# ΠΑΝΕΠΙΣΤΗΜΙΟ ΤΗΣ ΠΕΡΟΥΤΖΑ

Τμήμα Χημείας, Βιολογίας & Βιοτεχνολογίας

ΠΜΣ Τοξικολογία

Συσσώρευση **Hg** (Υδραργύρου) και άλλων χημικών στοιχείων σε επιλεγμένους ιστούς ενός 'επεμβατικού' είδους καραβίδας, **Procambarus clarkii,** από τη λίμνη Αλβιάνο

Επιβλέπων Καθηγητής:
**David Michele Cappelletti**

Διπλωματική εργασία της φοιτήτριας:
Χρυσοβαλάντου Μίχου

Ακαδημαϊκό έτος 2020/ 2021

# Università degli Studi di Perugia

Department of Chemistry, Biology and Biotechnology

MSc in Toxicology

# Accumulation of Hg and Other Trace Elements in Selected Tissues of an Invasive Crayfish Species, Procambarus clarkii, from Alviano Lake

Supervisor:
Prof. David Michele CAPPELLETTI

Master's thesis by:
Chrysovalantou MICHOU

Academic year 2020/21

# Abstract

Metal pollution is a global problem which represents a growing threat to the environment. Because of bioaccumulation and negative effects of heavy metals, their bioavailability needs to be monitored. Many studies showed accumulation of metals in crayfish tissues as dose- and time-dependent without significant differences in tissue concentration levels comparing males and females. The aim of this project was to estimate the levels of bioaccumulation in crayfish samples of Alviano, by ICP-MS-QQQ (triple quadrupole Iductively Coupled Plasma-Mass Spectometer), and the use of molecular markers (SOD, CAT,GPx, GST) to identify gene differences in the specimen. The present work details the analysis of Hg and other 29 elements concentrations in hepatopancreas and abdominal muscle tissues of 45 crayfish (Procrambarus clarkii) specimens collected from Alviano Lake, with the potential source of Hg located in Mountain Amiata, while a significant transport of mercury is documented in the streams draining the district. By far the largest output occurs to the southeast in the Paglia River catchment; this river is tributary of Tiber River, from which Alviano Lake derives. The elements Zn (15.8 mg/ kg) and Cd (0.01 mg/ kg) were the most and the least accumulated elements in the abdominal muscle tissue, while the elements Zn (18.97 mg/ kg) and Hg (0.03 mg/ kg) were the most and the least accumulated elements in hepatopancreas.

# Contents

# List of Figures

# List of Tables

# Chapter 1

# Introduction

## 1.1 General Properties of Mercury

The chemical symbol for mercury, Hg, is derived from the Greek word, hydrargyrum, which means silver water. Elemental mercury is found in the Earth's crust in only a limited number of regions in the world. Mercury is more abundant in mineral form, with cinnabar (HgS) being the most prevalent. Several of the less abundant minerals include calomel, Livingstonite, and Tiemannite. Mercury is found primarily in deposits formed by hydrothermal systems, which are more common at converging tectonic margins. It also tends to be enriched in some basic metallic minerals and presented with other chalcophilic (having a sulfur affinity) elements.The elemental form of mercury ($Hg^0$) has had a great number of uses historically, including barometers, thermometers, electrical switches, fluorescent light bulbs, and ballast for submarines. Elemental mercury has a unique combination of properties that seem to make it ideal for these applications. Hg0 is the only abundant metal that is liquid at room temperature. It has a melting point of –39°C and a boiling temperature of 357°C. It also has a rather high vapor pressure despite having a density 13 times greater than water and slightly greater than lead. This anomalous behavior is caused by weak inter-atomic bonding, which is due to the nucleus having a tight hold on its valence electrons. Hg0 is also relatively insoluble in water (49 $\mu$g/L or 4.4 ppt at 20°C which is 4 to 6 orders of magnitude smaller than the solubility of the predominant Hg compounds) and will readily avoid liquids. So, it is often described as preferring to be in the gas phase. Mercury can also be found in two ionic forms, oxidation states +1 and +2, which are more prevalent in water than in the atmosphere [1].

A number of the mercury compounds that occur in the environment have not been directly identified. Rather, several different fractions of mercury have been defined based on how they are collected (e.g., on a filter) and how elemental mercury can be released from them (e.g., heating the filter to 800°C). These distinctions, called "operationally defined fractions," are then used in place of specific compounds. The properties of the different fractions (e.g., solubility, volatility, etc.) are used in modeling the fate of mercury.

Mercury enters the waterways via deposition of particles or ionic compounds from the atmosphere, runoff and erosion from the land surface, leaching from landfills, geothermal inputs, combustion and industrial discharges. Once in the water environ-

1
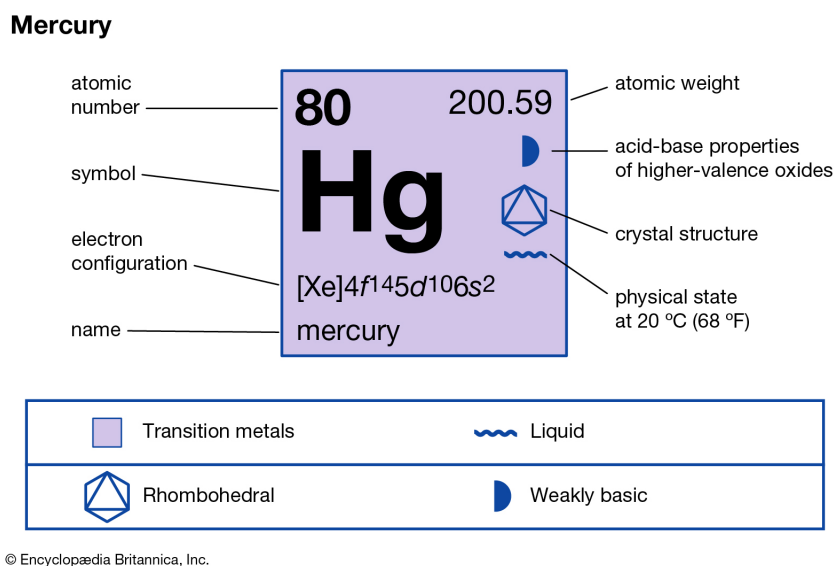
**Mercury**



Figure 1.1: Basic properties of Mercury (Encyclopedia Britannica, Inc.).

ment, mercury undergoes similar oxidation-reduction, sorption-desorption processes on to mineral surfaces and organic matter, and methylation-demethylation reactions as occur in the land environment.

In a similar manner to the land environment, elemental mercury can be evaporated back to the atmosphere directly from water (this process is also called evasion) or it can be oxidized to form Mercury(II). This ionic form of mercury can then be either reduced back to elemental mercury and again evaporate to the atmosphere, or it can form methylmercury. Mercury(II) can also form complexes with organic matter or be sorbed onto suspended particulate matter within the water environment. Mercury(II) complexes are thought to be the dominant form in which mercury is found in natural waters. Mercury(II) complexes can be transported over very long distances [2].

The methylation reactions in the aquatic environment are of particular concern due to the bioaccumulation of methylmercury in aquatic species. As a result, top-level predators acquire greater body burdens of mercury than the fish they consume. Bioaccumulation and biomagnification within the food chain can lead to top-level predators (fish-eating fish, birds and humans) having bioaccumulation factors of the order of 10 million [3]. In other words, concentrations within the bodies of these predators can be 10 million times higher than the environments in which they live.

Both oxidized mercury(II) and methylmercury can be deposited into the underlying sediments, where similar processes and transformations occur as those described for the land environment. Sediments at the bottom of water bodies can act as mercury sinks from which mercury can be distributed back into circulation for many years after initial deposition [4].

### 1.1.1 Chemical Species of Mercury

**Hg⁰** is elemental mercury. Hg0 has an anomalously high vapor pressure for a heavy metal. It is slightly water-soluble ( 50 $\mu$g/L at 20°C) and has a high Henry's law coefficient (729 at 20°C). In the natural environment, it can exist in the gaseous or

2

Table 1.1: Physical and chemical forms of mercury: Some recent and present pathways of human exposure

| | Inorganic mercury | |
|---|---|---|
| Hg vapor | Mercurous | Mercuric |
| $Hg^0$ | $Hg\text{-}Hg^2+$ | $Hg2+$ |
| Occupational | Laxatives | Skin creams |
| Dental amalgam | Teething powders | |
| | Organic mercury* | |
| Short chain alkyl | | Other organics |
| $CH_3(CH_2)_n\text{-}Hg^2$ | | $(R\text{-}C\text{-}Hg^+])$ |
| Mehtylmercury in fish | | Phenyl Hg antiseptic |
| Ethylmercury in preservatives | | Mercurial diureties |

*Some organic mercury compounds involve two carbon atoms attached to mercury, such as dimethylmercury ($CH_3\text{-}Hg\text{-}CH_3$)

liquid state. Gaseous element mercury (GEM), is the dominant form in the atmosphere. Most natural waters are nearly saturated, or are supersaturated with respect to atmospheric $Hg^0$.

**Hg(II)** or divalent mercury. Inorganic and organic divalent mercury compounds exist in gaseous, dissolved, and solid states. Their toxicity, solubility, vapor pressure, and reactivity vary greatly. Hg(II) is much more prevalent in waters than in the atmosphere. Methylated mercury compounds (below) are of particular interest because of their role in the biologic cycling of Hg and accordingly make up >95% of the mercury in fish [5].

**DMHg** is dimethylmercury, $(CH_3)_2Hg$. DMHg is significantly more toxic than $Hg^0$ on a milligrams per kilogram of body weight ingestion basis (due to more efficient absorption in the gut). It is believed to be present in the atmosphere in only negligible concentrations, but it is thought to be ubiquitous in the deeper ocean.

**MMHg** is monomethylmercury, $CH_3Hg^+$. MMHg is significantly more toxic than $Hg^0$ on a milligrams per kilogram of body weight ingestion basis (due to more efficient absorption in the gut) and readily bioaccumulates up the food chain. MMHg has not been reliably detected in the open oceans apart from the Equatorial Pacific Ocean [6].

### 1.1.2  Operational defined forms of Mercury

**DGHg** is dissolved gaseous Hg. It is a fraction of mercury measured in water that is defined by its ability to be volatilized only by purging with a clean, inert gas. It includes DMHg [6].

**HgR** is reactive Hg dissolved in water. It is defined based on its ability to be volatilized after reduction with $SnCl_2$, and purging with a clean, inert gas [6]. Hg(II) has also been used as an operationally defined fraction of dissolved Hg. It is determined by subtracting mercury that is readily volatilized (DGHg) from reactive Hg (HgR). It has been used as a measure of bio-available mercury, but is known to not be universally appropriate [6].

**Hg-Col** is colloidal mercury. It is mercury associated with colloidal matter that can be trapped on an ultrafine membrane after filtration of larger particulate matter. Col-

loidal mercury is generally considered to be larger than 1000 Da (molecular weight) but smaller than 0.1–0.5 $\mu$m.

**RGM** or reactive gaseous mercury, refers to Hg that can be captured on a KCl surface. RGM is believed to consist primarily of gaseous Hg(II) compounds. It is regarded as the fraction of airborne Hg that is readily deposited to the surface via wet or dry deposition. The exact chemical form of RGM is not known, but likely candidates include $Hg^O$, $HgCl_2$, and $HgBr_2$. In many reports, RGM and gaseous Hg(II) are used interchangeably, but it is important to recognize that RGM is an operation definition whereas Hg(II) is a chemical definition.

**PHg**, or particulate-bound mercury, refers to mercury that is extracted from particles, either airborne or waterborne. The observed PHg concentration can be dependent on the size of particles that are collected; for example, most airborne PHg measurements include only particles < 2.5 $\mu$m (aerodynamic diameter), so mercury on larger particles would be excluded from the reported concentration.

The amount of mercury extracted from the particles can be dependent on the technique used. Waterborne particulate mercury is generally determined by filtration, addition of BrCl, reduction with $SnCl_2$, and purging with a clean, inert gas. Measuring airborne PHg also requires capturing particles on a filter. The filters can be analyzed in the aqueous phase using the previously described technique. Or, the mercury on particles can be thermally reduced/desorbed, and quantified as GEM [7].
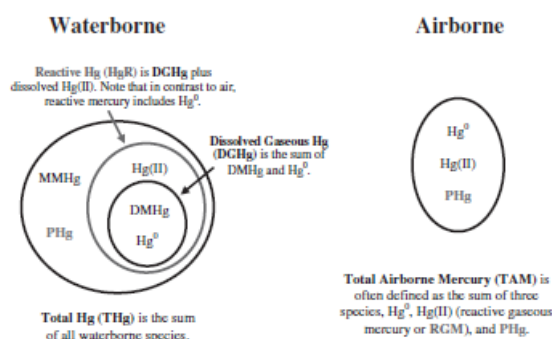


Figure 1.2: A simplified diagram of the major chemical forms of mercury found in water and air. (Mercury in the Environment, Michael S. Bank, University of California Press)

Any form of mercury in the environment may evolve into a more toxic species (methyl mercury) under biogeochemical transformation processes. Due to these processes and the high mobility of mercury species, a good understanding of how mercury species transform and accurate monitoring are essential for assessing the risk of mercury in the environment. The impact of mercury depends strongly on its chemical species; understanding mercury transformations and the impact of its various chemical forms are vital to preventing harmful effects on humans and the environment. Nevertheless, physicochemical characteristics of mercury are either useful or necessary for many industrial and agricultural applications, and mercury may be scattered over large area, depending on the source.

## 1.2 Production and Uses of Mercury

Mercury is a natural component of the earth, with an average abundance of approximately 0.05 mg/kg in the earth's crust, with significant local variations. Mercury ores that are mined generally contain about one percent mercury, although the strata mined in Spain typically contain up to 12-14 percent mercury. While about 25 principal mercury minerals are known, virtually the only deposits that have been harvested for the extraction of mercury are cinnabar. Mercury is also present at very low levels throughout the biosphere. Its absorption by plants may account for the presence of mercury within fossil fuels like coal, oil, and gas, since these fuels are conventionally thought to be formed from geologic transformation of organic residues.

The mercury available on the world market is supplied from a number of different sources, including (not listed in order of importance):

Mine production of primary mercury (meaning extracted from ores within the earth's crust):

1. Either as the main product of the mining activity, or as by-product of mining or refining of other metals (such as zinc, gold, silver) or minerals;

2. Recovered primary mercury from refining of natural gas (actually a by-product, when marketed, however, is not marketed in all countries);

3. Reprocessing or secondary mining of historic mine tailings containing mercury;

4. Recycled mercury recovered from spent products and waste from industrial production processes. Large amounts ("reservoirs") of mercury are "stored" in society within products still in use and "on the users' shelves";

5. Mercury from government reserve stocks, or inventories;

6. Private stocks (such as mercury in use in chlor-alkali and other industries), some of which may later be returned to the market.

The mining and other mineral extraction of primary mercury constitute the human mobilisation of mercury for intentional use in products and processes. Recycled mercury and mercury from stocks can be regarded as an anthropogenic re-mobilisation of mercury previously extracted from the Earth.

Despite a decline in global mercury consumption (global demand is less than half of 1980 levels), supply from competing sources and low prices, production of mercury from mining is still occurring in a number of countries. Spain, China, Kyrgyzstan and Algeria have dominated this activity in recent years, and several of the mines are state-owned. The table below gives information on recorded global primary production of mercury since 1981. There are also reports of small-scale, artisanal mining of mercury in China, Russia (Siberia), Outer Mongolia, Peru, and Mexico. It is likely that this production serves robust local demand for mercury, often for artisanal mining of gold – whether legal or illegal. Such mercury production would require both accessible mercury ores and low-cost labor in order for it to occur despite low-priced mercury available in the global commodity market.

In connection with its use, mercury has been found in Egyptian tombs dating back to 1500 B.C., and it has been used for centuries in medicines. While mercury is no longer sold as a dermal or oral antiseptic, an organic form continues to be used as

a vaccine preservative. The ancient Greeks and Romans used mercury in cosmetics and it was also one of the primary cures for syphilis in Europe before modern times. During the medieval period, alchemists thought mercury could be hardened to produce gold. In some cultures, spiritualists associate mercury with mystic qualities and it continues to be used to "bless" homes, cars and apartments. Although its toxic effects are well understood, mercury continues to be used in a wide variety of products and manufacturing processes because it is very useful.

Elemental mercury is used in thermometers, blood pressure devices, and thermostats because its ability to expand and contract uniformly makes it useful for measuring changes in temperature and pressure. Although many liquids could be used in pressure measuring devices, mercury is used because its high density requires less space. It is also a good conductor of electricity, so it is a useful component of electrical switches.

Mercury is also used in dental fillings, paints, soaps, batteries, and fluorescent lighting. Mercury will dissolve numerous metals to form amalgams and is used to extract gold dust from rocks by dissolving the gold and then boiling off the mercury. The amalgam used in dental fillings contains tin and silver alloyed with mercury. Because it works as a biocide, mercury has been used as a fungicide in paint, though this kind of paint is no longer sold.

### 1.2.1 Sources of Mercury in Water

#### 1.2.1.1 Atmospheric Wet and Dry Deposition

The largest and most important source of mercury in water is wet and dry deposition from the atmosphere. This includes both a natural and anthropogenic component. Globally, about 1% of the total oceanic burden is deposited and emitted each year. Most of the mercury deposited to oceans in precipitation is either bound to particles or is dissolved in an ionic state, Hg(II). Over the oceans, the overwhelming portion that is dry deposited is RGM, which has been produced near the water surface from photochemically driven oxidation by halogens. A portion ( 10%) of the RGM that is deposited to the ocean is reduced to elemental mercury in the surface waters, either directly by sunlight, or through biologic activity (Fitzgerald et al., 2007). This tends to make the surface waters supersaturated with respect to dissolved elemental mercury. Therefore, (gaseous) elemental mercury is generally evading from the ocean surface. Lakes and wetlands are more variable in their interaction with GEM.

Mercury that is bound to particles and bound to soluble organic complexes can also be incorporated into the hydrologic cycle as a part of runoff after rain or fl ooding events and through the movement of subsurface pore water. Subsurface geothermal and hydrothermal vents are also sources of mercury in the ocean, although the magnitude of these inputs is believed to be negligible as compared with the total oceanic burden. Subsurface vents may, nonetheless, be important in enhancing the concentrations in ambient waters and sediments near the vent site. Some mercury is also thought to enter (or perhaps reenter) the hydrologic cycle from diagenetic reactions, which are physical, chemical, or biologic changes that occur as sediment (settled particulate matter that contains mercury) is deposited, compressed, and transformed to rock.

### 1.2.1.2  Industrial Point Sources

Industrial waste is an important source of Hg to some watersheds. The most promi-
nent example of anthropogenic input of mercury to aquatic system occurred in Min-
imata, Japan, in the early 1950s. Throughout this period, the Chisso Corporation
dumped more than 20 tons of mercury that had been used as a catalyst in the pro-
duction of acetaldehyde, into Minamata Bay. The mercury contaminated the sedi-
ments, water, and ecosystem and ultimately the fish, which were a staple of the local
diet. In the following years, more than 100 people died and more than 1000 were per-
manently disabled from the resulting methylmercury poisoning, which consequently
bears the name, Minimata Disease.

It is also important to note that, by definition, the increased deposition (of RGM and
particulate-bound Hg) to oceans and lakes throughout the globe as compared with
preindustrial times is ultimately attributable to anthropogenic activities. Though the
input occurs after transport through the atmosphere, it is nonetheless of anthro-
pogenic origin.

### 1.2.1.3  Mining Runoff

An additional important source of mercury to aquatic systems is runoff or leach-
ing resulting from mining activities. Large-scale mercury mines often produce large
quantities of tailings or leave mining passages open after operations cease (e.g., Sul-
fur Bank Mercury Mine, California; Almadén, Spain; Idrija, Slovenia. Early gold and
silver mining also produced large quantities of Hg-enriched tailings because Hg was
added to crushed ore in order to amalgamate and extract the gold and silver. The
wastes, along with the open mine passages, allow rain and groundwater to leach
and mobilize mercury. Even smaller-scale mining activities, in particular artisanal
mining practiced in China, Indonesia, South America, and Africa produce significant
amounts of waste matter that is enriched in mercury. This is often dumped into
streams or lakes, or otherwise allowed to leach in an uncontrolled manner.

### 1.2.1.4  Methylated Species

Perhaps the most crucial process in the global cycling of mercury, at least from the
standpoint of toxicity, is the concentration and accumulation of MMHg or DMHg up
the food chain (called "bio-accumulation"). Most of the DMHg and MMHg that is
bio-accumulated is produced in situ in natural waters or near the sediment–water
interface. The production of MMHg and DMHg from dissolved Hg(II) (methylation)
occurs primarily in sulfate-reducing bacteria in anoxic environments and has been
hypothesized to be a cellular detoxification mechanism. A limited number of other
methylation mechanisms have been proposed, but bacteria appear to be the largest
producers in lakes and wetlands. Little DMHg and MMHg is found in the surface wa-
ters of the open ocean. Higher concentrations of DMHg can be found below the mixed
layer of the open ocean and peripheral seas, while MMHg has been unambiguously
detected only in coastal zones, peripheral seas, and the Equatorial Pacific Ocean [6].

## 1.3  Mercury in Nature

### 1.3.1  Mercury Cycle

The cycling of Hg in the environment is influenced by both natural and anthropogenic activities. The atmospheric transport is of particular importance for the dispersion of Hg in the global environment either released by natural or anthropogenic processes. Particularly, gaseous elemental Hg (Hg(0)) is efficiently transported over long distances with air masses and moves between the continents, thereby reaching even isolated regions. It is suggested that more than 90% of the Hg in surface waters results from atmospheric deposition. Consistently, several data on Hg contents in lake sediments, peat cores, and ice cores point out that the average global Hg deposition has increased by about a factor of 3 since preindustrial times ($\approx$1850), with more pronounced increases in regions influenced by regional sources.
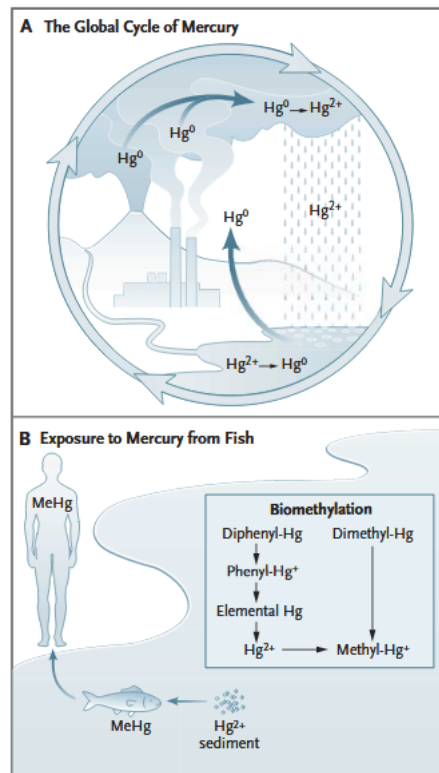


Figure 1.3: In nature, mercury vapor (Hg$^0$), a stable monatomic gas, evaporates from the earth's surface (both soil and water) and is emitted by volcanoes (Panel A). Anthropogenic sources include emissions from coal-burning power stations and municipal incinerators. After approximately one year, mercury vapor is converted to a soluble form (Hg$^2+$) and returned to the earth in rainwater. It may be converted back to the vapor form both in soil and in water by microorganisms and reemitted into the atmosphere. Thus, mercury may recirculate for long periods. Mercury attached to aquatic sediments is subject to microbial conversion to methyl mercury (MeHg), where up-on it enters the aquatic food chain. It reaches its highest concentrations in long-lived predatory fish, such as sharks. Panel B indicates the routes of transformation to methyl mercury as originally suggested by Jernelov.

The impact of mercury depends strongly on its chemical species; understanding mer-

8

cury transformations and the impact of its various chemical forms are vital to preventing harmful effects on humans and the environment. Nevertheless, the physico-chemical characteristics of mercury are either useful or necessary for many industrial and agricultural applications, and mercury may be scattered over large area, depending on the source.
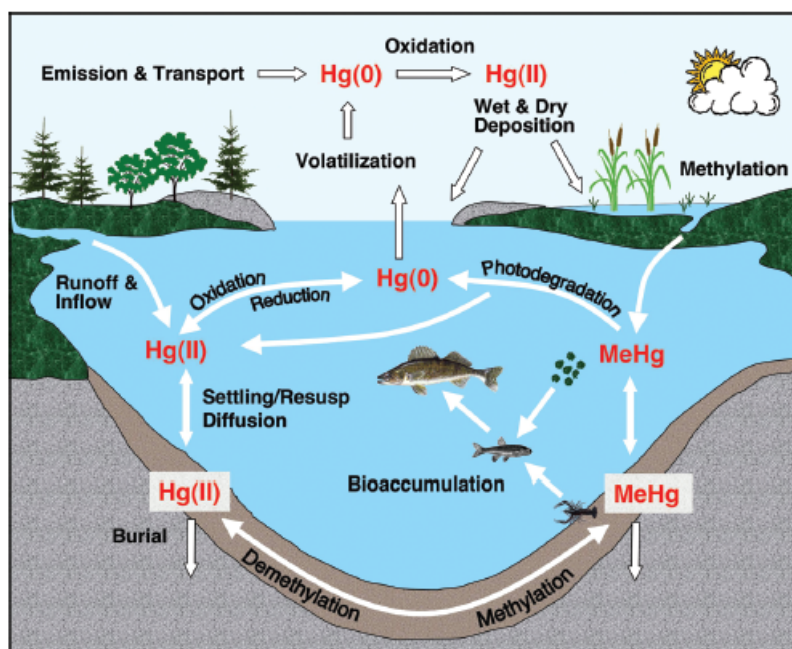


Figure 1.4: Mercury cycling in a lake and its watershed. Hg(0), mercury in its elemental form; Hg(II), divalent mercury; MeHg, methylmercury; Resusp, resuspension

Mercury in the environment is constantly cycled and recycled through a biogeochemical cycle 1.3. The cycle has six major steps:

1. Degassing of mercury from rock, soils, and surface waters, or emissions from volcanoes and from human activities.

2. Movement in gaseous form through the atmosphere.

3. Deposition of mercury on land and surface waters.

4. Conversion of the element into insoluble mercury sulfide.

5. Precipitation or bioconversion into more volatile or soluble forms such as methylmercury.

6. Reentry into the atmosphere or bioaccumulation in food chains.

The modern, industrial cycle of mercury differs from the preindustrial cycle 1.6 because of the extraction and mobilization of Hg from deep reservoirs. Deep reservoirs are defined as reservoirs that are physically below the surface ocean and land surface which contain a large mass of mercury relative to the mass that cycles through the land, air, and water, on an annual basis). Anthropogenic activities have greatly increased the mobilization of Hg (e.g., coal combustion and mining) from deep reservoirs. This enhanced Hg extraction is thought to have increased the total atmospheric burden of Hg by about a factor of 3, which has resulted in a nearly threefold increase

9
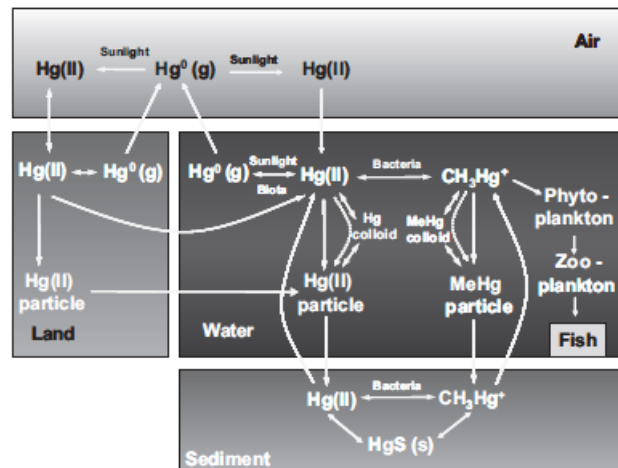
Figure 1.5: A biogeochemical cycle of mercury in the environment, illustrating the common forms of mercury often quantified.

in deposition to the land and ocean. But, it should be noted that the observational record of Hg in the atmosphere is relatively short, so no clear pattern of change has been found. Increased concentrations in the surface ocean and land surface have accordingly increased emissions back to the atmosphere. Thus, the total amount of mercury cycling through the land surface, surface oceans, and atmosphere, has increased significantly. The burden of total mercury in the deep oceans has also increased, but by a much smaller factor. The smaller increase in deep ocean concentrations is largely a result of the much greater reservoir of Hg and slower mixing and turnover times. This produces a lag in uptake on the order of decades to centuries in the surface waters and deep ocean, respectively.
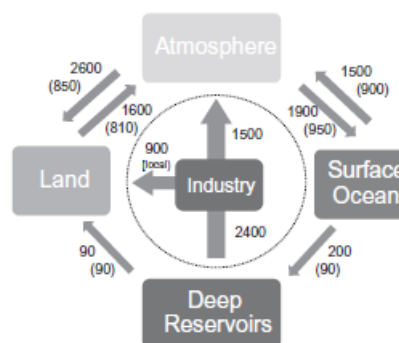


Figure 1.6: Simplified global geochemical mercury cycle. All values are tons per year. Preindustrial values are given in parentheses below the modern values. The inner, dashed circle indicates the perturbation of industrial activities that significantly increased the extraction of mercury from deep reservoirs. This results in significantly greater local deposition and also increased input to the global atmospheric pool, which increases global deposition. Upward arrows from the land and ocean are net evasion and downward arrows are wet and dry deposition.

The primary anthropogenic sources are: fossil fuel combustion and smelting activities. Both these natural and human activities release elemental mercury vapor ($Hg^0$)

into the atmosphere. Once in the atmosphere, the mercury vapor can circulate for up to a year, and hence become widely dispersed. The elemental mercury vapor can then undergo a photochemical oxidation to become inorganic mercury that can combine with water vapors and travel back to the Earth's surface as rain. This 'mercury-water' is deposited in soils and bodies of water. Once in soil, the mercury accumulates until a physical event causes it to be released again. In water, inorganic mercury can be converted into insoluble mercury sulfide which settles out of the water and into the sediment, or it can be converted by bacteria that process sulfate into methylmercury. The conversion of inorganic mercury to methylmercury is important for two reasons:

The conversion of inorganic mercury to methylmercury is important for two reasons:

1. Methylmercury is much more toxic than inorganic mercury.

2. Organisms require a long time to eliminate methylmercury, which leads to bioaccumulation.

Now the methylmercury-processing bacteria may be consumed by the next higher organism up the food chain, or the bacteria may release the methylmercury into the water where it can adsorb (stick) to plankton, which can also be consumed by the next higher organism up the food chain. This pattern continues as small fish/organisms get eaten by progressively bigger and bigger fish until the fish are finally eaten by humans or other animals. Alternatively, both elemental mercury and organic (methyl) mercury can vaporize and re-enter the atmosphere and cycle through the environment.

### 1.3.1.1  Transformation/Methylation Processes

An early advance in the understanding of Hg cycling in terrestrial/freshwater ecosystems was the recognition of MeHg as the form responsible for most bio-accumulation of Hg. The abundance of MeHg is controlled by two counteracting microbiologic processes: Hg methylation and MeHg demethylation. The pattern of net methylation in the landscape (i.e. the balance of these processes in space and time) determines the risk of biota to Hg bioaccumulation. Here we address terrestrial methylation, including wetlands. Until recently, Hg methylation was viewed primarily as an aquatic process affecting primarily the aquatic food web. However, aquatic MeHg finds its way into terrestrial food webs, and high MeHg has been documented in songbirds nourished from purely terrestrial food webs, making it clear that terrestrial Hg methylation cannot be ignored. The importance of terrestrial relative to aquatic methylation can be expected to vary with their relative areas on the landscape (e.g., the ratio of catchment to lake surface area), as well as the relative strength of the methylation sources (such as wetlands). There is great variability in MeHg concentrations in soil water and groundwater. They are generally low (up to a few tenths of a nanogram per liter) where there are low DOC concentrations and/or oxic conditions. However, in waters with more than a few milligrams per liter of DOC, MeHg concentrations are often higher, with concentrations of one to several nanograms per liter possible, but with considerable variations. These patterns, which reflect the local balance between methylation and demethylation, vary in space but are less well characterized in time.

Although elevated inputs of ionic Hg ($Hg^2+$) to ecosystems are generally thought to result in high concentrations in fish, there are many factors that mediate the ultimate fate and trophic transfer of Hg in the environment. Elevated MeHg bio-accumulation

in fish and piscivorous birds and mammals results from a complex sequence of biotic and abiotic mechanisms that control the transport and availability of $Hg^2+$, MeHg production, bio-accumulation, or biomagnification. These mechanisms occur at critical points in the transfer of Hg in the environment which include: (1) Hg supply and inputs to the ecosystem (e.g., deposition to the landscape); (2) transport to aquatic ecosystems (e.g., from terrestrial watersheds); (3) transformation in wetlands and sediments to MeHg; and finally, (4) bio-accumulation and trophic transfer in aquatic food webs. Moreover, the effect of each of these processes can be enhanced or diminished depending on environmental conditions.
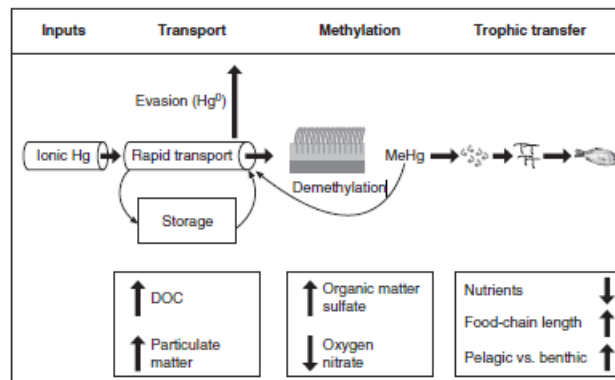


Figure 1.7: Conceptual model of important transformation and transfer points in the Hg cycle.

### 1.3.1.2 Bio-Availability and Transformation

An important factor controlling concentrations of Hg to fish and other biota is net methylation. Methylation is the process by which microbes convert $Hg^2+$ to MeHg. This process is important because MeHg is the form that readily bioaccumulates in the terrestrial and aquatic food chain resulting in potential exposure to wildlife and humans. Although methylation can be mediated by a variety of microbes, the most important of these is sulfate-reducing bacteria. Sulfate-reducing bacteria flourish in reducing environments, such as wetlands and lake and river sediments. As a result, zones of high methylation activity occur only at restricted locations on the landscape. Conditions that promote the methylation of Hg2+ are low oxygen, high inputs of labile organic carbon, and a supply of sulfate and $Hg^2+$. Inputs of oxygen or nitrate inhibit sulfate reduction and therefore methylation of $Hg^2+$. In the presence of elevated concentrations of sulfide, methylation of Hg2+ is also restricted because the sulfide binds $Hg^2+$, making it unavailable for methylation and because of the formation of charged Hg-sulfide complexes, which cannot be readily assimilated by sulfate-reducing bacteria. MeHg can be demethylated by oxidative or reductive processes, resulting in the formation of either $Hg^2+$ or GEM. Therefore, the net production of MeHg is the result of two processes: methylation and demethylation.

### 1.3.1.3 Bio-Accumulation and Trophic Transfer

The final process in the sequence is bio-accumulation (uptake from food and water) and trophic transfer of $Hg_2^+$ and MeHg. MeHg and $Hg_2^+$ are bioconcentrated (from water) and assimilated by phytoplankton. MeHg in phytoplankton is assimi-

12

lated more efficiently by zooplankton than $Hg_2^+$, resulting in an enrichment in MeHg content. Phytoplankton in the water column exhibit the largest bioconcentration step in aquatic food webs resulting in log bio-accumulation factors of 5–6. A bio-accumulation factor is the ratio of the concentration of a contaminant (e.g., MeHg) in the organism to the value in water. A number of mechanisms influence the bio-accumulation of MeHg in phytoplankton, including bio-availability of MeHg to algal uptake and phytoplankton growth. Phytoplankton bio-accumulate both Hg2+ and MeHg from water but partition the MeHg to the cytoplasm, leaving $Hg_2^+$ bound to the cell wall. Zooplankton appear to assimilate the MeHg inside algal cells and egest the $Hg_2^+$ with the cell walls. Fish also obtain MeHg from ingestion of food and take up far less directly from water. Enrichment of MeHg continues up the food chain to top consumers, who are found to have virtually all their Hg occurring as MeHg. Several factors influence this trophic transfer of MeHg in aquatic ecosystems. Elevated inputs of growth-limiting nutrients (e.g., P, N) increase biomass, resulting in a decrease in the Hg concentration of individual organisms; this phenomenon is called biodilution. Higher growth rates in individuals also result in lower mass-specific concentrations in their tissues because of growth dilution. Growth dilution has been hypothesized as the mechanism explaining lower MeHg concentrations in fish and shellfish from the more productive lakes. Differences in food-web structure and type affect the fate of MeHg as well. Several studies have found chain length to be positively related to MeHg concentrations in top-trophic level fish, suggesting that the increased number of trophic levels results in greater biomagnification of MeHg. Finally the Hg concentration of fish is greater for those species feeding from a pelagic food chain rather than a benthic food chain. Some studies have shown that bioaccumulation of MeHg also occurs along the terrestrial food chain.

### 1.3.2  Freshwater Systems

Much of the research that has been conducted on aquatic mercury cycling has occurred in freshwater ecosystems. Mercury contamination of freshwater systems is widespread, while ecosystems are also affected by point sources of mercury owing to local contamination issues.

In areas away from point sources, atmospheric mercury reaches freshwater ecosystems by direct deposition to lake surfaces and through runoff from watersheds. Wet and dry deposition to watersheds and lake surfaces, as in terrestrial systems, is predominantly as Hg(II). Hg(II) can reduce to Hg(0), which may then volatilize to the atmosphere. A small portion of Hg(II) is converted to the more toxic form of methylmercury (MeHg). Methylation of mercury is a biologically mediated process known to be facilitated by some strains of sulfate- and ironreducing bacteria ([10], [11], [12]). Wetlands and lake sediments are important environments where methylation occurs. The spatial extent of these areas in particular ecosystems influences net methylation. Methylmercury can bioconcentrate in living organisms and then further biomagnify up the food chain, as predators eat prey contaminated with methylmercury and further concentrate it in their tissues. This process of bioaccumulation means that methylmercury concentrations in predatory fish can be elevated relative to water by a factor of $\geq 106$.

In aquatic sediments, microbes convert a small fraction of inorganic mercury (Hg(II)) to MeHg over time. Sulfur, organic carbon, sediment structure, and composition

affect methylmercury production by changing the amount of bioavailable inorganic mercury and by stimulating microbial activity. In coastal sediments, sulfate-reducing bacteria are thought to be the principal agents responsible for MeHg production. These microbes thrive at the geochemical interface between oxic and anoxic conditions. A number of environmental factors are known to affect the rate of MeHg formation by influencing the supply of bioavailable Hg(II) and/or the activity of methylating microbes. In addition to Hg(II) concentrations, effective proxy indicators for MeHg production and accumulation identified by previous research include sulfide concentrations, total organic carbon, and redox potential. Methylmercury production has also been measured in the water column in lakes and in anoxic coastal waters.Ecosystems respond to changes in deposition on varying timescales, depending on ecosystem type and the influence of watersheds.

## 1.4 Enviromental and Health Concerns of Mercury

The primary motivations for researching mercury in the environment are related to its toxicity. The majority of the human population lives within 100 km of the ocean,and the benefits from marine ecosystems are greater than those from all other ecosystems combined. Those benefits include the consumption of seafood, which has many health benefits. Accordingly, the study of mercury biogeochemistry and environmental toxicology in marine systems is of great importance for both human and environmental health.

While mercury has long been recognized as a potent toxin, full appreciation of the threat of mercury contamination from environmental exposures has occurred only within the latter half of the past century. The environmental mercury problem was first documented in the 1950s in Minamata Bay, Japan, where many individuals suffered severe mercury poisoning from their consumption of seafood with elevated levels of methylmercury (5–35 $\mu g\ g^{-1}$). That contamination was traced to wastewater discharges of monomethylmercury to the bay from a chemical plant producing acetaldehyde and vinyl chloride. Since then, other cases of mercury poisoning have been chronicled, including in native populations of Arctic and sub-Arctic regions who consume relatively high amounts of fish, marine mammals, and marine birds. More recently, the focus has shifted to the potential sublethal or long-term toxicity of mercury to individuals consuming relatively large amounts of marine fish, and in a few cases marine mammals.

The greatest concern for human health related to environmental mercury pollution is the consumption of fish by the most susceptible populations, specifically pregnant women and children. Thus, while fish represent an important protein source for large segments of the population, and the consumption of fish has many health benefits, it is also the pathway responsible for most human exposure to mercury.

The growing awareness of mercury's sublethal toxicity in humans has increased concerns about mercury's adverse effects on other organisms. Ecosystems can be threatened by elevated environmental mercury levels, with higher trophic-level organisms considered most at risk. These include top predator fish, as well as piscivorous birds and mammals, which can have high body burdens of mercury (often described as "potentially toxic") because of the biomagnification of mercury in aquatic food chains. Some of the adverse effects associated with these elevated mercury concentrations

are reduced reproductive success in fish and birds, altered behavioral traits or neurologic effects in marine mammals, and immunotoxic effects in birds and marine mammals.

### 1.4.1 Effects of Mercury in Aquatic Environment

Mercury concentrations systematically increase with increasing trophic level in freshwater, estuary, and marine food chains (Figure 7 and Table 8). Mercury levels in apex predators in the aquatic environment may be more than 1 million–fold higher than in surrounding waters. This enrichment underlies mercury's persistent and bioaccumulative nature as a toxicant, representing a serious environmental and human health concern. Table 10.5 summarizes data from various marine ecosystems, illustrating the general trend of increasing total mercury concentrations and increasing % MMHg with trophic level. Central to mercury's biomagnification is that only MMHg, not Hg(II), is biomagnified in marine food webs. The preferential bioaccumulation of MMHg, due to its relatively low elimination rate and relatively high assimilation efficiency, has been shown in kinetic models, laboratory studies, and field studies of mercury uptake by aquatic organisms. Those reports demonstrate that in most cases MMHg is the only form of mercury biomagnified and that MMHg constitutes a larger fraction of the overall body burden of mercury in aquatic organisms with increasing trophic level.

### 1.4.2 Effects of Mercury in Human Health

#### 1.4.2.1 Potential Health Effects of Mercury

The toxicity of mercury depends on its chemical form, and thus symptoms and signs are rather different in exposure to elemental mercury, inorganic mercury compounds, or organic mercury compounds (notably alkylmercury compounds such as methylmercury and ethylmercury salts, and dimethylmercury). The sources of exposure are also markedly different for the different forms of mercury. For alkylmercury compounds, among which methylmercury is by far the most important, the major source of exposure is diet, especially fish and other seafood. For elemental mercury vapour, the most important source for the general population is dental amalgam, but exposure at work may in some situations exceed this by many times. For inorganic mercury compounds, diet is the most important source for the majority of people. However, for some segments of populations, use of skin-lightening creams and soaps that contain mercury, and use of mercury for cultural/ritualistic purposes or in traditional medicine, can also result in substantial exposures to inorganic or elemental mercury.

While it is fully recognised that mercury and its compounds are highly toxic substances for which potential impacts should be considered carefully, there is ongoing debate on how toxic these substances, especially methylmercury, are. New findings during the last decade indicate that toxic effects may be taking place at lower concentrations than previously thought, and potentially larger parts of the global population may be affected. As the mechanisms of subtle toxic effects – and proving whether such effects are taking place – are extremely complex issues, a complete understanding has so far not been reached on this very important question.

Of the organic mercury compounds, methylmercury occupies a special position in

that large populations are exposed to it, and its toxicity is better characterized than that of other organic mercury compounds. Within the group of organic mercury compounds, alkylmercury compounds (especially ethylmercury and methylmercury) are thought to be rather similar as to toxicity (and also historical use as pesticides), while other organic mercury compounds, such as phenylmercury, resemble more inorganic mercury in their toxicity.

Methylmercury is a well-documented neurotoxicant, which may in particular cause adverse effects on the developing brain. Moreover, this compound readily passes both the placental barrier and the blood-brain barrier, therefore, exposures during pregnancy are of highest concern. Also, some studies suggest that even small increases in methylmercury exposures may cause adverse effects on the cardiovascular system, thereby leading to increased mortality. Given the importance of cardiovascular diseases worldwide, these findings, although yet to be confirmed, suggest that methylmercury exposures need close attention and additional follow-up. Moreover, methylmercury compounds are considered possibly carcinogenic to humans according to the International Agency for Research on Cancer (IARC, 1993), based on their overall evaluation.

Methylmercury can be formed in the environment by microbial metabolism (biotic processes), such as by certain bacteria, and by chemical processes that do not involve living organisms (abiotic processes). Although, it is generally believed that its formation in nature is predominantly due to biotic processes. Significant direct anthropogenic (or human generated) sources of methylmercury are currently not known, although historic sources have existed. Indirectly, however, anthropogenic releases contribute to the methylmercury levels found in nature because of the transformation of other forms. Examples of direct release of organic mercury compounds are the Minamata methylmercury-poisoning event that occurred in the 1950's where organic mercury by-products of industrial-scale acetaldehyde production were discharged in the local bay, and the Iraqi poisoning events where wheat treated with a seed dressing containing organic mercury compounds were used for bread. Also, new research has shown that methylmercury can be released directly from municipal waste landfills and sewage treatment plants, but the general significance of this source is still uncertain.

Once in the food chain mercury can bioaccumulate causing adverse effects to human health. The exact mechanism(s) by which mercury enters the food chain remains largely unknown, and probably varies among ecosystems. Figure 1 presents multiple routes through which humans are exposed to mercury.

16

# Chapter 2

# Materials and Methods

In the present study, the red swamp crayfish, Procambarus clarkii of both sexes was collected from Lake Alviano. The sampling process was separated in two sections, site 1 and site 2, in e which

## 2.1 Study Area

Lake Alviano is an artificial basin, which was created by the construction of a dam on the Tiber river in 1963 for hydroelectric power production. The sampling site is affected by anthropic charge of the Tiber River with urban and industrial waste. The potential source of Hg is located in Mountain Amiata, while a significant transport of mercury is documented in the streams draining the district. By far the largest output occurs to the southeast in the Paglia River catchment; this river is tributary of Tiber River, from which Alviano Lake derives. Most transport is in particulate form, and mercury is temporarily stored in stream and overbank sediments, and can be significantly mobilized and redistributed by extreme events such as flash floods. This shallow reservoir has since turned into an interesting wetland, becoming a hotspot for thousands of migratory birds as well as an important nesting area. Alviano is situated below the confluence of the Paglia River with the Tiber, with an area of 3.49 $km^2$ and a maximum depth of 9 m.



Figure 2.1: Picture of Lake Alviano

The Alviano Lake is one of the widest WWF nature reservoirs and includes all the

17

typical habitat of the fresh water wetlands. The Oasis of Alviano Lake was created in 1990, it contains most of the wetland habitats, many of which disappeared more than 100 years ago. This makes it a special place; in fact with its 900 hectares, it protects a unique biodiversity from hunting and property speculation, and is one of the widest WWF nature reserves and includes all the typical habitat of the fresh water wetlands: swamps, ponds, morass, water meadows, and a hygrophilous woodland, one of the largest in central Italy.

The nature reserve is part of the largerest Umbria regional park which also includes the Corbara Lake and the Forello gorges. It contains all the common freshwater habitats of wetlands: swamps, ponds, morass, water meadows, hygrophilous woodland, among the largest in the Appennines.

Alviano is most famous for its rich bird diversity: species include mallards, Eurasian teals, northern shovelers, wigeons, great cormorants, herons, Eurasian bitterns, little bitterns, Western marsh-harriers, ospreys, glossy ibises and spoonbills. There are also many species of passerine, particularly Eurasian siskins and thrushes the mammal population contains [13].

Furthermore, the area of the Tiber River basin south of its confluence with the Paglia River, and especially south of Lake Alviano, has considerable urban, agricultural, and industrial activities, which constitute additional potential Hg sources.

### 2.1.1 Sample Collection and Processing

Specimens of P. clarkii were sampled monthly, from July 2019 to September 2019, from Alviano Lake. The samples were captured within the day using tophi (large pots with circular section typical of the region) placed at a depth of about 1.5 meters and up to 1500 meters from the southeastern shore.



Figure 2.2: Tophi for crayfishes capture.

For the processing, P. clarkii specimens were purchased alive from fishermen's cooperatives in the two sites examined. The crayfishes were immediately transported to the Ecotoxicology laboratory of the Department of Chemistry, Biology and Biotechnology of the University of Perugia, where they were separated on the basis of sex. The presence of modified pereiopods (hooks), suitable for holding the female during mating, is exclusive to male specimens if sexually active. Subsequently, the specimens were placed in bags appropriately labeled with the date and place of sampling and placed in the freezer at -20°C until the tissues of interest (hepatopancreas or muscle) were taken for morphometric, chemical and biochemical analysis.

18

## 2.2   Bioindicator : Red swamp crayfish (Procambarus clarkii)

Crayfish species have been used as a good bio-indicator species to determine the toxic metal contamination in the environment by many researchers. The red swamp crayfish (Procambarus clarkii), as a representative species of crustaceans, inhabits a wide range of aquatic environments, including those with heavy metals pollution. It is known for its hyperaccumulation potential and tolerance to various heavy metals. Several traits of its life history, e.g., polytrophism, rapid growth, high fecundity and disease resistance, make its invasion of the wild successful.



Figure 2.3: Procambarus clarkii in different color variations

It is widely used because of its following characteristics:

  i  can able to tolerate environmental stress better than other organisms;

 ii  have long life spans (2–5 years) and low fecundity with high juvenile survival;

iii  ability to survive in physical contact with contaminated water and soil;

 iv  occupy higher tropical level in the food chain;

  v  huge in size to get samples from different tissue organs, which make them a suitable study specimen for environmental monitoring studies [14, 15, 16].

Generally, crayfish have been classified as herbivores, detritivores and omnivores, which magnify the metal levels by feeding the contaminated organisms from the lower trophic levels of the food chain. It feeds on detritus, algae, plant matter, aquatic invertebrates, amphibians and fish [17]. Therefore, the current study was aimed at assessing the effect of Hg toxicity on the aquatic environment by using crayfish, Procambarus clarkii, as a fundamental bioindicator in the freshwater system.

19

## 2.3 Chemical Analysis

### 2.3.1 Optimization of the Digestion Method

The work in the laboratory is carried out according to the analysis of the samples by ICP-MS, which is used to determine the concentration of heavy metals present in the muscle and hepatopancreas of crabs taken from Lake Alviano.The sample preparation process has undergone, over time, an optimization of the method, as shown below:

1. Firstly, the thawed samples, were homogenized in small falcons while being kept in beakers with ice.

2. Following, the samples were prepared using a CEM Corporation MARS 6 microwave digestion system equipped with iWave technology. iWave is a novel technology advancement that utilizes Light Emitting Technology™ to accurately measure the temperature of the actual sample solution inside the vessel and does not require an internal probe. The samples were placed inside cylindrical PFA Teflon containers called vessels. The vessels were firsty weighed empty and subsequently they were reweighed containing the sample (which could be muscle or hepatopancreas). At this point, the calibration of the scale prior to the use is of big importance.

3. At this time, 5 ml of 67-69% $HNO_3$ Ultrapure NORMATOM is added in each sample. The vessels were capped hermetically and placed in the MARS 6 for digestion. The mixture is then heated in the microwave digestion system (MARS 6 ONE TOUCH CEM) as shown in Figure 2.3. The One Touch Technology automatically recognized the vessel type and counted the number of vessels. It then chosed the optimized conditions for the acid digestion.The maximum temperature achieved using this method is 180 °C. Animal tissue samples in general do not require extremely high temperatures to achieve complete digestion.



Figure 2.4: Microwave Digestion System MARS 6

20

4. Prior to the analysis of the elements, the sample must undergo acid mineralization. This procedure serves to destroy the organic part present in the sample and to form soluble salts of the metal of interest. The technique was applied using a MARS 6 (Microwave Accelerated Reaction System) which is a microwave digestion system. Microwave acid digestion is a technique to dissolve metals, bound within a sample matrix, into liquid. This is achieved by exposing a sample to a strong acid, in a closed vessel and raising the temperature and pressure through microwave irradiation. Both the speed of thermal decomposition of the sample, and the solubility of heavy metals in solution are increased. Once these heavy metals are in solution, they can be quantified through elemental techniques. This instrument is proprietary technology that utilizes the emission of light from the sample (solution) to rapidly and accurately measure temperature. It reads the temperature of the solution itself, instead of reading the temperature of the vessel. This makes it the most accurate temperature sensor. The sensors are floor-mounted inside the cavity of the MARS 6 microwave digestion system. Every time a vessel rotates past a sensor, the temperature is accurately measured in real time. This allows the advanced MARS 6 software to automatically make power adjustments to ensure for a successful acid digestion.

5. At the end of the digestion process, the samples were diluted with ultrapure water to 25ml.

### 2.3.2 Analysis with ICP-MS-QQQ

Inductively coupled plasma - mass spectrometry (ICP-MS) can be seen as one of the leading techniques in the field of elemental analysis, focusing on the determination of ultratrace levels of metals and metalloids in a large variety of sample types. It is a versatile, fast and extremely sensitive analytical technique, which allows to perform accurate multi-elementary analyzes. Some of the advantages of this technique are:

1. speed of analysis (35 elements can be determined in a sample within two minutes);

2. limits of detection for most elements in the parts per trillion range and for some parts per trillion (ppt) elements;

3. possibility of analyzing solid, liquid and gaseous samples;

4. ease of analysis of simple and complex matrices;

5. removal of uncertainty and ensurance of accuracy when using reaction gases;

6. consistent and reliable results, even when sample matrix and co-existing analytes change;

7. simplifcity in method development –same gas mode used for all samples;

8. enablement of accurate isotope analysis (no inter-isotope overlaps);

9. removal of direct isobaric overlaps.
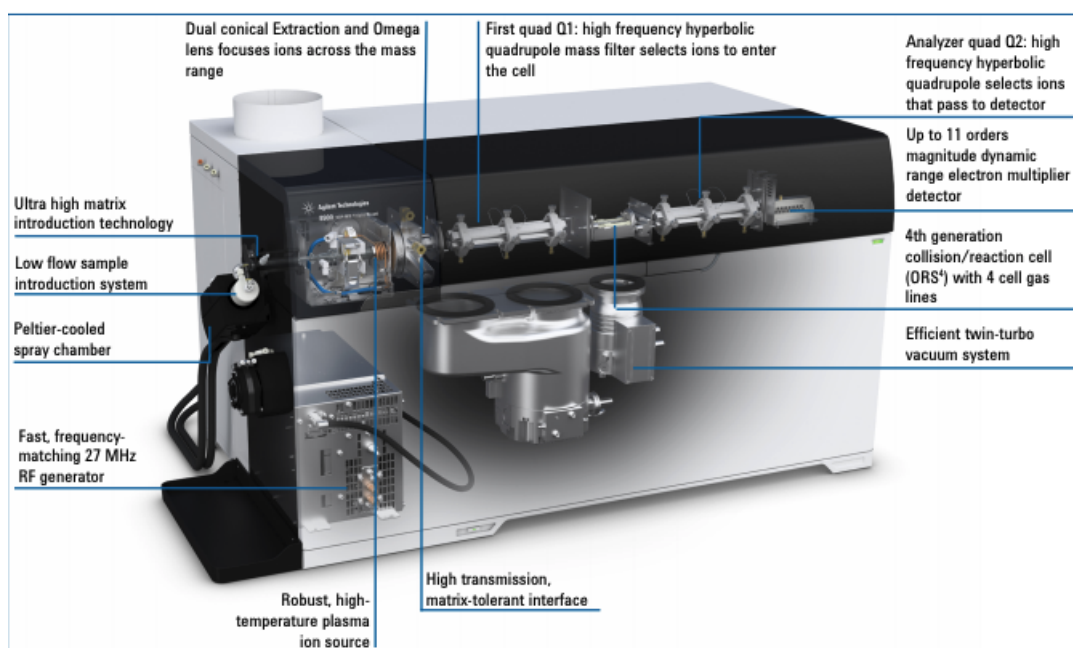
Figure 2.5: ICP-MS Agilent 8900 QQQ

The cell containing the ion guide—the Octopole Reaction System (ORS) in the case of Agilent ICP-QQQ—can be pressurized with a collision or reaction gas to allow the selective attenuation of potential interfering ions. In MS/MS operation, where both quadrupoles are operated as unit mass filters, ions at the target analyte mass are selected by the first quadrupole (Q1) and passed to the ORS cell, where the analyte ions are separated from overlapping interfering ions. The resulting product ions that emerge from the cell are then filtered by the second quadrupole (Q2) before being passed to the detector (Figure 2.5). . This configuration releases the full potential of reaction cell gas methods to resolve spectroscopic interferences including isobaric and doubly-charged interferences, as well as polyatomic ion overlaps. As a result, ICP-QQQ can determine a wider range of analytes at much lower concentrations with greater reliability and higher confidence.
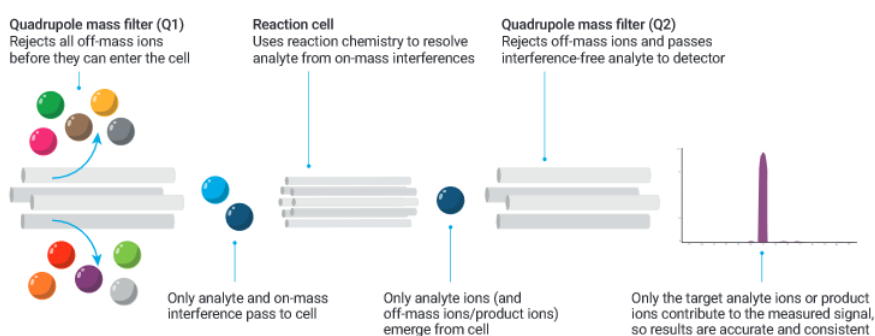


Figure 2.6: Schematics of the ICP-MS/MS system

The tandem MS configuration of Agilent ICP-QQQ instruments – with two fully functioning mass filters, one either side of the ORS cell – allows unprecedented control over the ions that enter the collision/reaction cell (CRC). Q1 rejects all non-target

masses/elements, ensuring more consistent reaction processes in the CRC, even when the sample composition varies. Precise mass selection by the first quadrupole, Q1, is crucial to the accurate analytical performance in MS/MS mode. For reliable, consistent control of reaction processes, Q1 must allow only ions at the target mass-to-charge ratio (m/z) to pass into the cell. Inefficient mass filtering would cause results to be compromised by interferences arising from non-target ions entering the cell. To ensure the most effective mass filtering and the best quality data, Agilent ICP-QQQ instruments use the same hyperbolic quadrupole mass spectrometer for Q1 and Q2. Both quadrupoles are placed in the high vacuum region to ensure optimum mass filtering. This arrangement allows both quadrupoles to operate at unit mass resolution and low abundance sensitivity while maintaining high transmission and sensitivity [18].

The elements under examination were analyzed in no gas mode and in collision-reaction cell (CRC) mode using helium or oxygen with a plasma configuration defined as "General Purpose".

The instrument was calibrated with standard solutions of known and certified concentration of metals (ICP multi-element standard solution CertiPUR, Merck Chemicals and Reagents), obtaining a calibration line for each metal with the least squares method (Ordinary Least Squares, OLS ).

The certified Internal standard mix for ICP-MS systems, 100 ppm of 6 solution was used as an internal standard to correct for changes in instrument operating conditions and sample-specific matrix effects, which could increase or suppress the analyte signal. -Li, Sc, Ge, Rh, In, Tb, Lu, Bi produced by Agilent Technologies.

A parameter strictly connected with the instrumental and analytical performance of the method adopted is the Limit Of Detection (LOD) which indicates the minimum concentration of analyte capable of producing a signal / response, significantly different from that of the blank. LOD was estimated using the slopes of the calibration lines constructed with certified standard solutions of the metals examined (determination with the least squares method using the standard deviation of the residuals of the linear regression Sy/x).

Experimental repeatability was calculated by performing three replicate analyzes of two multi-element standard solutions (1 and 10 $\mu$g/L). The % RSDs obtained from the repeatability test of the metal solutions were good and included in the 0.1-10.0% range.

The procedure followed the order listed below:

1. The sample analysis instrument, the triple quadrupole mass ICP, set itself automatically before starting its program (it takes about 30 minutes); first it directed the plasma (8000 Kelvin), then it adjusted the discs inserted between plasma and quadrupole and between the three quadrupoles themselves in order not to disperse ions (provided with a central hole with potential difference).

2. The instrument ebulized the solution under examination; the aerosol that is formed was transported in a high frequency plasma in which the analytes were atomized and ionized. The ions were extracted from the high-frequency plasma through a cone and separated according to their mass-to-charge ratio. The poles were used to differentiate the inherent atom from analytes with equivalent mass.

3. The separation took place at the level of the central octupole, thanks to the use of gases connected to the machinery (for example, it has oxygen, nitrogen and argon available) which through chemical reactions modify the molecules (or ions) consequently varying the weight, allowing so the selection.

4. After separation, they were recorded in a detector and the created signals were evaluated by the software. Quantitative determination was possible after calibration with standard solutions since there is a linear relationship between the intensity of the ionic signals and the concentration of an element.

## 2.4 Biochemical Analysis

Reactive oxygen species (ROS) are produced in metabolic and physiological processes, and harmful oxidative reactions may occur in organisms, which remove them via enzymatic and non-enzymatic antioxidative mechanisms. Under some conditions, the increase in oxidants and decrease in antioxidants cannot be prevented, and the oxidative/ antioxidative balance shifts toward the oxidative status. Consequently, oxidative stress, which has been implicated in over 100 disorders, develops [19].
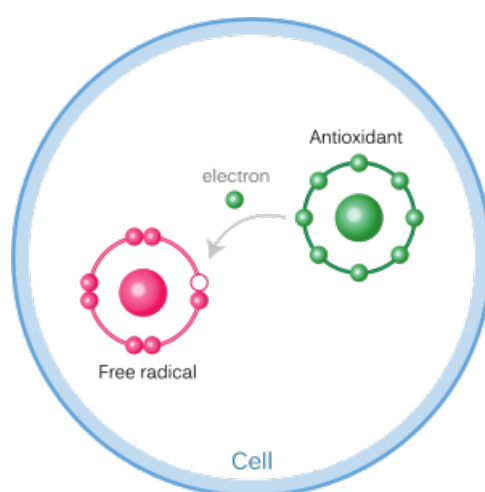


Figure 2.7: Free radical electrons.

Hydroxyl radical (OH·) and its subsequent radicals are the most harmful ROS and they are mainly responsible for the oxidative injury of biomolecules. Alone hydrogen peroxide and superoxide molecules cannot directly oxidize lipids, nucleic acids and sugars. These species can lead to oxidative injury in the biomolecules indirectly by producing OH· via Fenton reaction and/or iron-catalyzed Haber– Weiss reaction [20] Oxidized molecules generally form new radicals leading to radical chain reactions or they are neutralized by antioxidants. Antioxidant molecules prevent and/or inhibit these harmful reactions [21].

24
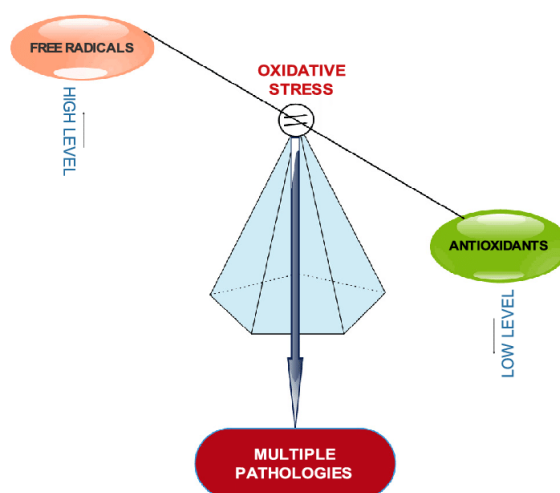
Figure 2.8: Oxidative stress: Imbalance between free radicals and antioxidants.

In this study, we studied the activity of four biomarkers, glutathione (GSH), super-oxide dismutase (SOD), catalase (CAT), and glutathione peroxidase (GPx). Mechanisms that involve GSH, and related antioxidants superoxide dismutase (SOD), catalase (CAT), and glutathione peroxidase (GPx) represent important protective metabolic pathways [22], and serve as biomarkers of xenobiotic-mediated oxidative stress. Glutathione in its reduced form is an important non-enzymatic scavenger of oxyradicals, and is involved in metabolism of toxic compounds and endogenous substances [23]. Both SOD and CAT enzymes catalyze the breakdown of ROS-generating $O_2^-$ and hydrogen peroxide ($H_2O_2$) respectively and are key components within the primary defense system against oxidative stress-induced damage. GPx affects only organic hydroperoxides.

Levels of biomarkers (total $GSH^+$ 2GSSG levels and activities of SOD, CAT, and GPx) were measured in cytosolic fraction of muscle and hepatopancreas by spectrophotometric analysis (Varian Cary 50 spectrophotometer at $25^oC$, Figure 2.9). The muscle and hepatopancreas tissue from one individual crab was divided into two portions prior to homogenization with an Ultraturrax homogenizer for different analyses (enzymatic markers and total glutathione). Muscles and hepatopancreas tissues were homogenized in 100 mM KP buffer (pH 7.5) containing 0.1 mg bacitracin/mL, 0.008 TIU aprotinin/ml, 100 $\mu$M PMSF (phenylmethylsulphonyl fluoride) and 2.5% NaCl. Homogenates were centrifuged at 18,000 x g (45 min, $4^oC$) and resulting supernatants further centrifuged at 50,000 x g (90 min, $4^oC$). Protein concentrations in the cytosol determined [24], were used to normalize enzyme levels. All analyses were performed in triplicate along with blank samples (buffer and reagents only). These absorbance values were subtracted from those of the sample.

1. SOD activity was determined according to an established method [25] following modifications [26]. The analysis was performed at 550 nm in buffer (50 mM $Na_2CO_3$ 0.1 mM EDTA, 500 mM cytochrome C, 1 mM hypoxanthine, and xanthine oxidase, pH 10). A standard curve of SOD units was used. One unit of SOD was defined as the amount of enzyme needed to inhibit 50% of the reduction of cytochrome C.

2. CAT activity was determined by following the decrease in absorbance at 240 nm

25

Figure 2.9: Picture of Varian Cary 50 spectrophotometer

owing to the consumption of $H_2O_2$ [27]. The assay was performed in 100 mM sodium phosphate buffer ($NaH_2PO_4$ + $Na_2HPO_4$, pH 7, with 12 mM $H_2O_2$).

3. GPx activity was determined following the oxidation of nicotinamide adenine dinucleotide phosphate reduced form (NADPH) at 340 nm [28]. Each assay was performed in 100 mM sodium phosphate buffer ($NaH_2PO_4$ + $Na_2HPO_4$, 1mM EDTA, 0.12 mM NADPH, 2 mM GSH, 1U GR, pH 7.5).

4. Total glutathione (GSH+ 2GSSG) was measured following homogenization in 5% sulfosalicilic acid with 4 mM EDTA (1:3 and 1:4 w/v ratios for muscles and hepatopancreas tissues, respectively). Homogenates were maintained for 30 min on ice and then centrifuged at 30,000 × g for 15 min. Total GSH+ 2GSSG content was determined by the GR recycling assay at 412 nm [29].

## 2.5  Statistical Analysis

The data were processed using the statistical programming environment R (R Version 3.4.4) and the packages tidyverse, ggplot2 [30], corrgram, corrplot, qwraps2, dplyr, ggpubr and lubridate. In order to verify differences between the biometric variables of males and females, the Student's t test was performed, using a level of statistical significance equal to 0.05. Barlett's test was used for the homogeneity of variances, while comparisons with counting data were carried out using the Shapiro-Wilk hypothesis test.Biomarker levels were compared by one -way ANOVA with post-hoc Tukey test treating each exposure group separately.

26

# Chapter 3

# Results & Conclusions

## 3.1 Statistical Analysis Results with R

With the use of the statistical programming environment R, and in order to see if the samples obtained were following a normal distribution, the following histogram was taken. In addition, the same procedure was followed for all the elements detected, as seen in the B.2.
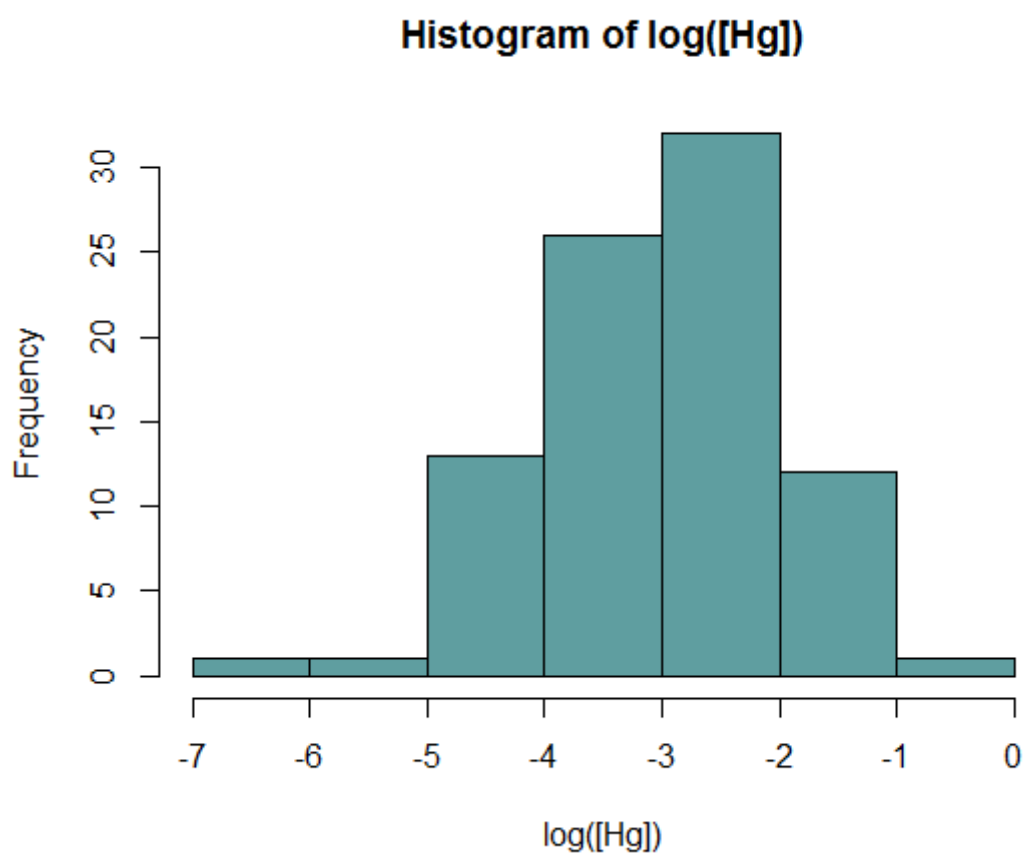
**Histogram of log([Hg])**



Figure 3.1: Histogram of the logarithm of Hg concentration.

27

The density plot obtained is used to observe the distribution of the numeric variable (Hg) in the dataset. Thus, the plot is smooth across bins and is not affected by the number of bins created, which helps create a more defined distribution shape. The peaks of the density plot help display where values are concentrated over the interval.
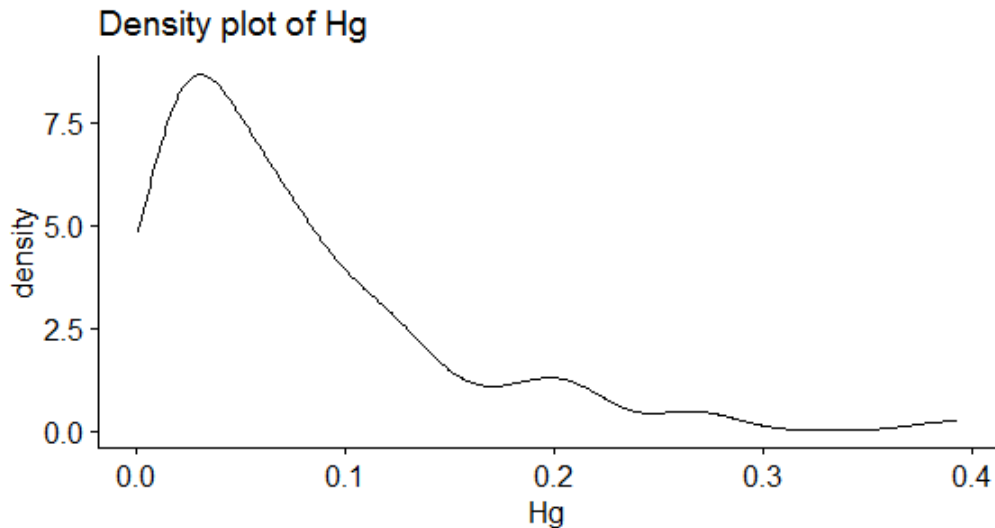


Figure 3.2: Density plot of Hg, obtained from the statistical programming environment R.

The Q-Q plot, or quantile-quantile plot, is a graphical tool to help us assess if a set of data plausibly came from some theoretical distribution such as a normal or exponential. As seen in the tables below, since the points are forming a line that is roughly straight, both sets of quantiles came from the same distribution.
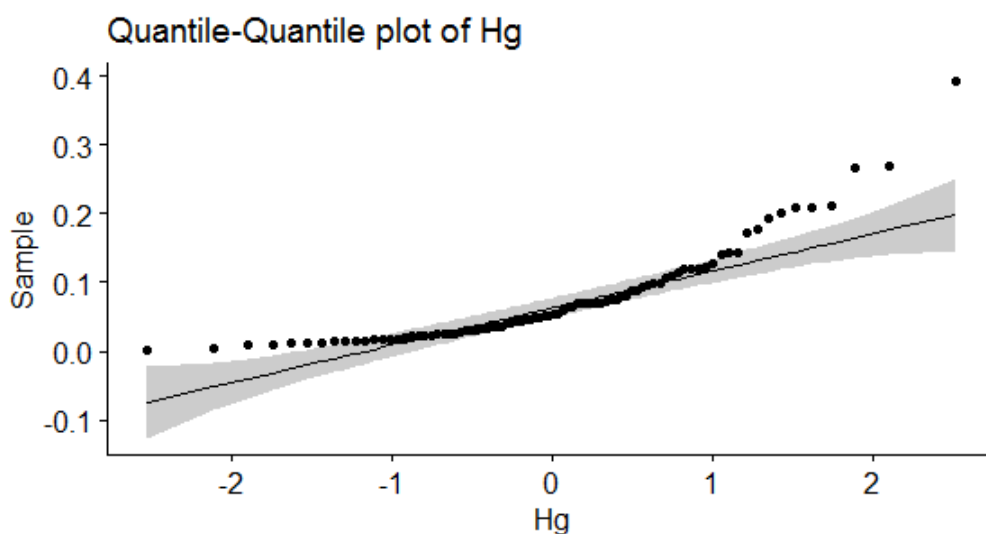


Figure 3.3: Quantile - quantile plot of Hg, obtained from the statistical programming environment R.

28
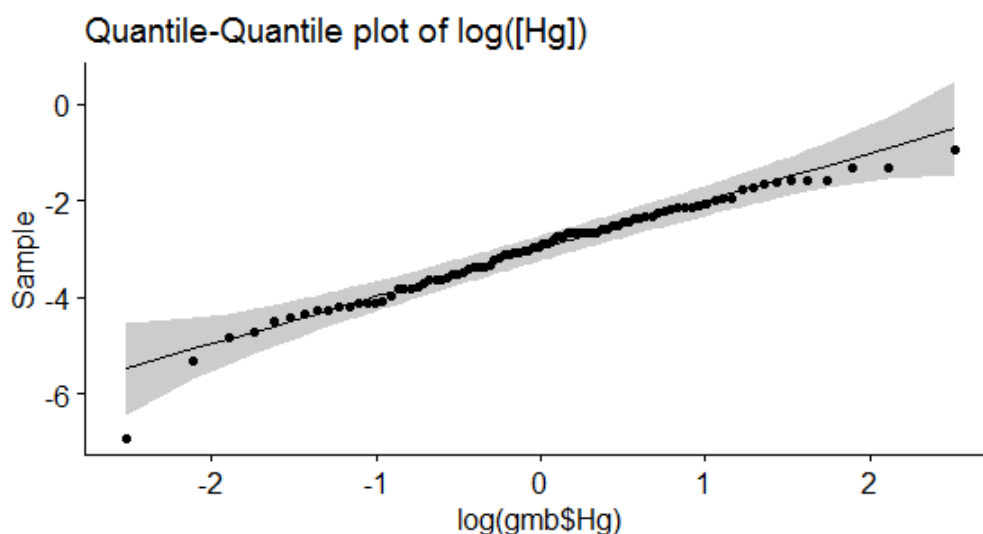
Figure 3.4: Quantile - quantile plot of log ([Hg]), obtained from the statistical programming environment R.

In the process, box plots were conducted in order to provide a visual summary of the data enabling a quick identification of the mean values, the dispersion of the data set, and signs of skewness. Box plots divide the data into sections that each contain approximately 25% of the data in that set.
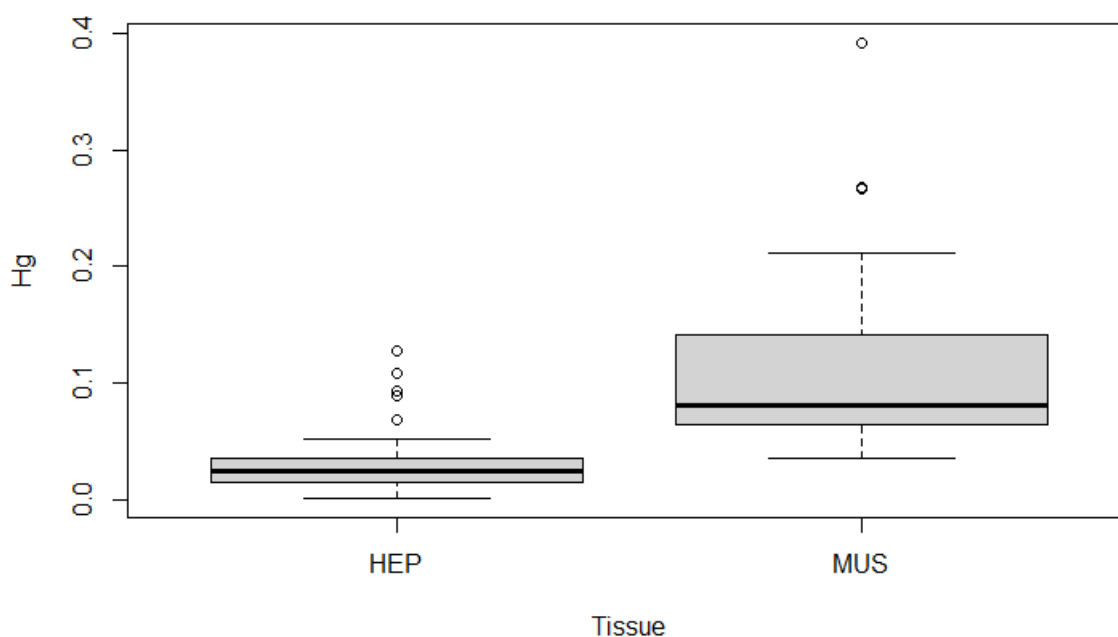


Figure 3.5: Boxplot graph of Hg for hepatopancreas and muscle tissues.

29
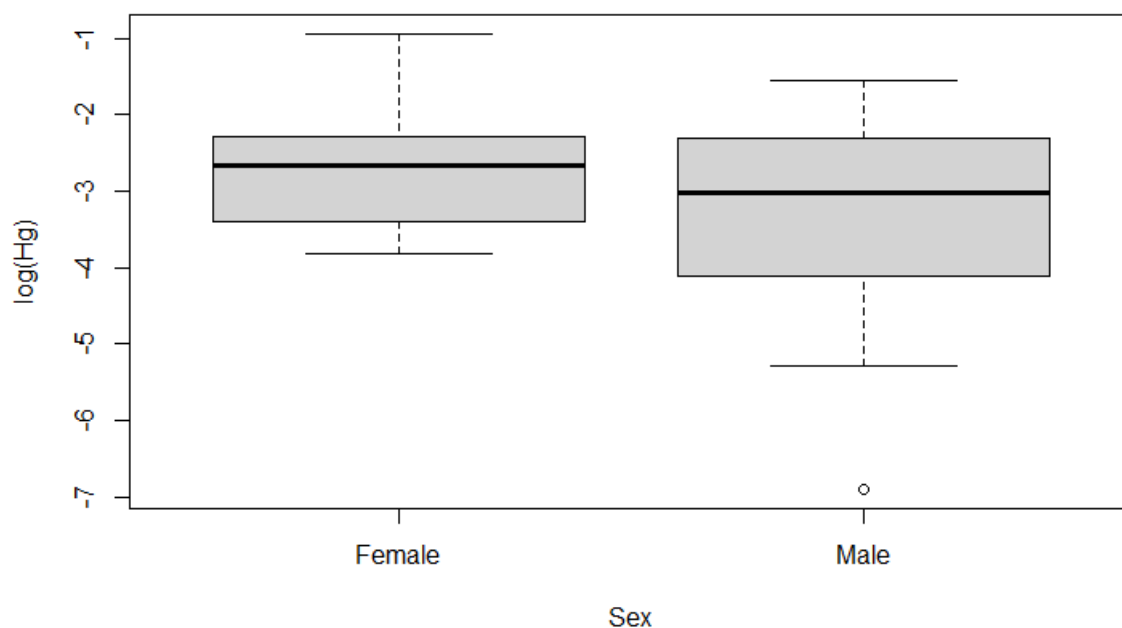
Figure 3.6: Boxplot graph of Hg for hepatopancreas and muscle tissues.

With the use of the statistical programming environment R, the data were processed in order to obtain the correlations matrix. In table 3.1 presented the positive correlations can be seen. Cr and Ni showed a perfect positive correlation. Also As, Mn, Co and Cd showed high positive correlation , while Pb with Zn and Hg with Ni showed low positive correlation.

Table 3.1: Correlation table of metals' concentrations in P.clarkii hepatopancreas and muscle tissues.

| Parameters | Mn | Co | Ni | Cu | Zn | Cd | Pb | Hg | As | Cr |
|---|---|---|---|---|---|---|---|---|---|---|
| Mn | 1.00 | | | | | | | | | |
| Co | 0.74 | 1.00 | | | | | | | | |
| Ni | -0.04 | 0.03 | 1.00 | | | | | | | |
| Cu | 0.16 | 0.22 | -0.24 | 1.00 | | | | | | |
| Zn | 0.50 | 0.45 | -0.03 | 0.37 | 1.00 | | | | | |
| Cd | 0.62 | 0.59 | -0.22 | 0.40 | 0.45 | 1.00 | | | | |
| Pb | 0.09 | 0.25 | -0.04 | 0.29 | 0.32 | 0.19 | 1.00 | | | |
| Hg | -0.16 | -0.14 | 0.40 | 0.04 | 0.18 | -0.32 | 0.09 | 1.00 | | |
| As | 0.77 | 0.84 | -0.15 | 0.31 | 0.49 | 0.80 | 0.25 | -0.28 | 1.00 | |
| Cr | -0.14 | -0.09 | 0.98 | -0.29 | -0.08 | -0.30 | -0.06 | 0.43 | -0.27 | 1.00 |

30
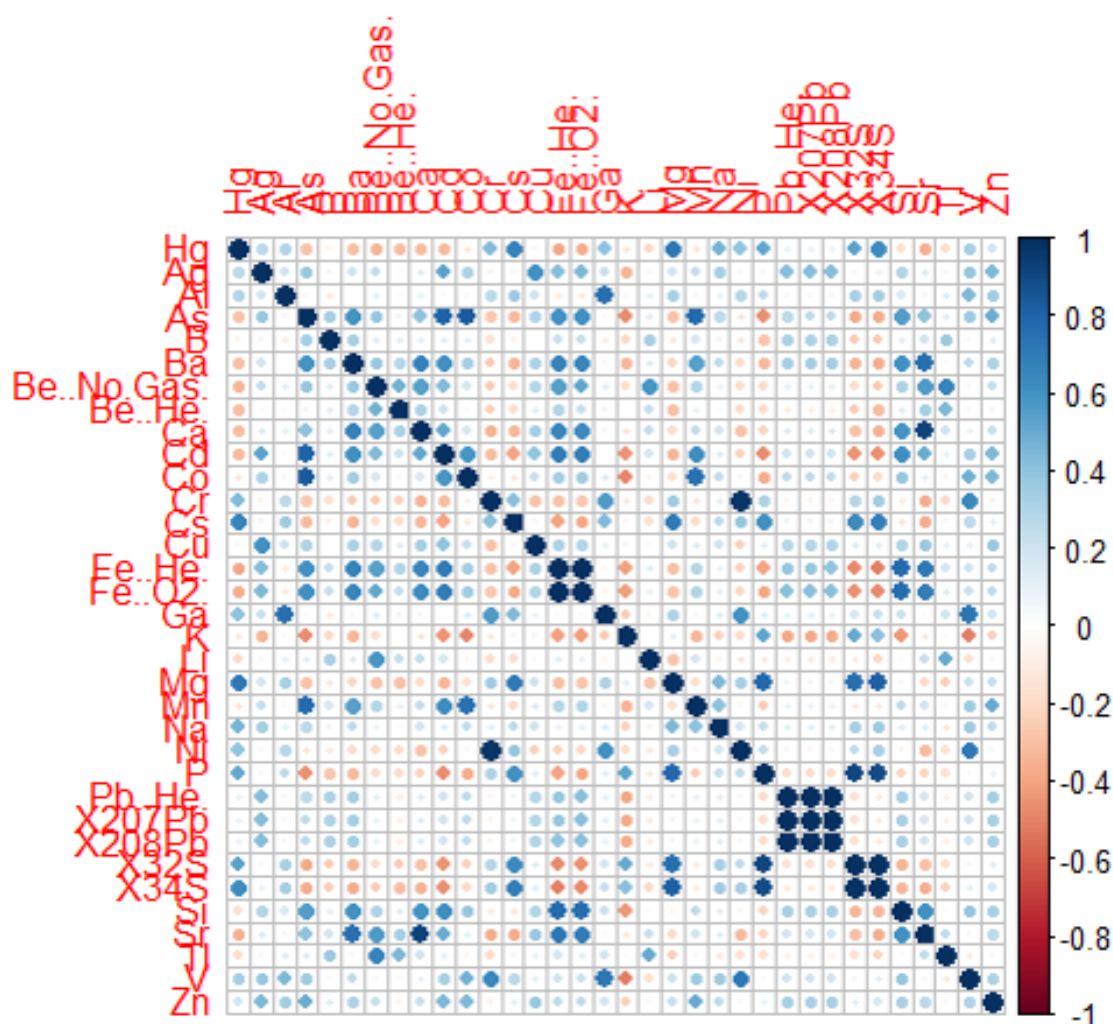
Figure 3.7: Correlations matrix obtained from the statistical programming environment R.

## 3.2   Chemical Analysis Results

In the tables below, the graphs of Hg concentrations for both sexes, male and female, and for both tissues, muscle and hepatopancreas (y axis = samples, x axis= mean value in ppb) are presented. With respect to the tissue comparison, the difference between muscle and hepatopancreas is directly observd. Hg is accumulated in higher level in muscle, compared to hepatopancreas. As for the comparison between males and females, it is observed that females tend to have higher Hg concentrations compared to males. Moreover, a higher accumulation in the summer months compared to September is also observed.

31
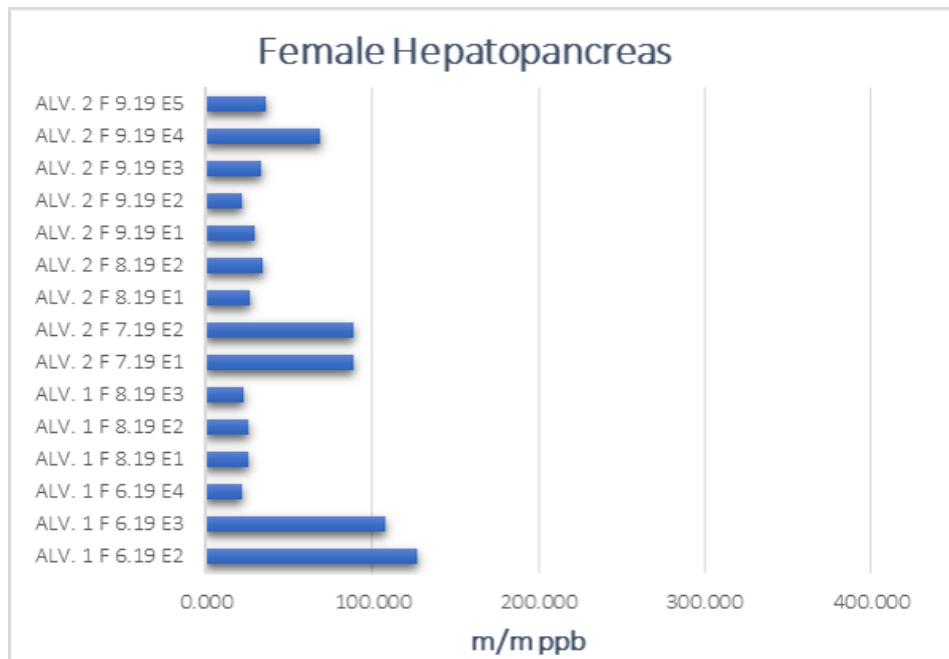
Figure 3.8: Mercury (Hg) concentration in samples of P. clarkii female hepatopancreas tissues.
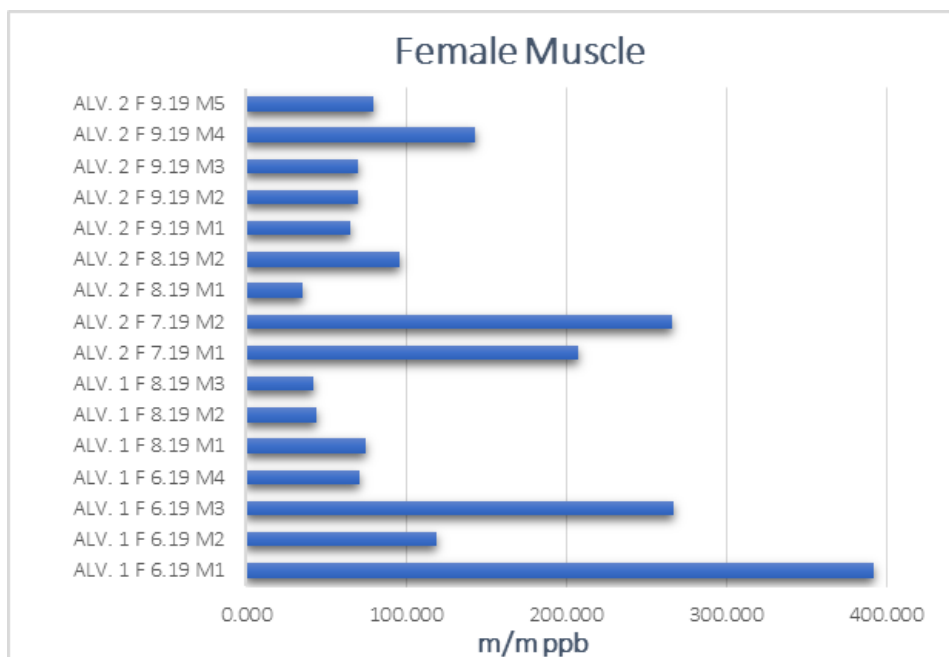


Figure 3.9: Mercury (Hg) concentration in samples of P. clarkii female muscle tissues.

The graphs 3.8, 3.9 above show the accumulation in the female hepatopancreas and muscle tissues respectively. In both tissues, the Hg accumulation is higher in June, while the muscle has significantly higher Hg concentration than the hepatopancreas.

32
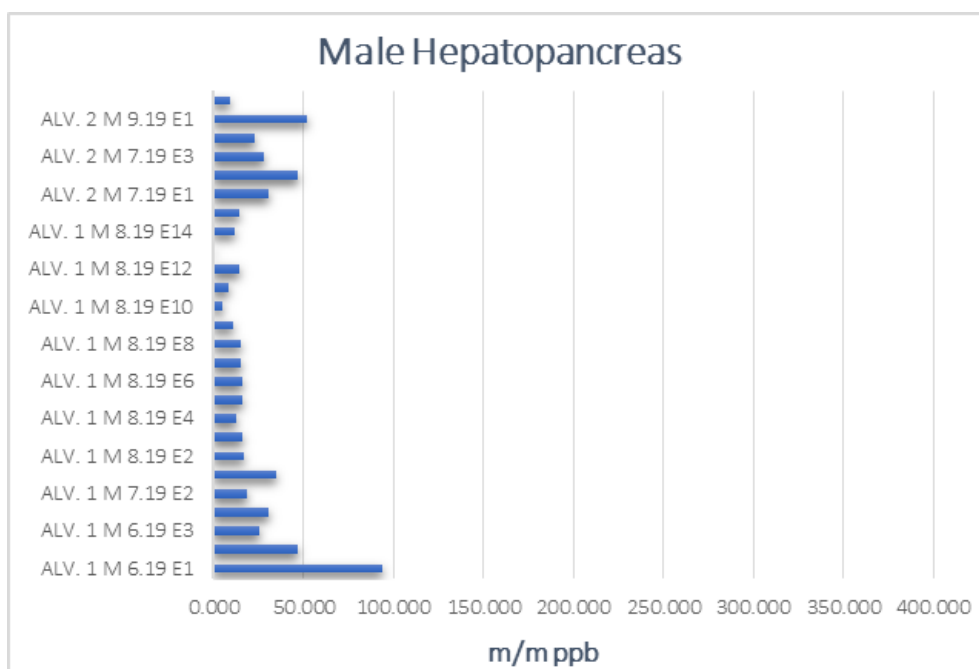
Figure 3.10: Mercury (Hg) concentration in samples of P. clarkii male hepatopancreas tissues.
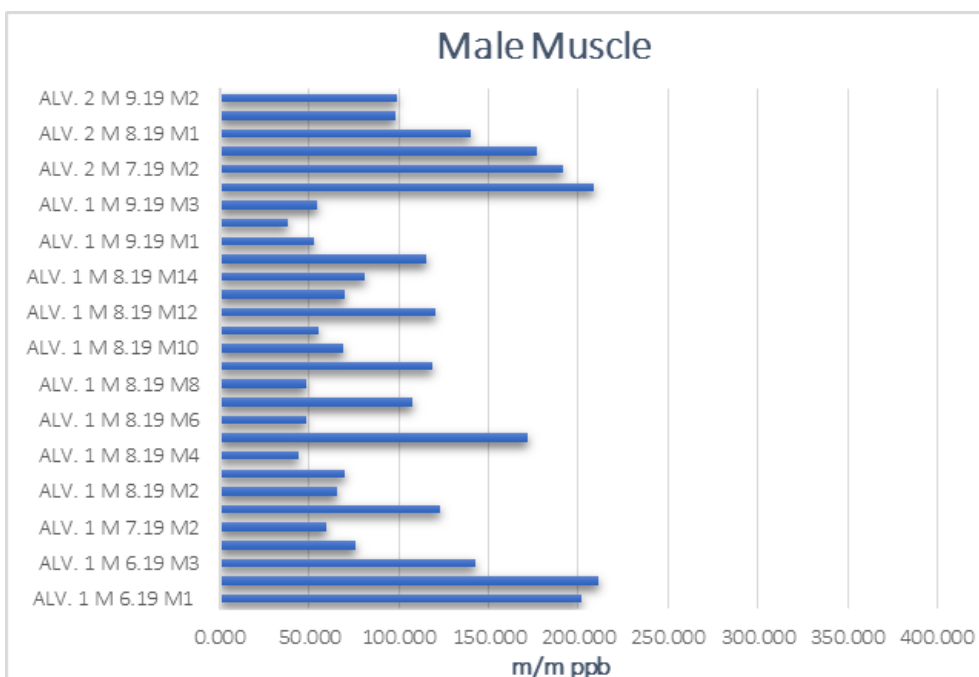


Figure 3.11: Mercury (Hg) concentration in samples of P. clarkii male muscle tissues.

The graphs 3.10, 3.11 above show the accumulation in the male hepatopancreas and muscle tissues respectively. In contrast with the female tissues, a different result is observed.While in the male hepatopancreas the higher concentration is in June too, in the muscle tissue very high concentrations are also observed in also July and August. As for the comparison between the two tissues, as in the female tissues, the

Hg accumulation is higher in the male muscle than in hepatopancreas. Summing up, as seen in table 3.2 the mean Hg concentration in muscle tissues is 0.117 ppm, which is more than three times higher compared to hepatopancreas with 0.037 ppm.

Table 3.2: Comparison of Hg concentrations between sexes and specific tissues of P.clarkii.

|  | mean | stdev | median | rsd |
|---|---|---|---|---|
| muscle - female | 0.128 | 0.103 | 0.077 | 80% |
| muscle - male | 0.106 | 0.054 | 0.098 | 52% |
| hepatopancreas - female | 0.051 | 0.036 | 0.033 | 71% |
| hepatopancreas - male | 0.023 | 0.019 | 0.016 | 82% |
| total muscle | 0.117 | 0.075 | 0.081 | 64% |
| total hepatopancreas | 0.037 | 0.029 | 0.025 | 79% |

Consecutively,using some of the most important elements, the figure 3.13 with the means, medians, standard deviations and relative standard deviations was conducted. As compared with the results of a previous study, in Trasimeno Lake, shown in figure 3.13, it is observed that:

1. Mn is higher concentrated in Alv. Lk compared to Tras.Lk, in both sexes and both tissues;

2. Co in Alviano Lake is in the same amounts as in Trasimeno Lake

3. Ni is in lower concentration in Alviano Lake, and significantly lower in hepatopancreas. The total mean of hepatopancreas in Alviano Lake is 0,73 ppm, when in Trasimeno Lake is 14,4 ppm;

4. Zn is higher concentrated in Alviano Lake than in Trasimeno Lake, with the exception of male hepatopancreas. In Trasimeno Lake the mean concentration of Zn is 28,98 ppm whereas in Alviano Lake it is 16,48 ppm;

5. as for Cd, even though the muscle concentrations in Alviano Lake are lower, the hepatopancreas concentrations are higher;

6. Pb is around the same numbers in both tissues, with the exception of the only higher concentration in female hepatoncreas in Alviano Lake, compared to Trasimeno Lake;

7. Hg is significantly higher in muscle tissues in Alviano Lake compared to Trasimeno Lake. An increase in the concentration in hepatopancreas is also observed in Alviano Lake compared to Trasimeno Lake.

34

| mg/Kg | Mn | Co | NI | Cu | Zn | Ag | Cd | Pb | Hg |
|---|---|---|---|---|---|---|---|---|---|
| **MUSCOLO MASCHIO** | | | | | | | | | |
| MEDIA | 1.13 | 0.03 | 4.45 | 8.42 | 13.46 | 0.011 | 0.004 | 0.041 | 0.027 |
| DS | 0.57 | 0.02 | 5.52 | 2.51 | 4.01 | 0.004 | 0.004 | 0.022 | 0.008 |
| RSD% | 51 | 64 | 124 | 30 | 30 | 31 | 95 | 54 | 30 |
| | | | | | | | | | |
| **MUSCOLO FEMMINA** | | | | | | | | | |
| MEDIA | 1.02 | 0.03 | 3.97 | 8.78 | 14.06 | 0.010 | 0.003 | 0.060 | 0.016 |
| DS | 0.40 | 0.02 | 5.85 | 4.07 | 1.24 | 0.002 | 0.002 | 0.043 | 0.006 |
| RSD% | 39 | 67 | 148 | 46 | 9 | 15 | 65 | 72 | 38 |
| | | | | | | | | | |
| **MUSCOLO TOTALE** | | | | | | | | | |
| MEDIA | 1.08 | 0.03 | 4.25 | 8.56 | 13.71 | 0.011 | 0.004 | 0.049 | 0.021 |
| DS | 0.51 | 0.02 | 5.67 | 3.25 | 3.20 | 0.003 | 0.004 | 0.034 | 0.009 |
| RSD% | 47 | 66 | 133 | 38 | 23 | 27 | 92 | 70 | 43 |
| | | | | | | | | | |
| **EPATOPANCREAS MASCHIO** | | | | | | | | | |
| MEDIA | 16.79 | 0.60 | 19.62 | 17.84 | 28.98 | 0.035 | 0.101 | 0.114 | 0.011 |
| DS | 9.75 | 0.29 | 29.96 | 21.16 | 17.40 | 0.051 | 0.040 | 0.178 | 0.006 |
| RSD% | 58 | 48 | 153 | 119 | 60 | 145 | 39 | 155 | 52 |
| | | | | | | | | | |
| **EPATOPANCREAS FEMMINA** | | | | | | | | | |
| MEDIA | 9.32 | 0.36 | 5.10 | 11.16 | 19.41 | 0.023 | 0.128 | 0.084 | 0.015 |
| DS | 4.39 | 0.10 | 3.42 | 6.64 | 4.53 | 0.018 | 0.060 | 0.066 | 0.007 |
| RSD% | 47 | 29 | 67 | 60 | 23 | 81 | 47 | 80 | 48 |
| | | | | | | | | | |
| **EPATOPANCREAS TOTALE** | | | | | | | | | |
| MEDIA | 14.10 | 0.51 | 14.40 | 15.44 | 25.53 | 0.031 | 0.111 | 0.103 | 0.013 |
| DS | 8.98 | 0.26 | 25.05 | 17.69 | 14.91 | 0.043 | 0.050 | 0.148 | 0.007 |
| RSD% | 64 | 51 | 174 | 115 | 58 | 139 | 45 | 143 | 53 |
| | | | | | | | | | |
| LOD | 0.0002 | 0.00002 | 0.0028 | 0.0003 | 0.0063 | 0.00002 | 0.00003 | 0.00004 | 0.00004 |

Figure 3.12: Metals concentration in P. clarkii hepatopancreas and muscle tissues in Trasimeno Lake.

| mg/kg (ppm) | Mn | Co | Ni | Cu | Zn | Cd | Pb | Hg | As | Cr |
|---|---|---|---|---|---|---|---|---|---|---|
| **Muscle - Male** | | | | | | | | | | |
| Mean | 2.17 | 0.05 | 2.19 | 6.14 | 14.76 | 0.01 | 0.04 | 0.11 | 0.25 | 3.47 |
| Median | 2.37 | 0.04 | 0.80 | 6.00 | 14.15 | 0.01 | 0.03 | 0.10 | 0.23 | 1.19 |
| SD | 1.91 | 0.05 | 3.60 | 2.17 | 3.28 | 0.00 | 0.03 | 0.05 | 0.11 | 5.97 |
| RSD% | 87.82 | 93.74 | 164.21 | 35.29 | 22.22 | 52.53 | 98.32 | 51.60 | 43.29 | 171.97 |
| **Muscle- Female** | | | | | | | | | | |
| Mean | 1.74 | 0.05 | 2.43 | 7.53 | 16.21 | 0.01 | 0.05 | 0.13 | 0.20 | 3.76 |
| Median | 1.44 | 0.04 | 2.08 | 6.87 | 16.21 | 0.01 | 0.02 | 0.08 | 0.18 | 3.28 |
| SD | 1.50 | 0.03 | 1.97 | 1.71 | 2.87 | 0.01 | 0.09 | 0.10 | 0.06 | 3.21 |
| RSD% | 86.34 | 59.25 | 80.95 | 22.74 | 17.71 | 73.17 | 168.27 | 80.35 | 29.92 | 85.28 |
| **Muscle Total** | | | | | | | | | | |
| Mean | 2.02 | 0.05 | 2.28 | 6.63 | 15.28 | 0.01 | 0.04 | 0.11 | 0.23 | 3.58 |
| Median | 1.46 | 0.04 | 0.92 | 6.41 | 15.66 | 0.01 | 0.03 | 0.08 | 0.22 | 1.42 |
| SD | 1.77 | 0.04 | 3.09 | 2.11 | 3.19 | 0.00 | 0.06 | 0.07 | 0.10 | 5.12 |
| RSD% | 87.67 | 83.40 | 135.96 | 31.77 | 20.85 | 62.64 | 142.87 | 65.94 | 41.50 | 143.24 |
| **Hepatopancreas - Male** | | | | | | | | | | |
| Mean | 23.25 | 0.33 | 0.77 | 6.55 | 16.48 | 0.16 | 0.08 | 0.02 | 0.77 | 0.19 |
| Median | 12.81 | 0.20 | 0.60 | 6.68 | 12.43 | 0.14 | 0.07 | 0.02 | 0.75 | 0.03 |
| SD | 28.13 | 0.41 | 0.63 | 3.03 | 12.75 | 0.10 | 0.06 | 0.02 | 0.45 | 0.36 |
| RSD% | 120.97 | 124.80 | 81.72 | 46.23 | 77.33 | 63.03 | 66.51 | 82.37 | 58.32 | 190.32 |
| **Hepatopancreas - Female** | | | | | | | | | | |
| Mean | 11.70 | 0.30 | 0.67 | 10.48 | 23.28 | 0.17 | 0.30 | 0.05 | 0.72 | 0.23 |
| Median | 8.60 | 0.22 | 0.62 | 9.87 | 21.51 | 0.15 | 0.05 | 0.03 | 0.69 | 0.05 |
| SD | 11.18 | 0.18 | 0.31 | 2.90 | 8.36 | 0.11 | 0.47 | 0.04 | 0.24 | 0.33 |
| RSD% | 95.62 | 61.35 | 45.88 | 27.65 | 35.89 | 62.85 | 157.26 | 70.89 | 33.15 | 144.68 |
| **Hepatopancreas Total** | | | | | | | | | | |
| Mean | 19.02 | 0.32 | 0.73 | 7.99 | 18.97 | 0.16 | 0.17 | 0.03 | 0.75 | 0.20 |
| Median | 11.29 | 0.21 | 0.62 | 7.86 | 15.21 | 0.15 | 0.07 | 0.03 | 0.73 | 0.04 |
| SD | 23.88 | 0.34 | 0.53 | 3.51 | 11.70 | 0.10 | 0.30 | 0.03 | 0.38 | 0.34 |
| RSD% | 125.50 | 107.65 | 72.51 | 43.98 | 61.69 | 62.30 | 178.00 | 87.82 | 50.90 | 169.89 |
| **LOD** | 0.00004 | 0.000000004 | 0.00001 | 0.00001 | 0.00003 | 0.000001 | 0.000003 | 0.000002 | 0.000002 | 0.000004 |

Figure 3.13: Metals concentration in P. clarkii hepatopancreas and muscle tissues in Alviano Lake.

As seen in figure 3.14 both Ni and Cr are higher concentrated in muscle tissues, and higher concentrated in females compared to hepatopancreas and males, respectively. In figure 3.15 Hg shows significantly higher concentrations in muscle tissues, with higher concentration in females, while Cd shows significantly higher concentrations in hepatopancreas, with higher concentration in females. Figure 3.16 shows the concentrations of As, Co and Pb in both sexes and both tissues detected. As and Co are significantly higher concentrated in hepatopancreas, with higher concentration in males. However, although Pb is also significantly higher concentrated in hepatopancreas, higher concentration is observed in females compared to males. Moreover, as observed in figure 3.17 Cu and Zn are higher concentrated in hepatopancreas, with significantly higher concentration in female hepatopancreas compared to male hepatopancreas. Mn is significantly higher concentrations in hepatopancreas, with higher concentration in males.
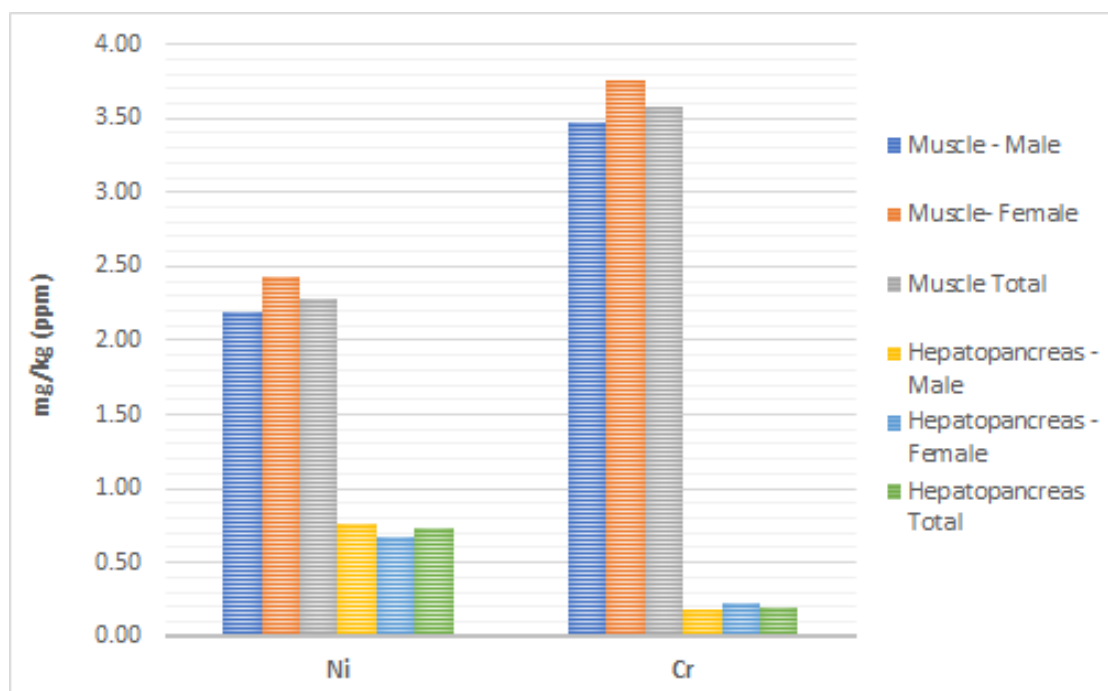
Figure 3.14: Concentrations of Ni and Cr in abdominal muscle tissues and hepatopancreas of P. clarkii in Alviano Lake.
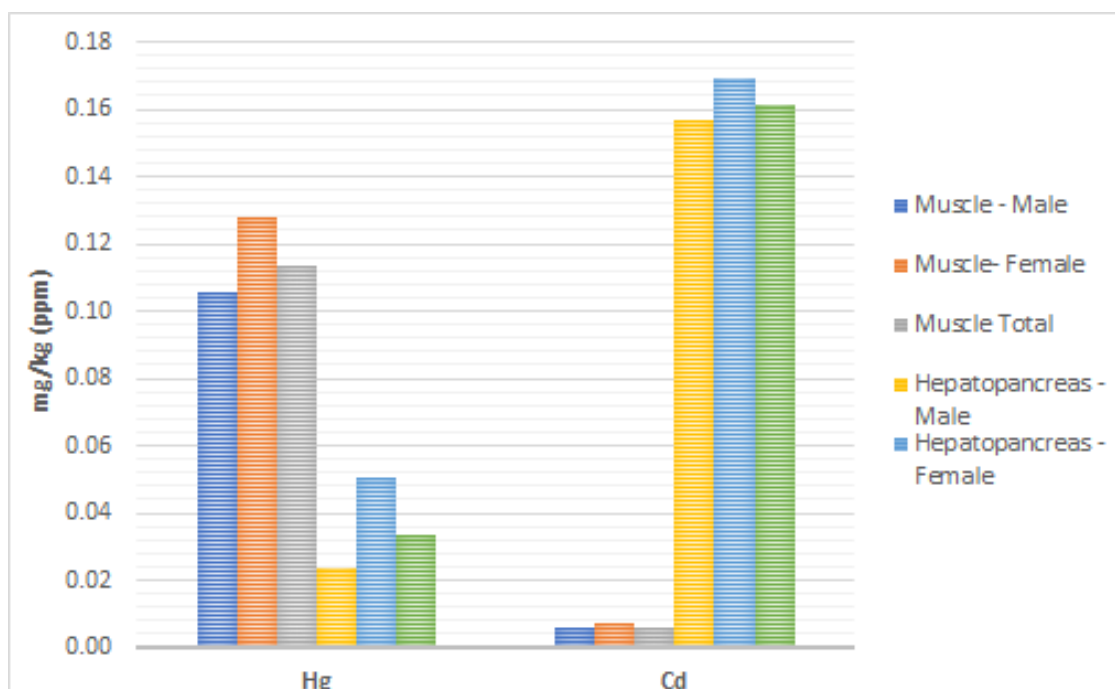


Figure 3.15: Concentrations of Hg and Cd in abdominal muscle tissues and hepatopancreas of P. clarkii in Alviano Lake.

37
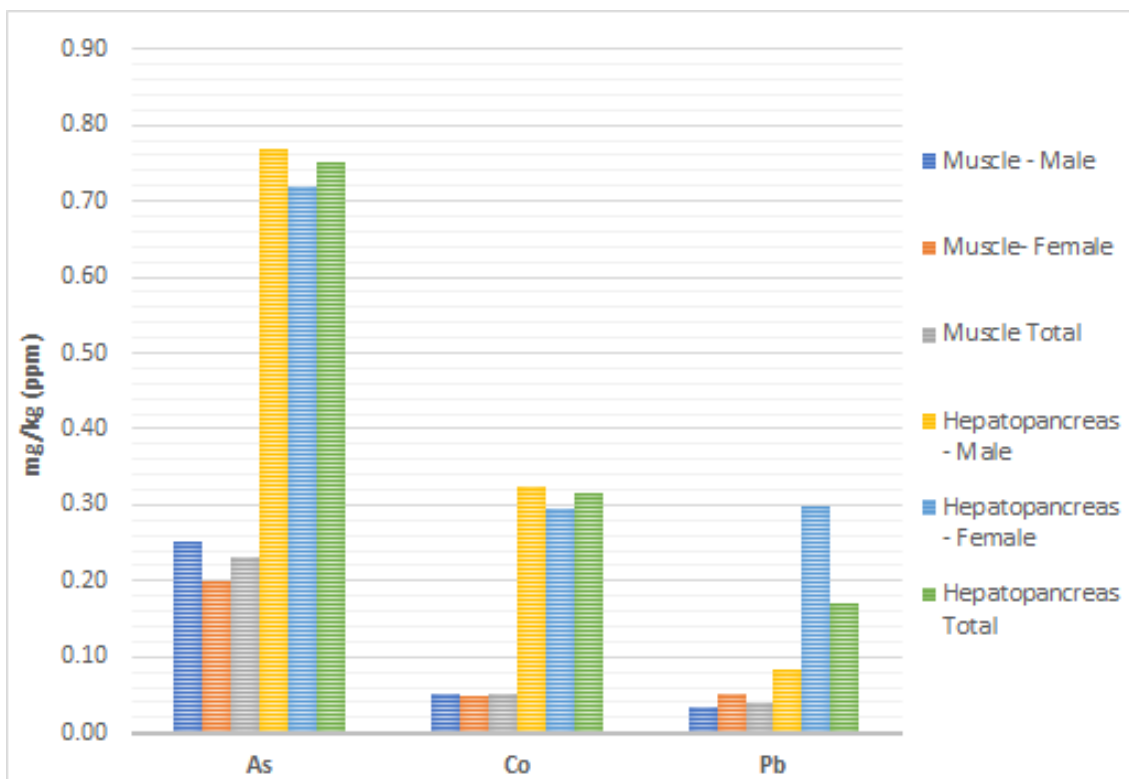
Figure 3.16: Concentrations of As, Co and Pb in abdominal muscle tissues and hepatopancreas of P. clarkii in Alviano Lake.
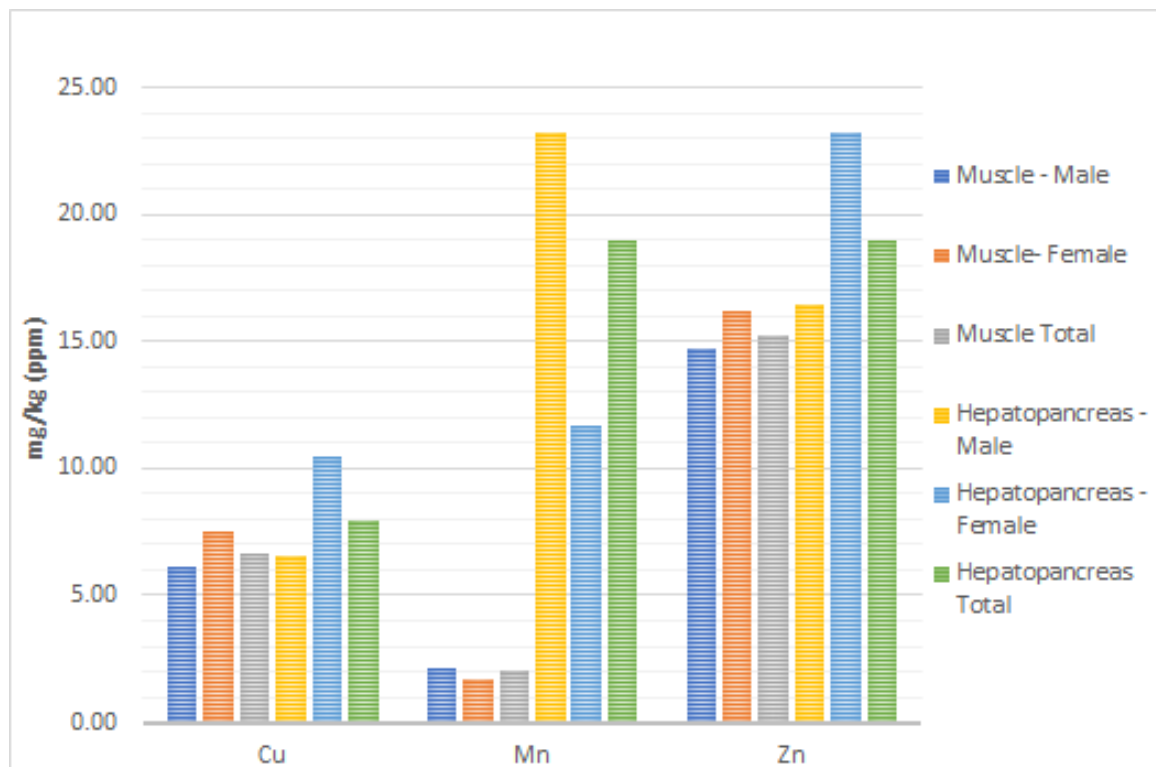


Figure 3.17: Concentrations of Cu, Mn and Zn in abdominal muscle tissues and hepatopancreas of P. clarkii in Alviano Lake.

38

In table 3.2, an examination of the total average concentration data shows that the levels of accumulation are always greater in the muscle tissue, which is know to reflect a chronic exposure to pollutant inputs, while hepatopancreas, major tissue for detoxification, is the organ that reflects short term contaminant exposure. Total mean concentrations decrease in the following order: Zn> Cu> Cr> Ni> Mn> As> Hg> Co> Pb> Cd in the muscle and Mn> Zn> Cu> As> Ni> Co> Cr> Pb> Cd> Hg in hepatopancreas.

Table 3.3: Mean values of elements accumulation in different tissues of the crayfish species P. clarkii.

| Species | Tissue | Order |
|---|---|---|
| *P. clarkii* | Muscle | Zn >Cu >Cr >Ni >Mn >As >Hg >Co >Pb >Cd |
| *P. clarkii* | Hepatopancreas | Mn >Zn >Cu >As >Ni >Co >Cr >Pb >Cd >Hg |

Table 3.4: Elements accumulation in different tissues of the crayfish species P.clarkii.

| Species | Sex | Tissue | Order |
|---|---|---|---|
| *P. clarkii* | Female | Muscle | Zn >Cu >Cr >Mn >As >Hg >Pb >Cd |
| *P. clarkii* | Male | Muscle | Zn >Cu >Cr >Mn >As >Hg >Pb >Cd |
| *P. clarkii* | Female | Hepatopancreas | Zn >Mn >Cu >As >Pb >Cr >Cd >Hg |
| *P. clarkii* | Male | Hepatopancreas | Mn >Zn >Cu >As >Cr >Cd >Pb >Hg |

As regards the trends with respect to sex, the average concentrations of metals in the muscle are almost equal and decrease as follows: Zn> Cu> Ni> Mn> Pb> Co> Hg> Ag> Cd in the muscle of male specimens and Zn> Cu > Ni> Mn> Pb> Co> Ag> Hg> Cd in that of females.

Differences in concentration are instead observed in the muscles with higher values in the tissues of female specimens with the exception of Ag and Hg which have higher concentrations in males. In the hepatopancreas the average concentrations of metals decrease in the following order: Zn> Ni> Cu> Mn> Co> Pb> Cd> Ag> Hg in males and Zn> Cu> Mn> Ni> Co> Cd> Pb> Ag> Hg in females.

The results obtained are generally comparable with the values reported in the literature. There are some exceptions with some of the studies reporting lower or higher values than those observed in this study, for the same species, which could be justified by the different geological nature and biovailability of the metals in the study area.

Finally, it should be noted that the average concentrations of mercury, cadmium and lead in the muscle and in the hepatopancreas for both genders are below the maximum permissible limits (0.5 mg / kg of fresh weight) prescribed by Regulation (EC) No. 1881/2006 and 2014.

| Standard's | Cu | Cr | Pb | Cd | Zn | Mn | Hg | As |
|---|---|---|---|---|---|---|---|---|
| WHO (1989) | 30 | 50 | 2 | 1 | 100 | 0.5-1 | – | |
| CFHC (1994) | 50 | 2 | 0.5 | 0.1 | 50 | – | 0.5 | 0.1 |
| FAO (1983) | 30 | – | 0.5 | 0.5 | 40 | – | 0.5 | 1.4 |
| HKG (1987) | | | | | | | 0.5 | 2.3 |
| USEPA (2000) | 120 | 8 | 4 | 2 | 120 | – | – | |
| EC (2014) | – | – | 0.3 | 0.5 | 30 | – | – | |
| FSSAI (2015) | – | – | 0.3 | 0.3 | – | – | – | |

Figure 3.18: Maximum Permissible Limit of trace metals in fish muscles (mg kg$^{-1}$) according to International Guideline values.

Additionally, in figure 3.18 the Maximum Permissible Limit (MPL) of trace metals in fish muscles according to International Guideline values is shown.In accordance with table 3.1 which presents the mean, median and standard deviation values of metals concentrations in crayfish tissues of this study, Mn reaches the Maximum Permissible Limit based on the World's Health Organization Standard. In contrast, both Cr and As exceed the MPL of Chinese Food Health Criterions Standard. Notably, the MPL of Hg, Cd and Pb based on EC/2006, is 0,5 pmm of fresh fish. So these elements concentrations in this study, even though are higher compared to the Trasimeno Lake results, they are not exceeding the MPL based on the European and Internaltional Standards.

Table 3.5: Mean, median and standard deviation (SD) values of metals concentrations (mg kg$^{-1}$) in P.clarkii hepatopancreas and muscle tissues.

| | | Cu | Zn | Mn | Cr | Cd | Pb | Hg | As |
|---|---|---|---|---|---|---|---|---|---|
| **Hepatopancreas** | **Mean** | 7.99 | 18.97 | 19.02 | 0.20 | 0.16 | 0.17 | 0.03 | 0.75 |
| | **Median** | 7.86 | 15.21 | 11.29 | 0.04 | 0.15 | 0.07 | 0.03 | 0.73 |
| | **SD** | 3.51 | 11.70 | 23.88 | 0.34 | 0.10 | 0.30 | 0.03 | 0.38 |
| **Abdominal muscle** | **Mean** | 6.63 | 15.28 | 2.02 | 3.58 | 0.01 | 0.04 | 0.11 | 0.23 |
| | **Median** | 6.41 | 15.66 | 1.46 | 1.42 | 0.01 | 0.03 | 0.08 | 0.22 |
| | **SD** | 2.11 | 3.19 | 1.77 | 5.12 | 0.00 | 0.06 | 0.07 | 0.10 |

Table 3.6 shows the total mean concentrations by gender, the median values, the standard deviation and the RSD% values of the metals detected in the abdominal muscle and hepatopancreas tissues of P. clarkii and the respective LODs. All metal concentrations are expressed in mg/kg of wet weight and each metal investigated has a defined instrumental detection limit (LOD).

40

Table 3.6: Mean (mg/kg) and median values by gender, the standard deviation,the RSD% and LOD values of metals in abdomincal muscle and hepatopancreas tissues.

| mg/kg (ppm) | Mn | Co | Ni | Cu | Zn | Cd | Pb | Hg | As | Cr |
|---|---|---|---|---|---|---|---|---|---|---|
| **Muscle - Male** | | | | | | | | | | |
| Mean | 2.17 | 0.05 | 2.19 | 6.14 | 14.76 | 0.01 | 0.04 | 0.11 | 0.25 | 3.47 |
| Median | 2.37 | 0.04 | 0.80 | 6.00 | 14.15 | 0.01 | 0.03 | 0.10 | 0.23 | 1.19 |
| SD | 1.91 | 0.05 | 3.60 | 2.17 | 3.28 | 0.00 | 0.03 | 0.05 | 0.11 | 5.97 |
| RSD% | 87.82 | 93.74 | 164.21 | 35.29 | 22.22 | 52.53 | 98.32 | 51.60 | 43.29 | 171.97 |
| **Muscle- Female** | | | | | | | | | | |
| Mean | 1.74 | 0.05 | 2.43 | 7.53 | 16.21 | 0.01 | 0.05 | 0.13 | 0.20 | 3.76 |
| Median | 1.44 | 0.04 | 2.08 | 6.87 | 16.21 | 0.01 | 0.02 | 0.08 | 0.18 | 3.28 |
| SD | 1.50 | 0.03 | 1.97 | 1.71 | 2.87 | 0.01 | 0.09 | 0.10 | 0.06 | 3.21 |
| RSD% | 86.34 | 59.25 | 80.95 | 22.74 | 17.71 | 73.17 | 168.27 | 80.35 | 29.92 | 85.28 |
| **Muscle Total** | | | | | | | | | | |
| Mean | 2.02 | 0.05 | 2.28 | 6.63 | 15.28 | 0.01 | 0.04 | 0.11 | 0.23 | 3.58 |
| Median | 1.46 | 0.04 | 0.92 | 6.41 | 15.66 | 0.01 | 0.03 | 0.08 | 0.22 | 1.42 |
| SD | 1.77 | 0.04 | 3.09 | 2.11 | 3.19 | 0.00 | 0.06 | 0.07 | 0.10 | 5.12 |
| RSD% | 87.67 | 83.40 | 135.96 | 31.77 | 20.85 | 62.64 | 142.87 | 65.94 | 41.50 | 143.24 |
| **Hepatopancreas - Male** | | | | | | | | | | |
| Mean | 23.25 | 0.33 | 0.77 | 6.55 | 16.48 | 0.16 | 0.08 | 0.02 | 0.77 | 0.19 |
| Median | 12.81 | 0.20 | 0.60 | 6.68 | 12.43 | 0.14 | 0.07 | 0.02 | 0.75 | 0.03 |
| SD | 28.13 | 0.41 | 0.63 | 3.03 | 12.75 | 0.10 | 0.06 | 0.02 | 0.45 | 0.36 |
| RSD% | 120.97 | 124.80 | 81.72 | 46.23 | 77.33 | 63.03 | 66.51 | 82.37 | 58.32 | 190.32 |
| **Hepatopancreas - Female** | | | | | | | | | | |
| Mean | 11.70 | 0.30 | 0.67 | 10.48 | 23.28 | 0.17 | 0.30 | 0.05 | 0.72 | 0.23 |
| Median | 8.60 | 0.22 | 0.62 | 9.87 | 21.51 | 0.15 | 0.05 | 0.03 | 0.69 | 0.05 |
| SD | 11.18 | 0.18 | 0.31 | 2.90 | 8.36 | 0.11 | 0.47 | 0.04 | 0.24 | 0.33 |
| RSD% | 95.62 | 61.35 | 45.88 | 27.65 | 35.89 | 62.85 | 157.26 | 70.89 | 33.15 | 144.68 |
| **Hepatopancreas Total** | | | | | | | | | | |
| Mean | 19.02 | 0.32 | 0.73 | 7.99 | 18.97 | 0.16 | 0.17 | 0.03 | 0.75 | 0.20 |
| Median | 11.29 | 0.21 | 0.62 | 7.86 | 15.21 | 0.15 | 0.07 | 0.03 | 0.73 | 0.04 |
| SD | 23.88 | 0.34 | 0.53 | 3.51 | 11.70 | 0.10 | 0.30 | 0.03 | 0.38 | 0.34 |
| RSD% | 125.50 | 107.65 | 72.51 | 43.98 | 61.69 | 62.30 | 178.00 | 87.82 | 50.90 | 169.89 |
| **LOD** | 0.00004 | 0.000000004 | 0.00001 | 0.00001 | 0.00003 | 0.000001 | 0.000003 | 0.000002 | 0.000002 | 0.000004 |

Furthermore, in figure 3.19, there is a comparison of the elemental concentrations in the muscle tissues between this study and studies from other regions. Generally, it is observed that Alviano Lake is not as contaminated as other areas, like Ebro river in Spain ([Hg] = 0,76-1,64 ppm), Chech Republic area ([Hg] = 1,18 ppm) and Luisiana in USA with Cu concentration as high as 204 ppm.

| Location | Sex | Tissue | Cu | Zn | Mn | Cr | Cd | Pb | Hg | As |
|---|---|---|---|---|---|---|---|---|---|---|
| *Present Study* | *Female* | *Muscle* | *7.53* | *16.21* | *1.74* | *3.76* | *0.01* | *0.05* | *0.13* | *0.20* |
| *Present Study* | *Female* | *Hepatopancreas* | *10.48* | *23.28* | *11.70* | *0.23* | *0.17* | *0.30* | *0.05* | *0.72* |
| *Present Study* | *Male* | *Muscle* | *6.14* | *14.76* | *2.17* | *3.47* | *0.01* | *0.04* | *0.11* | *0.25* |
| *Present Study* | *Male* | *Hepatopancreas* | *6.55* | *16.48* | *23.25* | *0.19* | *0.16* | *0.08* | *0.02* | *0.77* |
| *Czech Republic* | *-* | *Muscle* | *32.9* | *76.9* | *-* | *4.2* | *0.05* | *<0.5* | *1.18* | *-* |
| *Luisiana, USA* | *-* | *Muscle* | *31* | *61* | *-* | *-* | *0.06* | *4.5* | *-* | *0.2-3.7* |
| *Luisiana, USA* | *-* | *Gill* | *204* | *113* | *-* | *-* | *0.23* | *4.2* | *-* | *0.6-8.7* |
| *Ebro river, Spain* | *-* | *Muscle* | *12.1-82.3* | *49.2-127* | *1.7-2.6* | *-* | *0.03-0.41* | *0.22-3.1* | *0.76-1.64* | *12.1-82.3* |
| *Egypt* | *-* | *Muscle* | *32.7* | *125* | *-* | *5.1* | *-* | *15.9* | *-* | *-* |
| *South- Western Sicily, Italy* | *-* | *Muscle* | *17.3* | *74.9* | *-* | *0.81* | *-* | *0.2* | *-* | *-* |
| *California, USA* | *-* | *Muscle* | *44.6* | *76.9* | *-* | *0.43* | *-* | *0.2* | *-* | *0.7* |
| *China* | *-* | *Muscle* | *10.7* | *11.7* | *-* | *0.4* | *0.1* | *0.72* | *0.024* | *0.028* |

Figure 3.19: Comparison of elemental concentrations (mg kg$^{-1}$ dry weight) in the muscle tissues of P.clarkii from the present study with other regions.

41

## 3.3 Biochemical Analysis Results

Superoxide dismutase (SOD): is known to catalyze the dismutation of superoxide ($O_2^-$) to hydrogen peroxide ($H_2O_2$) and $O_2$. SOD is present in most aerobic organisms and is assumed to play a central role in providing defense against oxidative stress.

In the first graph 3.20 we observe that the SOD activity in hepatopancreas, is lower in summer and higher in autumn, both in males and females. Based also on the chemical analysis results, where we observed higher concentrations of Hg and other metals in summer, we could interpret that the decrease in SOD activity, in summer, is due to the presence of free radicals. In the second graph 3.21, compared to hepatopancreas results, we observe a more persistent decrease in the SOD activity in muscle, in both seasons, to both males and females. We could assume that this result is logical since muscle is a tissue that reflects chronic exposure, while hepatopancreas is the major tissue for detoxification.



Figure 3.20: Superoxide dismutase activity (mean values ±SD) in hepatopancreas of both sexes of P. clarkii. Different lower case letters indicate statistically significant differences among seasons (Two-way ANOVA with Tukey's multiple comparisons test $P<0.05$).
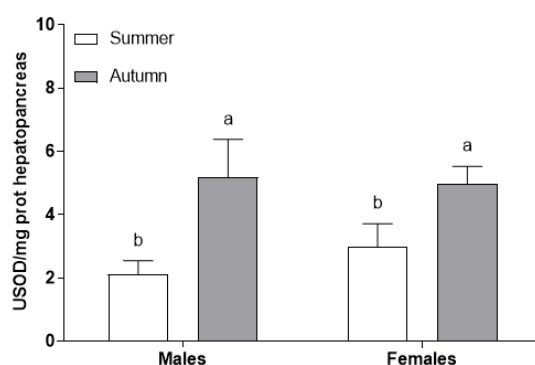


Figure 3.21: Superoxide dismutase activity (mean values ±SD) in muscle of both sexes of P. clarkii. Different lower case letters indicate statistically significant differences among seasons (Two-way ANOVA with Tukey's multiple comparisons test $P<0.05$).

42

Catalase is a common enzyme found in nearly all living organisms exposed to oxygen (such as bacteria, plants, and animals) which catalyzes the decomposition of hydrogen peroxide to water and oxygen. It is a very important enzyme in protecting the cell from oxidative damage by reactive oxygen species (ROS).

Similarly to SOD activity, the graph 3.22 shows that the CAT activity in hepatopancreas, is lower in summer and higher in autumn, both in males and females. Therefore, it would appear that, in summer, crayfishes, especially females, are subjected to more harmful effects of free radicals and lipid peroxidation. Continuously, the muscle graph 3.23, shows again a lower activity of CAT to both sexes and seasons compared to hepatopancreas.



Figure 3.22: Catalase activity (mean values ±SD) in hepatopancreas of both sexes of P. clarkii. Different lower case letters indicate statistically significant differences among seasons (Two-way ANOVA with Tukey's multiple comparisons test P<0.05).
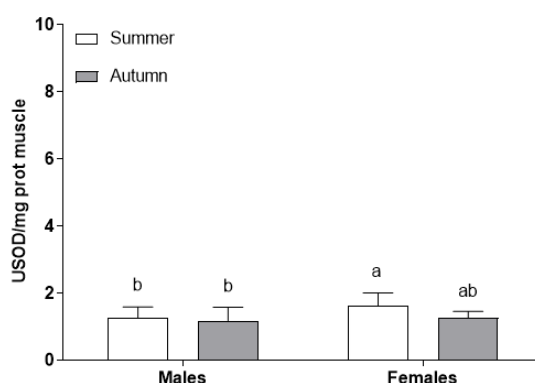


Figure 3.23: Catalase activity (mean values ±SD) in muscle of both sexes of P. clarkii. Different lower case letters indicate statistically significant differences among seasons (Two-way ANOVA with Tukey's multiple comparisons test P<0.05).

Glutathione peroxidase (GPx) is a cytosolic enzyme that catalyzes the reduction of hydrogen peroxide to water and oxygen as well as catalyzing the reduction of peroxide radicals to alcohols and oxygen.

43

As seen in graph 3.24, the GPx activity in hepatopancreas, is lower in summer and higher in autumn, both in males and females. Therefore, it would appear that crayfishes, especially females, are subjected to more harmful effects of free radicals and consequently to oxidative stress. As for the graph 3.25, in comparison with the graph 3.24, a smaller decrease in the GPx activity to both male and female muscle tissues is observed, between summer and autumn.
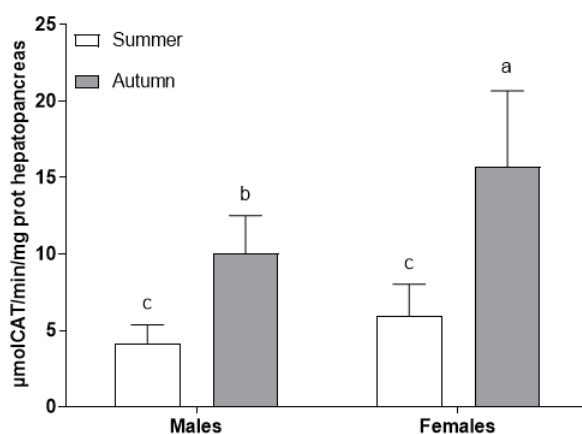


Figure 3.24: Glutathione peroxidase activity (mean values ±SD) in hepatopancreas of both sexes of P. clarkii. Different lower case letters indicate statistically significant differences among seasons (Two-way ANOVA with Tukey's multiple comparisons test $P<0.05$).
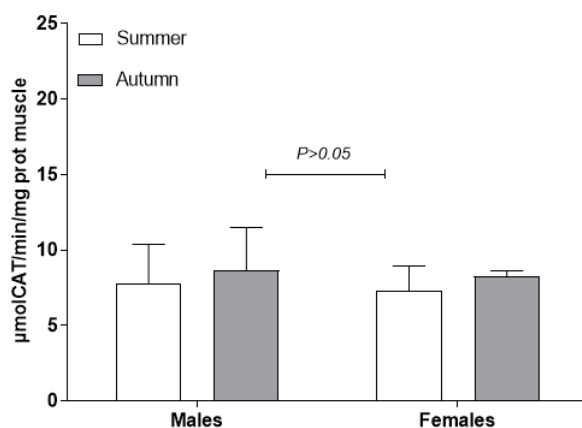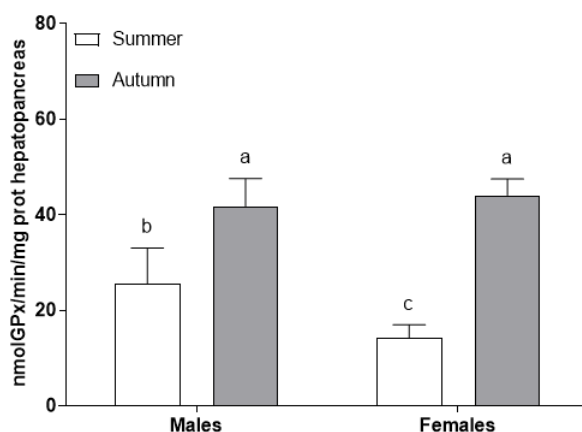


Figure 3.25: Glutathione peroxidase activity (mean values ±SD) in muscle of both sexes of P. clarkii. Different lower case letters indicate statistically significant differences among seasons (Two-way ANOVA with Tukey's multiple comparisons test $P<0.05$).

Glutathione S- transferase is best known for its ability to catalyze the conjugation of the reduced form of glutathione (GSH) to xenobiotic substrates for the purpose of detoxification.

Additionally, in the graph 3.26 the GST activity in hepatopancreas, is lower in summer and higher in autumn, both in males and females. So we could interpret that

44

the result of lower GST activity, in summer, is explained of a potential defense mechanism against free radicals. Similarly to the other enzymes activity, as seen in the muscle graph 3.27, a lower activity of GST is observed to both sexes and seasons compared to hepatopancreas.



Figure 3.26: Glutathione S- transferase activity (mean values ±SD) in hepatopancreas of both sexes of P. clarkii. Different lower case letters indicate statistically significant differences among seasons (Two-way ANOVA with Tukey's multiple comparisons test $P<0.05$).
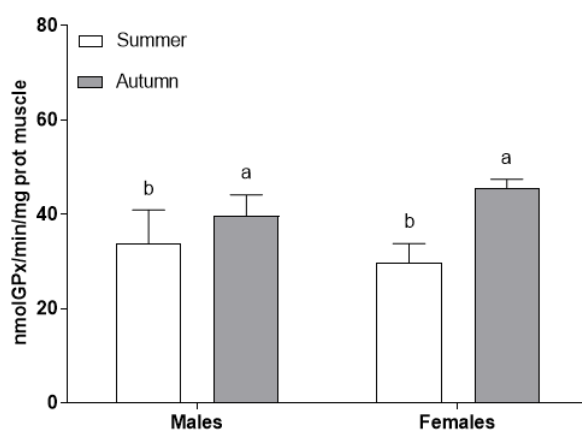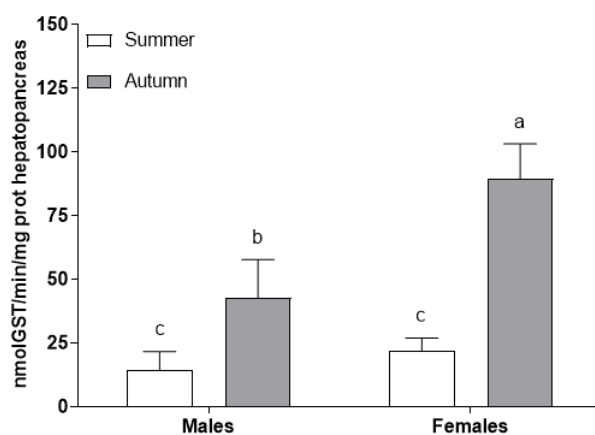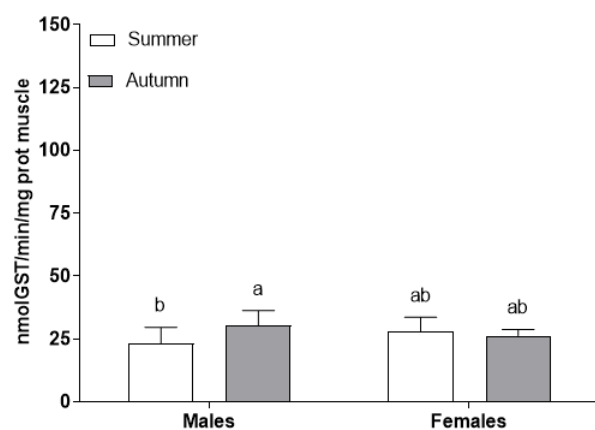


Figure 3.27: Glutathione S- transferase activity (mean values ±SD) in muscle of both sexes of P. clarkii. Different lower case letters indicate statistically significant differences among seasons (Two-way ANOVA with Tukey's multiple comparisons test $P<0.05$)..

As for the biochemical analysis results, in the hepatopancreas, all four biomarkers showed a decrease in the activity in summer, and an increase in autumn for both sexes, with bigger concentrations in females compared to males. Generally, in muscle tissues, even though there was not a significant difference among seasons and sexes,lower enzymes activities were observed compared to the activity in hepatopancreas.

The mode and action of chemicals, like heavy metals, play different role in the ac-

tion of antioxidant enzymes. Different researchers point out that metals decrease the antioxidant's activity which is time dependent, and it also depends on the study area and the animal model used. But, generally, lots of literature and experimental analysis proves that, the level of antioxidant enzyme decreases as the level of free radicals increase. Because decrease of antioxidant level means, increase of free radicals, which ultimately increase the oxidative stress.

So based on both chemical and biochemical analysis, the results are consistent with each other. In chemical analysis higher contamination was found in summer months, and this explains the decrease in biomarkers' activity, which are considered the first defense line against oxyradicals, which triggers an interdependent enzymes cascade that offsets oxidative stress.

Moreover, the invasive red swamp crayfish, Procambarus clarkii, poses a serious threat to native freshwater species, causing significant economic damage every year. The high ecological value, resistance to environmental stresses, plasticity of the reproductive cycle, aggressiveness, ability to locomotion and dispersion and parental care make its eradication almost impossible and successful only if the diffusion environment is very limited spatially. Consequently, in large lakes such as Alviano, its eradication does not seem possible to date. Currently, the only way to mitigate the adverse effects of this alien species on lake ecosystems is to implement containment maneuvers, mainly based on large-scale sampling. These actions have produced positive environmental implications, but also led to the reconversion of this invasive species into a resource of considerable economic value for the fish market and the food chain. In fact, both recreational and professional fishing is rapidly increasing and is expanding all over the world, thanks also to the high economic performance of this species.

For the red shrimp population, which has settled in Alviano for 20 years and difficult to eradicate, a feasible and economically convenient choice is to adopt a policy of containment and control of the population through fishing, as a source of income. additional for lake fishermen. The adequate assessment of the chemical contamination of meat is therefore crucial for the maintenance and implementation of production, in order to support the seafood sector with a product of excellent quality and high commercial value.

The reported dataset from the present study clearly documents that the muscle tissue is the main storage organs for analyzed elements in the P.clarkii species followed by walking leg and abdominal muscle tissues. Compared to the international (WHO/-FAO) fishery products guidelines the accumulation of elements in the muscle tissues of crayfish were below the maximum permissible limits (0.5 mg / kg of fresh weight) prescribed by the regulation, (EC) No. 1881/2006, with few exceptions and considered safe for human consumption by avoiding the muscle tissues because these tissues contains elevated concentration of As, Mn and Cr. Since, the crayfish is an invasive species and have the capacity to tolerate high level of metal content compared to the native species. The both analyzed species from the study area can be consumed safely by humans and it can be used as a sentinel species for assessing the heavy metals contamination in freshwater ecosystems and culturing areas.

This study represents a first monitoring of the metal accumulaton in P. clarkii in the Alviano Lake. In the later stages of this research, you will need:

1. increase the number of samples analyzed,

2. extend the sampling area to other sites in order to have more data available,

3. use comparison populations also from other continents and already available in the literature.

# Bibliography

[1] Schroeder, W. H., K. Anlauf, L. A. Barrie, J. Y. Lu, A. Steffen,D. R. Schneeberger, and T, Berg. 1998. Arctic springtime depletion of mercury. Nature 394: 331–332.

[2] Lin C.and Pehkonen, S.O. 1999. The chemistry of atmospheric mercury: a review. Atmospheric Environment,33: 2067–2079.

[3] Boudou, A., and F. Ribeyre. 1997. Mercury in the food web: accumulation and transfer mechanisms, in metal ions in biological systems, Vol. 34, Mercury and Its Effects on Environment and Biology, Sigel, A. and Sigel, H., Eds., Marcel Dekker, New York, 1997, 289–319.

[4] United Nations Environment Programme. "Chapter 7: current production and use of mercury." in Global Mercury Assessment. pp. 117–134. Geneva, Switzerland: UNEP Chemicals, 2002. http://new.unep.org/gc/gc22/Document/UNEP-GC22-INF3.pdf (accessed February 5,2008).

[5] Chen, C., A. Amirbahman, N. Fisher, G. Harding, C. Lamborg, D. Nacci, and D. Taylor. 2008. Methylmercury in Marine Ecosystems: Spatial Patterns and Processes of Production, Bioaccumulation, and Biomagnification. EcoHealth doi:10.1007/s10393-008-0201-1.

[6] Fitzgerald, W. F., C. H. Lamborg, and C. R. Hammerschmidt. 2007. Marine biogeochemical cycling of mercury. Chemical Reviews 107: 641–662.

[7] Landis, M. S., R. K. Stevens, F. Schaedlich, and E. M. Prestbo. 2002. Development and characterization of an annular denuder methodology for the measurement of divalent inorganic reactive gaseous mercury in ambient air. Environmental Science and Technology 36: 3000–3009.

[8] Adriano, D. C. (2001). Trace elements in terrestrial environments. New York: Springer-Verlag. Agnan, Y., Le Dantec, T., Moore, C. W., Edwards, G. C., and Obrist, D. (2016). New Constraints on Terrestrial Surface¡Atmosphere Fluxes of Gaseous Elemental Mercury Using a Global Database. Environ. Sci. Technol. 50:507–524.

[9] Hazen, R. M., Golden, J., Downs, R. T., Hystad, G., Grew, E. S., Azzolini, D., and Sverjensky, D.A. (2012). Mercury (Hg) mineral evolution: A mineralogical record of supercontinent assembly, changing ocean geochemistry, and the emerging terrestrial biosphere. Am. Miner.97:1013–1042.

[10] Gilmour CC, Riedel GS, Ederington MC, Bell JT, Benoit JM, et al. 1998. Methylmercury concentrations and production rates across a trophic gradient in the northern everglades. Biogeochemistry 40:327–45

[11] Benoit JM, Gilmour CC, Heyes A, Mason RP, Miller C. 2003. Geochemical and biological controls over methylmercury production and degradation in aquatic ecosystems. In ACS Symp. Ser. 835, ed. Y Chai, OC Braids, pp. 262–97.Washington, DC: Am. Chem. Soc.

[12] Kerin EJ, Gilmour CC, Roden E, Suzuki MT, Coates JD, Mason RP. 2006. Mercury methylation by dissimilatory iron-reducing bacteria. Appl. Environ. Microbiol. 72:7919

[13] Website:Lago di Alviano | WWF Italy

[14] Alcorlo, P., Otero, M., Crehuet, M., Baltanás, A., Montes, C., 2006. The use of the red swamp crayfish (Procambarus clarkii, Girard) as indicator of the bioavailability of heavy metals in environmental monitoring in the River Guadiamar (SW, Spain). Sci. Total Environ. 366 (1), 380–390. https://doi.org/10.1016/j.scitotenv.2006.02.023.

[15] Suárez-Serrano, A., Alcaraz, C., Ibáñez, C., Trobajo, R., Barata, C., 2010. Procambarus clarkii as a bioindicator of heavy metal pollution sources in the lower Ebro River and Delta. Ecotoxicol. Environ. Saf. 73 (3), 280–286. https://doi.org/10.1016/j.ecoenv.2009.11.001.

[16] Gedik, K., Kongchum, M., DeLaune, R.D., Sonnier, J.J., 2017. Distribution of arsenic and other metals in crayfish tissues (Procambarus clarkii) under different production practices. Sci. Total Environ. 574, 322–331. https://doi.org/10.1016/j.scitotenv.2016.09.060.

[17] Gherardi, F., 2006. Crayfish invading Europe: the case study of Procambarus clarkii. Mar. Freshw. Behav. Physiol. 39 (3), 175–191. https://doi.org/10.1080/10236240600869702.

[18] Handbook of ICP-QQQ Applications using the Agilent 8800 and 8900 - 4th Edition

[19] Halliwell B, Gutteridge JMC, editors. Free radicals in biology and medicine. Third ed. Oxford: Oxford Science Publications; 2000.p. 617– 24.

[20] Thomas CE, Morehouse LA, Aust SD. Ferritin and superoxide-dependent lipid peroxidation. J Biol Chem 1995;260(6):3275– 80.

[21] Young IS, Woodside JV. Antioxidants in health and disease. J Clin Pathol 2001;54:176–86.

[22] Livingstone, David W. "Adults' informal learning: Definitions, findings, gaps and future research." (2001).

[23] Meister, Alton, and Mary E. Anderson. "Glutathione." Annual review of biochemistry 52.1 (1983): 711-760.

[24] Lowry, Oliver H., et al. "Protein measurement with the Folin phenol reagent." Journal of biological chemistry 193 (1951): 265-275.

[25] McCord, Joe M., and Irwin Fridovich. "Superoxide dismutase: an enzymic function for erythrocuprein (hemocuprein)." Journal of Biological chemistry 244.22 (1969): 6049-6055.

[26] Pacini, Nicole, et al. "Antioxidant response versus selenium accumulation in the liver and kidney of the Siberian sturgeon (Acipenser baeri)." Chemosphere 93.10 (2013): 2405-2412.

[27] Beutler, B., et al. "Identity of tumour necrosis factor and the macrophage-secreted factor cachectin." Nature 316.6028 (1985): 552-554.

[28] Lawrence, Richard A., and Raymond F. Burk. "Glutathione peroxidase activity in selenium-deficient rat liver." Biochemical and biophysical research communications 71.4 (1976): 952-958.

[29] Akerboom, Theodorus PM, and Helmut Sies. "[48] Assay of glutathione, glutathione disulfide, and glutathione mixed disulfides in biological samples." Methods in enzymology. Vol. 77. Academic Press, 1981. 373-382.

[30] Wickham, Hadley, and Garrett Grolemund. R for data science: import, tidy, transform, visualize, and model data. " O'Reilly Media, Inc.", 2016.

# Appendix A

# Tables

## A.1 Female Data

Table A.1: Elements concentrations(mg/kg) in female hepatopancreas and muscle tissues.

| Sample Name | Sex | Tissue | Ca | Cd | Co | Cr | Cs | Cu | Fe [He] | Fe [O2] |
|---|---|---|---|---|---|---|---|---|---|---|
| ALV. 1 F 6.19 M1 | F | m | 307,665 | 0,022 | 0,106 | 3,997 | 0,012 | 10,380 | 30,718 | 30,491 |
| ALV. 1 F 6.19 M2 | F | m | 98,673 | 0,012 | 0,088 | 5,814 | 0,026 | 5,831 | 29,749 | 39,635 |
| ALV. 1 F 6.19 M3 | F | m | 65,996 | 0,004 | 0,109 | 12,515 | 0,029 | 5,433 | 44,602 | 59,357 |
| ALV. 1 F 6.19 M4 | F | m | 95,300 | 0,004 | 0,017 | 0,049 | 0,019 | 8,751 | 10,383 | 8,444 |
| ALV. 1 F 8.19 M1 | F | m | 141,475 | 0,011 | 0,038 | 1,736 | 0,015 | 9,562 | 25,635 | 23,871 |
| ALV. 1 F 8.19 M2 | F | m | 137,562 | 0,010 | 0,035 | 1,610 | 0,012 | 7,596 | 16,334 | 16,550 |
| ALV. 1 F 8.19 M3 | F | m | 145,460 | 0,003 | 0,030 | 2,468 | 0,011 | 6,036 | 17,514 | 16,890 |
| ALV. 2 F 7.19 M1 | F | m | 140,277 | 0,007 | 0,039 | 0,112 | 0,030 | 10,302 | 8,534 | 9,402 |
| ALV. 2 F 7.19 M2 | F | m | 188,203 | 0,003 | 0,024 | 0,912 | 0,041 | 6,410 | 13,406 | 14,030 |
| ALV. 2 F 8.19 M1 | F | m | 109,581 | 0,003 | 0,032 | 1,203 | 0,012 | 7,893 | 10,686 | 8,451 |
| ALV. 2 F 8.19 M2 | F | m | 125,025 | 0,005 | 0,029 | 3,443 | 0,031 | 5,653 | 21,479 | 21,166 |
| ALV. 2 F 9.19 M1 | F | m | 130,952 | 0,003 | 0,035 | 5,255 | 0,016 | 6,577 | 36,267 | 35,504 |
| ALV. 2 F 9.19 M2 | F | m | 288,097 | 0,007 | 0,059 | 5,504 | 0,023 | 9,841 | 51,207 | 50,313 |
| ALV. 2 F 9.19 M3 | F | m | 135,104 | 0,004 | 0,072 | 7,514 | 0,017 | 6,790 | 39,500 | 40,513 |
| ALV. 2 F 9.19 M4 | F | m | 162,807 | 0,005 | 0,046 | 4,930 | 0,015 | 6,521 | 26,903 | 26,493 |
| ALV. 2 F 9.19 M5 | F | m | 208,217 | 0,007 | 0,028 | 3,114 | 0,014 | 6,950 | 22,091 | 19,817 |
| ALV. 1 F 6.19 E2 | F | h | 218,074 | 0,504 | 0,616 | 0,400 | 0,007 | 14,766 | 1118,963 | 1543,630 |
| ALV. 1 F 6.19 E3 | F | h | 87,393 | 0,142 | 0,413 | 1,174 | 0,010 | 11,417 | 173,011 | 227,689 |
| ALV. 1 F 6.19 E4 | F | h | 161,017 | 0,063 | 0,112 | 0,048 | 0,005 | 8,150 | 153,528 | 129,144 |
| ALV. 1 F 8.19 E1 | F | h | 287,987 | 0,207 | 0,211 | 0,050 | 0,004 | 14,531 | 387,855 | 434,913 |
| ALV. 1 F 8.19 E2 | F | h | 287,696 | 0,179 | 0,210 | 0,109 | 0,007 | 9,144 | 296,623 | 348,401 |
| ALV. 1 F 8.19 E3 | F | h | 298,704 | 0,136 | 0,215 | 0,042 | 0,006 | 9,733 | 401,979 | 462,004 |
| ALV. 2 F 7.19 E1 | F | h | 675,000 | 0,198 | 0,772 | 0,341 | 0,010 | 7,864 | 469,638 | 594,374 |
| ALV. 2 F 7.19 E2 | F | h | 351,427 | 0,065 | 0,312 | 0,733 | 0,017 | 10,031 | 1057,043 | 1382,928 |
| ALV. 2 F 8.19 E1 | F | h | 142,389 | 0,137 | 0,347 | 0,013 | 0,005 | 10,469 | 328,712 | 365,345 |
| ALV. 2 F 8.19 E2 | F | h | 219,546 | 0,055 | 0,162 | 0,040 | 0,008 | 7,166 | 372,053 | 417,393 |
| ALV. 2 F 9.19 E1 | F | h | 473,226 | 0,212 | 0,197 | 0,050 | 0,007 | 12,405 | 734,054 | 838,934 |
| ALV. 2 F 9.19 E2 | F | h | 271,717 | 0,212 | 0,294 | 0,038 | 0,008 | 9,055 | 770,273 | 822,785 |
| ALV. 2 F 9.19 E3 | F | h | 236,198 | 0,119 | 0,210 | 0,054 | 0,011 | 16,201 | 132,195 | 144,987 |
| ALV. 2 F 9.19 E4 | F | h | 377,347 | 0,164 | 0,247 | 0,053 | 0,008 | 9,868 | 526,505 | 574,479 |
| ALV. 2 F 9.19 E5 | F | h | 330,964 | 0,148 | 0,134 | 0,267 | 0,007 | 6,341 | 552,713 | 608,795 |

53

Table A.2: Elements concentrations(mg/kg) in female hepatopancreas and muscle tissues.

| Sample Name | Sex | Tissue | Ca | Cd | Co | Cr | Cs | Cu | Fe [He] | Fe [O2] |
|---|---|---|---|---|---|---|---|---|---|---|
| ALV. 1 F 6.19 M1 | F | m | 307.665 | 0.022 | 0.106 | 3.997 | 0.012 | 10.380 | 30.718 | 30.491 |
| ALV. 1 F 6.19 M2 | F | m | 98.673 | 0.012 | 0.088 | 5.814 | 0.026 | 5.831 | 29.749 | 39.635 |
| ALV. 1 F 6.19 M3 | F | m | 65.996 | 0.004 | 0.109 | 12.515 | 0.029 | 5.433 | 44.602 | 59.357 |
| ALV. 1 F 6.19 M4 | F | m | 95.300 | 0.004 | 0.017 | 0.049 | 0.019 | 8.751 | 10.383 | 8.444 |
| ALV. 1 F 8.19 M1 | F | m | 141.475 | 0.011 | 0.038 | 1.736 | 0.015 | 9.562 | 25.635 | 23.871 |
| ALV. 1 F 8.19 M2 | F | m | 137.562 | 0.010 | 0.035 | 1.610 | 0.012 | 7.596 | 16.334 | 16.550 |
| ALV. 1 F 8.19 M3 | F | m | 145.460 | 0.003 | 0.030 | 2.468 | 0.011 | 6.036 | 17.514 | 16.890 |
| ALV. 2 F 7.19 M1 | F | m | 140.277 | 0.007 | 0.039 | 0.112 | 0.030 | 10.302 | 8.534 | 9.402 |
| ALV. 2 F 7.19 M2 | F | m | 188.203 | 0.003 | 0.024 | 0.912 | 0.041 | 6.410 | 13.406 | 14.030 |
| ALV. 2 F 8.19 M1 | F | m | 109.581 | 0.003 | 0.032 | 1.203 | 0.012 | 7.893 | 10.686 | 8.451 |
| ALV. 2 F 8.19 M2 | F | m | 125.025 | 0.005 | 0.029 | 3.443 | 0.031 | 5.653 | 21.479 | 21.166 |
| ALV. 2 F 9.19 M1 | F | m | 130.952 | 0.003 | 0.035 | 5.255 | 0.016 | 6.577 | 36.267 | 35.504 |
| ALV. 2 F 9.19 M2 | F | m | 288.097 | 0.007 | 0.059 | 5.504 | 0.023 | 9.841 | 51.207 | 50.313 |
| ALV. 2 F 9.19 M3 | F | m | 135.104 | 0.004 | 0.072 | 7.514 | 0.017 | 6.790 | 39.500 | 40.513 |
| ALV. 2 F 9.19 M4 | F | m | 162.807 | 0.005 | 0.046 | 4.930 | 0.015 | 6.521 | 26.903 | 26.493 |
| ALV. 2 F 9.19 M5 | F | m | 208.217 | 0.007 | 0.028 | 3.114 | 0.014 | 6.950 | 22.091 | 19.817 |
| ALV. 1 F 6.19 E2 | F | h | 218.074 | 0.504 | 0.616 | 0.400 | 0.007 | 14.766 | 1118.963 | 1543.630 |
| ALV. 1 F 6.19 E3 | F | h | 87.393 | 0.142 | 0.413 | 1.174 | 0.010 | 11.417 | 173.011 | 227.689 |
| ALV. 1 F 6.19 E4 | F | h | 161.017 | 0.063 | 0.112 | 0.048 | 0.005 | 8.150 | 153.528 | 129.144 |
| ALV. 1 F 8.19 E1 | F | h | 287.987 | 0.207 | 0.211 | 0.050 | 0.004 | 14.531 | 387.855 | 434.913 |
| ALV. 1 F 8.19 E2 | F | h | 287.696 | 0.179 | 0.210 | 0.109 | 0.007 | 9.144 | 296.623 | 348.401 |
| ALV. 1 F 8.19 E3 | F | h | 298.704 | 0.136 | 0.215 | 0.042 | 0.006 | 9.733 | 401.979 | 462.004 |
| ALV. 2 F 7.19 E1 | F | h | 675.000 | 0.198 | 0.772 | 0.341 | 0.010 | 7.864 | 469.638 | 594.374 |
| ALV. 2 F 7.19 E2 | F | h | 351.427 | 0.065 | 0.312 | 0.733 | 0.017 | 10.031 | 1057.043 | 1382.928 |
| ALV. 2 F 8.19 E1 | F | h | 142.389 | 0.137 | 0.347 | 0.013 | 0.005 | 10.469 | 328.712 | 365.345 |
| ALV. 2 F 8.19 E2 | F | h | 219.546 | 0.055 | 0.162 | 0.040 | 0.008 | 7.166 | 372.053 | 417.393 |
| ALV. 2 F 9.19 E1 | F | h | 473.226 | 0.212 | 0.197 | 0.050 | 0.007 | 12.405 | 734.054 | 838.934 |
| ALV. 2 F 9.19 E2 | F | h | 271.717 | 0.212 | 0.294 | 0.038 | 0.008 | 9.055 | 770.273 | 822.785 |
| ALV. 2 F 9.19 E3 | F | h | 236.198 | 0.119 | 0.210 | 0.054 | 0.011 | 16.201 | 132.195 | 144.987 |
| ALV. 2 F 9.19 E4 | F | h | 377.347 | 0.164 | 0.247 | 0.053 | 0.008 | 9.868 | 526.505 | 574.479 |
| ALV. 2 F 9.19 E5 | F | h | 330.964 | 0.148 | 0.134 | 0.267 | 0.007 | 6.341 | 552.713 | 608.795 |

Table A.3: Elements concentrations(mg/kg) in female hepatopancreas and muscle tissues.

| Sample Name | Sex | Tissue | Ga | K | Li | Mg | Mn | Na | Ni | P |
|---|---|---|---|---|---|---|---|---|---|---|
| ALV. 1 F 6.19 M1 | F | m | 0,0053 | 1584,819 | <DL | 334,796 | 6,909 | 1601,710 | 2,494 | 1646,518 |
| ALV. 1 F 6.19 M2 | F | m | 0,0033 | 1504,490 | <DL | 292,828 | 1,589 | 671,328 | 4,283 | 1533,789 |
| ALV. 1 F 6.19 M3 | F | m | 0,0063 | 2100,710 | <DL | 328,776 | 2,463 | 785,831 | 7,636 | 1980,472 |
| ALV. 1 F 6.19 M4 | F | m | 0,0010 | 26483,080 | 0,070 | 285,703 | 2,038 | 749,395 | 0,172 | 2173,706 |
| ALV. 1 F 8.19 M1 | F | m | 0,0011 | 27795,556 | 0,029 | 277,957 | 1,221 | 579,716 | 1,293 | 1978,889 |
| ALV. 1 F 8.19 M2 | F | m | 0,0002 | 24007,383 | <DL | 228,352 | 1,451 | 778,360 | 1,166 | 1940,612 |
| ALV. 1 F 8.19 M3 | F | m | 0,0013 | 23110,835 | 0,022 | 222,930 | 0,724 | 540,754 | 1,583 | 1818,249 |
| ALV. 2 F 7.19 M1 | F | m | 0,0006 | 2557,827 | <DL | 535,250 | 0,780 | 988,328 | 0,205 | 2419,830 |
| ALV. 2 F 7.19 M2 | F | m | 0,0038 | 1836,383 | <DL | 386,441 | 0,847 | 1147,025 | 0,603 | 1635,544 |
| ALV. 2 F 8.19 M1 | F | m | 0,0009 | 30494,693 | <DL | 309,808 | 0,600 | 562,641 | 0,808 | 2143,246 |
| ALV. 2 F 8.19 M2 | F | m | 0,0021 | 26402,240 | <DL | 255,146 | 0,874 | 525,995 | 2,215 | 2218,332 |
| ALV. 2 F 9.19 M1 | F | m | 0,0050 | 22615,685 | 0,006 | 252,203 | 2,143 | 580,674 | 3,108 | 1864,456 |
| ALV. 2 F 9.19 M2 | F | m | 0,0098 | 26540,681 | 0,064 | 311,108 | 2,249 | 684,828 | 3,578 | 2128,868 |
| ALV. 2 F 9.19 M3 | F | m | 0,0044 | 25972,822 | 0,152 | 273,220 | 1,540 | 674,495 | 4,741 | 2467,033 |
| ALV. 2 F 9.19 M4 | F | m | 0,0023 | 17331,004 | 0,108 | 217,137 | 1,428 | 669,279 | 3,021 | 1565,366 |
| ALV. 2 F 9.19 M5 | F | m | 0,0009 | 26442,831 | 0,062 | 296,960 | 0,928 | 741,076 | 1,936 | 1986,936 |
| ALV. 1 F 6.19 E2 | F | h | 0,0036 | 1220,968 | 0,019 | 263,253 | 46,205 | 1140,910 | 0,991 | 1072,016 |
| ALV. 1 F 6.19 E3 | F | h | 0,0027 | 726,635 | <DL | 112,685 | 11,735 | 498,383 | 1,003 | 676,769 |
| ALV. 1 F 6.19 E4 | F | h | 0,0033 | 12696,551 | 0,309 | 113,237 | 18,863 | 816,790 | 1,275 | 823,650 |
| ALV. 1 F 8.19 E1 | F | h | 0,0013 | 17587,287 | <DL | 160,190 | 11,515 | 472,063 | 0,620 | 1085,984 |
| ALV. 1 F 8.19 E2 | F | h | 0,0038 | 13630,033 | <DL | 134,729 | 22,493 | 609,322 | 0,518 | 831,605 |
| ALV. 1 F 8.19 E3 | F | h | 0,0038 | 12872,244 | 0,091 | 149,495 | 5,439 | 590,992 | 0,671 | 987,921 |
| ALV. 2 F 7.19 E1 | F | h | 0,0095 | 745,673 | <DL | 214,528 | 11,295 | 550,726 | 1,149 | 824,606 |
| ALV. 2 F 7.19 E2 | F | h | 0,0018 | 1087,470 | <DL | 340,406 | 6,284 | 936,591 | 0,565 | 1251,514 |
| ALV. 2 F 8.19 E1 | F | h | 0,0014 | 12052,424 | 0,040 | 116,621 | 2,789 | 386,453 | 0,380 | 1066,305 |
| ALV. 2 F 8.19 E2 | F | h | 0,0027 | 11021,891 | <DL | 143,505 | 4,829 | 415,548 | 0,425 | 926,141 |
| ALV. 2 F 9.19 E1 | F | h | 0,0027 | 15517,509 | 0,060 | 281,303 | 12,496 | 657,549 | 0,238 | 1742,595 |
| ALV. 2 F 9.19 E2 | F | h | 0,0010 | 11766,867 | 0,073 | 204,182 | 8,179 | 462,289 | 0,511 | 1541,316 |
| ALV. 2 F 9.19 E3 | F | h | 0,0012 | 15088,090 | 0,027 | 182,084 | 2,366 | 571,097 | 0,764 | 1182,729 |
| ALV. 2 F 9.19 E4 | F | h | 0,0099 | 13473,606 | 0,127 | 237,615 | 8,601 | 759,683 | 0,617 | 1148,813 |
| ALV. 2 F 9.19 E5 | F | h | 0,0013 | 12497,303 | <DL | 219,856 | 2,344 | 470,028 | 0,335 | 1350,366 |

Table A.4: Elements concentrations(mg/kg) in female hepatopancreas and muscle tissues.

| Sample Name | Sex | Tissue | Ga | K | Li | Mg | Mn | Na | Ni | P |
|---|---|---|---|---|---|---|---|---|---|---|
| ALV. 1 F 6.19 M1 | F | m | 0,0053 | 1584,819 | <DL | 334,796 | 6,909 | 1601,710 | 2,494 | 1646,518 |
| ALV. 1 F 6.19 M2 | F | m | 0,0033 | 1504,490 | <DL | 292,828 | 1,589 | 671,328 | 4,283 | 1533,789 |
| ALV. 1 F 6.19 M3 | F | m | 0,0063 | 2100,710 | <DL | 328,776 | 2,463 | 785,831 | 7,636 | 1980,472 |
| ALV. 1 F 6.19 M4 | F | m | 0,0010 | 26483,080 | 0,070 | 285,703 | 2,038 | 749,395 | 0,172 | 2173,706 |
| ALV. 1 F 8.19 M1 | F | m | 0,0011 | 27795,556 | 0,029 | 277,957 | 1,221 | 579,716 | 1,293 | 1978,889 |
| ALV. 1 F 8.19 M2 | F | m | 0,0002 | 24007,383 | <DL | 228,352 | 1,451 | 778,360 | 1,166 | 1940,612 |
| ALV. 1 F 8.19 M3 | F | m | 0,0013 | 23110,835 | 0,022 | 222,930 | 0,724 | 540,754 | 1,583 | 1818,249 |
| ALV. 2 F 7.19 M1 | F | m | 0,0006 | 2557,827 | <DL | 535,250 | 0,780 | 988,328 | 0,205 | 2419,830 |
| ALV. 2 F 7.19 M2 | F | m | 0,0038 | 1836,383 | <DL | 386,441 | 0,847 | 1147,025 | 0,603 | 1635,544 |
| ALV. 2 F 8.19 M1 | F | m | 0,0009 | 30494,693 | <DL | 309,808 | 0,600 | 562,641 | 0,808 | 2143,246 |
| ALV. 2 F 8.19 M2 | F | m | 0,0021 | 26402,240 | <DL | 255,146 | 0,874 | 525,995 | 2,215 | 2218,332 |
| ALV. 2 F 9.19 M1 | F | m | 0,0050 | 22615,685 | 0,006 | 252,203 | 2,143 | 580,674 | 3,108 | 1864,456 |
| ALV. 2 F 9.19 M2 | F | m | 0,0098 | 26540,681 | 0,064 | 311,108 | 2,249 | 684,828 | 3,578 | 2128,868 |
| ALV. 2 F 9.19 M3 | F | m | 0,0044 | 25972,822 | 0,152 | 273,220 | 1,540 | 674,495 | 4,741 | 2467,033 |
| ALV. 2 F 9.19 M4 | F | m | 0,0023 | 17331,004 | 0,108 | 217,137 | 1,428 | 669,279 | 3,021 | 1565,366 |
| ALV. 2 F 9.19 M5 | F | m | 0,0009 | 26442,831 | 0,062 | 296,960 | 0,928 | 741,076 | 1,936 | 1986,936 |
| ALV. 1 F 6.19 E2 | F | h | 0,0036 | 1220,968 | 0,019 | 263,253 | 46,205 | 1140,910 | 0,991 | 1072,016 |
| ALV. 1 F 6.19 E3 | F | h | 0,0027 | 726,635 | <DL | 112,685 | 11,735 | 498,383 | 1,003 | 676,769 |
| ALV. 1 F 6.19 E4 | F | h | 0,0033 | 12696,551 | 0,309 | 113,237 | 18,863 | 816,790 | 1,275 | 823,650 |
| ALV. 1 F 8.19 E1 | F | h | 0,0013 | 17587,287 | <DL | 160,190 | 11,515 | 472,063 | 0,620 | 1085,984 |
| ALV. 1 F 8.19 E2 | F | h | 0,0038 | 13630,033 | <DL | 134,729 | 22,493 | 609,322 | 0,518 | 831,605 |
| ALV. 1 F 8.19 E3 | F | h | 0,0038 | 12872,244 | 0,091 | 149,495 | 5,439 | 590,992 | 0,671 | 987,921 |
| ALV. 2 F 7.19 E1 | F | h | 0,0095 | 745,673 | <DL | 214,528 | 11,295 | 550,726 | 1,149 | 824,606 |
| ALV. 2 F 7.19 E2 | F | h | 0,0018 | 1087,470 | <DL | 340,406 | 6,284 | 936,591 | 0,565 | 1251,514 |
| ALV. 2 F 8.19 E1 | F | h | 0,0014 | 12052,424 | 0,040 | 116,621 | 2,789 | 386,453 | 0,380 | 1066,305 |
| ALV. 2 F 8.19 E2 | F | h | 0,0027 | 11021,891 | <DL | 143,505 | 4,829 | 415,548 | 0,425 | 926,141 |
| ALV. 2 F 9.19 E1 | F | h | 0,0027 | 15517,509 | 0,060 | 281,303 | 12,496 | 657,549 | 0,238 | 1742,595 |
| ALV. 2 F 9.19 E2 | F | h | 0,0010 | 11766,867 | 0,073 | 204,182 | 8,179 | 462,289 | 0,511 | 1541,316 |
| ALV. 2 F 9.19 E3 | F | h | 0,0012 | 15088,090 | 0,027 | 182,084 | 2,366 | 571,097 | 0,764 | 1182,729 |
| ALV. 2 F 9.19 E4 | F | h | 0,0099 | 13473,606 | 0,127 | 237,615 | 8,601 | 759,683 | 0,617 | 1148,813 |
| ALV. 2 F 9.19 E5 | F | h | 0,0013 | 12497,303 | <DL | 219,856 | 2,344 | 470,028 | 0,335 | 1350,366 |

Table A.5: Elements concentrations(mg/kg) in female hepatopancreas and muscle tissues.

| Sample Name | Sex | Tissue | Tl | V | Zn |
|---|---|---|---|---|---|
| ALV. 1 F 6.19 M1 | F | m | 0,0003 | 0,082 | 22,648 |
| ALV. 1 F 6.19 M2 | F | m | <DL | 0,058 | 18,444 |
| ALV. 1 F 6.19 M3 | F | m | <DL | 0,147 | 16,598 |
| ALV. 1 F 6.19 M4 | F | m | 0,0009 | 0,017 | 14,895 |
| ALV. 1 F 8.19 M1 | F | m | 0,0009 | 0,014 | 15,813 |
| ALV. 1 F 8.19 M2 | F | m | 0,0006 | 0,012 | 12,586 |
| ALV. 1 F 8.19 M3 | F | m | 0,0008 | 0,027 | 12,732 |
| ALV. 2 F 7.19 M1 | F | m | <DL | 0,038 | 19,662 |
| ALV. 2 F 7.19 M2 | F | m | <DL | 0,051 | 16,667 |
| ALV. 2 F 8.19 M1 | F | m | 0,0012 | 0,017 | 16,640 |
| ALV. 2 F 8.19 M2 | F | m | 0,0017 | 0,041 | 15,692 |
| ALV. 2 F 9.19 M1 | F | m | 0,0007 | 0,057 | 13,206 |
| ALV. 2 F 9.19 M2 | F | m | 0,0013 | 0,085 | 18,343 |
| ALV. 2 F 9.19 M3 | F | m | 0,0007 | 0,051 | 15,683 |
| ALV. 2 F 9.19 M4 | F | m | 0,0015 | 0,037 | 11,706 |
| ALV. 2 F 9.19 M5 | F | m | 0,0003 | 0,028 | 18,006 |
| ALV. 1 F 6.19 E2 | F | h | 0,0007 | 0,117 | 36,765 |
| ALV. 1 F 6.19 E3 | F | h | 0,0002 | 0,076 | 18,918 |
| ALV. 1 F 6.19 E4 | F | h | 0,0013 | 0,047 | 15,210 |
| ALV. 1 F 8.19 E1 | F | h | <DL | 0,035 | 14,324 |
| ALV. 1 F 8.19 E2 | F | h | 0,0031 | 0,080 | 12,818 |
| ALV. 1 F 8.19 E3 | F | h | 0,0048 | 0,048 | 15,990 |
| ALV. 2 F 7.19 E1 | F | h | 0,0002 | 0,105 | 29,832 |
| ALV. 2 F 7.19 E2 | F | h | <DL | 0,046 | 31,115 |
| ALV. 2 F 8.19 E1 | F | h | 0,0020 | 0,023 | 14,918 |
| ALV. 2 F 8.19 E2 | F | h | 0,0025 | 0,022 | 30,171 |
| ALV. 2 F 9.19 E1 | F | h | 0,0031 | 0,047 | 21,507 |
| ALV. 2 F 9.19 E2 | F | h | 0,0028 | 0,042 | 19,959 |
| ALV. 2 F 9.19 E3 | F | h | 0,0019 | 0,036 | 27,301 |
| ALV. 2 F 9.19 E4 | F | h | 0,0070 | 0,073 | 37,983 |
| ALV. 2 F 9.19 E5 | F | h | 0,0018 | 0,035 | 22,443 |

# A.2 Male Data

Table A.6: Elements concentrations(mg/kg) in males hepatopancreas and muscle tissues.

| Sample Name | Sex | Tissue | Hg | Ag | Al | As | B | Ba | Be [No Gas] | Be [He] |
|---|---|---|---|---|---|---|---|---|---|---|
| ALV. 1 M 6.19 M1 | M | m | 0,201 | 0,020 | 9,158 | 0,291 | 0,442 | 0,645 | <DL | 0,000 |
| ALV. 1 M 6.19 M2 | M | m | 0,211 | 0,018 | 6,101 | 0,297 | 0,414 | 0,466 | <DL | 0,000 |
| ALV. 1 M 6.19 M3 | M | m | 0,142 | 0,009 | 10,265 | 0,221 | 0,312 | 0,612 | <DL | 0,000 |
| ALV. 1 M 7.19 M1 | M | m | 0,076 | 0,016 | 3,925 | 0,265 | 0,416 | 1,247 | <DL | 0,007 |
| ALV. 1 M 7.19 M2 | M | m | 0,060 | 0,010 | 1,783 | 0,148 | 0,256 | 0,379 | 0,0016 | 0,003 |
| ALV. 1 M 7.19 M3 | M | m | 0,123 | 0,011 | 10,402 | 0,162 | 0,182 | 0,240 | 0,0023 | 0,001 |
| ALV. 1 M 8.19 M2 | M | m | 0,065 | 0,012 | 2,938 | 0,262 | 0,170 | 0,482 | <DL | 0,000 |
| ALV. 1 M 8.19 M3 | M | m | 0,069 | 0,017 | 3,588 | 0,165 | 0,149 | 0,313 | <DL | 0,001 |
| ALV. 1 M 8.19 M4 | M | m | 0,044 | 0,007 | 2,134 | 0,169 | 0,253 | 0,471 | <DL | 0,000 |
| ALV. 1 M 8.19 M5 | M | m | 0,172 | 0,009 | 1,936 | 0,158 | 0,423 | 0,234 | <DL | 0,000 |
| ALV. 1 M 8.19 M6 | M | m | 0,048 | 0,010 | 3,088 | 0,278 | 0,342 | 1,286 | <DL | 0,000 |
| ALV. 1 M 8.19 M7 | M | m | 0,107 | 0,023 | 2,258 | 0,219 | 0,333 | 0,810 | <DL | 0,001 |
| ALV. 1 M 8.19 M8 | M | m | 0,049 | 0,012 | 0,809 | 0,152 | 0,191 | 0,261 | <DL | 0,000 |
| ALV. 1 M 8.19 M9 | M | m | 0,119 | 0,008 | 2,408 | 0,236 | 0,278 | 0,672 | <DL | 0,001 |
| ALV. 1 M 8.19 M10 | M | m | 0,069 | 0,009 | 2,895 | 0,262 | 0,294 | 0,863 | <DL | 0,001 |
| ALV. 1 M 8.19 M11 | M | m | 0,055 | 0,012 | 2,595 | 0,212 | 0,273 | 1,035 | <DL | 0,000 |
| ALV. 1 M 8.19 M12 | M | m | 0,120 | 0,019 | 1,719 | 0,158 | 0,362 | 1,041 | <DL | <DL |
| ALV. 1 M 8.19 M13 | M | m | 0,070 | 0,009 | 1,335 | 0,184 | 0,230 | 0,735 | <DL | 0,000 |
| ALV. 1 M 8.19 M14 | M | m | 0,081 | 0,019 | 0,324 | 0,708 | 2,865 | 0,197 | 0,0009 | 0,010 |
| ALV. 1 M 8.19 M15 | M | m | 0,115 | 0,023 | 1,717 | 0,423 | 1,272 | 0,800 | <DL | 0,004 |
| ALV. 1 M 9.19 M1 | M | m | 0,052 | 0,013 | 3,988 | 0,311 | 0,661 | 1,005 | <DL | 0,001 |
| ALV. 1 M 9.19 M2 | M | m | 0,040 | 0,012 | 3,580 | 0,195 | 0,407 | 0,885 | <DL | 0,001 |
| ALV. 1 M 9.19 M3 | M | m | 0,055 | 0,018 | 3,866 | 0,283 | 0,419 | 1,004 | <DL | 0,003 |
| ALV. 2 M 7.19 M1 | M | m | 0,209 | 0,020 | 9,112 | 0,337 | 0,510 | 0,366 | 0,0017 | 0,003 |
| ALV. 2 M 7.19 M2 | M | m | 0,192 | 0,017 | 3,618 | 0,230 | 0,327 | 0,556 | <DL | 0,000 |
| ALV. 2 M 7.19 M3 | M | m | 0,177 | 0,034 | 3,938 | 0,235 | 0,394 | 0,990 | <DL | 0,000 |
| ALV. 2 M 8.19 M1 | M | m | 0,140 | 0,016 | 3,906 | 0,264 | 0,660 | 0,248 | <DL | 0,004 |
| ALV. 2 M 9.19 M1 | M | m | 0,098 | 0,014 | 7,270 | 0,223 | 0,173 | 0,262 | <DL | 0,003 |
| ALV. 2 M 9.19 M2 | M | m | 0,099 | 0,010 | 3,986 | 0,216 | 0,766 | 0,849 | <DL | 0,001 |
| ALV. 1 M 6.19 E1 | M | h | 0,094 | 0,027 | 8,518 | 1,689 | 0,873 | 5,488 | <DL | <DL |
| ALV. 1 M 6.19 E2 | M | h | 0,047 | 0,024 | 1,959 | 2,262 | 0,621 | 1,467 | 0,0014 | 0,001 |
| ALV. 1 M 6.19 E3 | M | h | 0,026 | 0,014 | 3,113 | 0,908 | 0,340 | 1,590 | <DL | <DL |
| ALV. 1 M 7.19 E1 | M | h | 0,030 | 0,024 | 11,015 | 0,814 | 0,412 | 4,741 | 0,0077 | 0,014 |
| ALV. 1 M 7.19 E2 | M | h | 0,019 | 0,016 | 0,754 | 0,353 | 0,003 | 1,088 | 0,0109 | 0,023 |
| ALV. 1 M 7.19 E3 | M | h | 0,035 | 0,012 | 2,026 | 0,391 | 0,104 | 0,616 | 0,0081 | 0,016 |
| ALV. 1 M 8.19 E2 | M | h | 0,017 | 0,017 | 0,469 | 0,714 | 0,440 | 1,786 | 0,0024 | 0,002 |
| ALV. 1 M 8.19 E3 | M | h | 0,016 | 0,007 | -0,006 | 0,727 | 0,291 | 0,724 | 0,0002 | <DL |
| ALV. 1 M 8.19 E4 | M | h | 0,013 | 0,015 | 2,228 | 0,761 | 1,039 | 4,554 | 0,0046 | 0,007 |
| ALV. 1 M 8.19 E5 | M | h | 0,016 | 0,008 | -0,231 | 0,592 | 0,512 | 0,883 | <DL | <DL |
| ALV. 1 M 8.19 E6 | M | h | 0,016 | 0,013 | 0,572 | 0,845 | 0,638 | 3,100 | 0,0028 | 0,004 |
| ALV. 1 M 8.19 E7 | M | h | 0,015 | 0,018 | 2,074 | 0,839 | 1,018 | 4,587 | 0,0040 | 0,013 |
| ALV. 1 M 8.19 E8 | M | h | 0,015 | 0,029 | 1,161 | 0,883 | 0,726 | 3,967 | 0,0018 | 0,016 |
| ALV. 1 M 8.19 E9 | M | h | 0,011 | 0,008 | 0,252 | 0,448 | 0,430 | 0,517 | 0,0001 | 0,002 |
| ALV. 1 M 8.19 E10 | M | h | 0,005 | 0,009 | 0,025 | 1,148 | 0,604 | 1,558 | 0,0010 | 0,006 |
| ALV. 1 M 8.19 E11 | M | h | 0,008 | 0,015 | 0,193 | 0,797 | -0,005 | 3,768 | 0,0033 | <DL |
| ALV. 1 M 8.19 E12 | M | h | 0,014 | 0,014 | 1,330 | 0,334 | 0,429 | 2,123 | 0,0012 | 0,018 |
| ALV. 1 M 8.19 E13 | M | h | 0,001 | 0,003 | 0,097 | 0,107 | 0,166 | 0,447 | 0,0009 | 0,000 |
| ALV. 1 M 8.19 E14 | M | h | 0,012 | 0,021 | 0,932 | 0,446 | 0,596 | 2,769 | 0,0031 | 0,005 |
| ALV. 1 M 8.19 E15 | M | h | 0,014 | 0,016 | 0,799 | 0,584 | 0,658 | 1,972 | 0,0006 | 0,000 |
| ALV. 2 M 7.19 E1 | M | h | 0,031 | 0,017 | 5,920 | 0,991 | 1,372 | 2,457 | 0,0141 | <DL |
| ALV. 2 M 7.19 E2 | M | h | 0,047 | 0,019 | 2,520 | 0,940 | 0,958 | 1,352 | 0,0003 | 0,001 |
| ALV. 2 M 7.19 E3 | M | h | 0,028 | 0,024 | 2,840 | 1,005 | 0,757 | 1,678 | 0,0002 | 0,000 |
| ALV. 2 M 8.19 E1 | M | h | 0,023 | 0,024 | 3,031 | 0,428 | 0,316 | 1,173 | 0,0013 | 0,003 |
| ALV. 2 M 9.19 E1 | M | h | 0,052 | 0,045 | 13,361 | 0,748 | 0,189 | 2,693 | 0,0052 | 0,005 |
| ALV. 2 M 9.19 E2 | M | h | 0,009 | 0,003 | 1,363 | 0,233 | 1,361 | 2,873 | 0,0007 | 0,007 |

56

Table A.7: Elements concentrations(mg/kg) in males hepatopancreas and muscle tissues.

| Sample Name | Sex | Tissue | Ca | Cd | Co | Cr | Cs | Cu | Fe [He] | Fe [O2] |
|---|---|---|---|---|---|---|---|---|---|---|
| ALV. 1 M 6.19 M1 | M | m | 103,407 | 0,004 | 0,237 | 23,431 | 0,022 | 3,114 | 93,981 | 135,185 |
| ALV. 1 M 6.19 M2 | M | m | 98,914 | 0,004 | 0,046 | 1,618 | 0,025 | 4,849 | 16,220 | 17,493 |
| ALV. 1 M 6.19 M3 | M | m | 90,926 | 0,002 | 0,157 | 19,122 | 0,023 | 2,834 | 66,019 | 90,579 |
| ALV. 1 M 7.19 M1 | M | m | 285,088 | 0,007 | 0,059 | 0,356 | 0,019 | 7,567 | 16,670 | 14,709 |
| ALV. 1 M 7.19 M2 | M | m | 151,975 | 0,002 | 0,045 | 0,054 | 0,019 | 6,552 | 7,503 | 6,174 |
| ALV. 1 M 7.19 M3 | M | m | 111,136 | 0,009 | 0,017 | 0,078 | 0,012 | 6,266 | 17,498 | 14,852 |
| ALV. 1 M 8.19 M2 | M | m | 112,020 | 0,005 | 0,064 | 12,156 | 0,010 | 5,367 | 41,961 | 52,866 |
| ALV. 1 M 8.19 M3 | M | m | 109,740 | 0,011 | 0,019 | 0,695 | 0,008 | 7,318 | 11,600 | 11,004 |
| ALV. 1 M 8.19 M4 | M | m | 125,545 | 0,007 | 0,032 | 1,222 | 0,002 | 4,909 | 20,294 | 18,676 |
| ALV. 1 M 8.19 M5 | M | m | 128,698 | 0,001 | 0,027 | 2,772 | 0,008 | 6,230 | 18,725 | 17,996 |
| ALV. 1 M 8.19 M6 | M | m | 203,420 | 0,005 | 0,056 | 4,165 | 0,008 | 5,997 | 34,810 | 33,234 |
| ALV. 1 M 8.19 M7 | M | m | 168,493 | 0,006 | 0,052 | 1,792 | 0,007 | 10,504 | 23,499 | 23,461 |
| ALV. 1 M 8.19 M8 | M | m | 100,907 | 0,002 | 0,023 | 0,433 | 0,005 | 5,797 | 14,148 | 13,683 |
| ALV. 1 M 8.19 M9 | M | m | 171,968 | 0,002 | 0,030 | 1,187 | 0,012 | 7,200 | 18,841 | 17,359 |
| ALV. 1 M 8.19 M10 | M | m | 151,759 | 0,005 | 0,050 | 1,197 | 0,007 | 4,715 | 23,418 | 20,519 |
| ALV. 1 M 8.19 M11 | M | m | 144,732 | 0,008 | 0,043 | 2,802 | 0,007 | 5,944 | 32,812 | 30,134 |
| ALV. 1 M 8.19 M12 | M | m | 212,068 | 0,006 | 0,032 | 1,272 | 0,004 | 10,496 | 15,707 | 14,170 |
| ALV. 1 M 8.19 M13 | M | m | 145,488 | 0,006 | 0,050 | 4,289 | 0,007 | 5,750 | 34,933 | 30,664 |
| ALV. 1 M 8.19 M14 | M | m | 60,289 | 0,009 | 0,018 | 0,248 | 0,014 | 2,596 | 5,502 | 4,741 |
| ALV. 1 M 8.19 M15 | M | m | 164,909 | 0,011 | 0,066 | 1,416 | 0,011 | 9,039 | 21,048 | 18,693 |
| ALV. 1 M 9.19 M1 | M | m | 187,720 | 0,010 | 0,042 | 1,058 | 0,006 | 6,923 | 21,056 | 18,983 |
| ALV. 1 M 9.19 M2 | M | m | 120,252 | 0,004 | 0,017 | 0,437 | 0,010 | 4,774 | 12,368 | 10,797 |
| ALV. 1 M 9.19 M3 | M | m | 151,867 | 0,007 | 0,029 | 0,900 | 0,015 | 6,197 | 14,365 | 15,403 |
| ALV. 2 M 7.19 M1 | M | m | 187,530 | 0,006 | 0,021 | 0,090 | 0,019 | 10,152 | 15,420 | 12,474 |
| ALV. 2 M 7.19 M2 | M | m | 96,454 | 0,006 | 0,144 | 14,688 | 0,018 | 3,823 | 50,412 | 66,700 |
| ALV. 2 M 7.19 M3 | M | m | 184,642 | 0,011 | 0,089 | 0,574 | 0,021 | 7,815 | 22,205 | 23,113 |
| ALV. 2 M 8.19 M1 | M | m | 146,749 | 0,005 | 0,022 | 0,654 | 0,016 | 7,683 | 15,895 | 13,965 |
| ALV. 2 M 9.19 M1 | M | m | 122,959 | 0,001 | 0,018 | 1,152 | 0,018 | 4,417 | 15,929 | 14,108 |
| ALV. 2 M 9.19 M2 | M | m | 183,534 | 0,002 | 0,019 | 0,879 | 0,009 | 3,102 | 19,971 | 18,098 |
| ALV. 1 M 6.19 E1 | M | h | 193,056 | 0,447 | 0,854 | 1,154 | 0,010 | 7,278 | 153,245 | 199,521 |
| ALV. 1 M 6.19 E2 | M | h | 97,327 | 0,224 | 2,048 | 0,424 | 0,011 | 9,216 | 173,753 | 241,244 |
| ALV. 1 M 6.19 E3 | M | h | 79,182 | 0,061 | 0,771 | 1,188 | 0,008 | 5,649 | 263,072 | 348,010 |
| ALV. 1 M 7.19 E1 | M | h | 532,610 | 0,156 | 0,424 | 0,042 | 0,010 | 12,675 | 397,220 | 472,455 |
| ALV. 1 M 7.19 E2 | M | h | 361,675 | 0,080 | 0,182 | 0,024 | 0,012 | 7,460 | 164,972 | 185,780 |
| ALV. 1 M 7.19 E3 | M | h | 168,966 | 0,179 | 0,203 | 0,025 | 0,006 | 4,163 | 247,798 | 209,325 |
| ALV. 1 M 8.19 E2 | M | h | 277,795 | 0,246 | 0,239 | 0,025 | 0,006 | 7,936 | 473,005 | 627,351 |
| ALV. 1 M 8.19 E3 | M | h | 355,324 | 0,263 | 0,108 | 0,019 | 0,004 | 4,591 | 89,820 | 84,361 |
| ALV. 1 M 8.19 E4 | M | h | 395,040 | 0,206 | 0,207 | 0,039 | 0,005 | 6,507 | 502,273 | 640,466 |
| ALV. 1 M 8.19 E5 | M | h | 306,204 | 0,050 | 0,189 | 0,036 | 0,003 | 3,617 | 347,147 | 455,417 |
| ALV. 1 M 8.19 E6 | M | h | 388,302 | 0,100 | 0,239 | 0,028 | 0,006 | 5,387 | 381,380 | 537,504 |
| ALV. 1 M 8.19 E7 | M | h | 461,574 | 0,191 | 0,203 | 0,030 | 0,004 | 7,962 | 546,632 | 588,842 |
| ALV. 1 M 8.19 E8 | M | h | 428,382 | 0,227 | 0,144 | 0,021 | 0,003 | 10,022 | 911,527 | 1143,909 |
| ALV. 1 M 8.19 E9 | M | h | 240,888 | 0,052 | 0,111 | 0,008 | 0,007 | 3,716 | 126,898 | 149,026 |
| ALV. 1 M 8.19 E10 | M | h | 244,855 | 0,116 | 0,229 | 0,021 | 0,007 | 4,777 | 326,982 | 424,487 |
| ALV. 1 M 8.19 E11 | M | h | 452,802 | 0,140 | 0,196 | 0,020 | 0,007 | 4,398 | 861,612 | 1214,718 |
| ALV. 1 M 8.19 E12 | M | h | 287,833 | 0,147 | 0,113 | 0,045 | 0,003 | 3,797 | 581,105 | 739,175 |
| ALV. 1 M 8.19 E13 | M | h | 44,185 | 0,013 | 0,030 | 0,018 | 0,002 | 0,648 | 97,604 | 106,380 |
| ALV. 1 M 8.19 E14 | M | h | 375,542 | 0,106 | 0,119 | 0,042 | 0,004 | 7,033 | 438,376 | 543,594 |
| ALV. 1 M 8.19 E15 | M | h | 230,220 | 0,103 | 0,202 | 0,027 | 0,004 | 6,857 | 384,125 | 479,408 |
| ALV. 2 M 7.19 E1 | M | h | 515,912 | 0,092 | 0,198 | 0,020 | 0,009 | 7,799 | 529,778 | 657,501 |
| ALV. 2 M 7.19 E2 | M | h | 279,409 | 0,285 | 0,558 | 0,912 | 0,007 | 4,915 | 334,973 | 463,865 |
| ALV. 2 M 7.19 E3 | M | h | 200,432 | 0,201 | 0,508 | 0,586 | 0,008 | 9,101 | 696,840 | 932,629 |
| ALV. 2 M 8.19 E1 | M | h | 331,444 | 0,105 | 0,102 | 0,039 | 0,005 | 9,450 | 381,145 | 484,460 |
| ALV. 2 M 9.19 E1 | M | h | 508,699 | 0,266 | 0,242 | 0,068 | 0,011 | 13,445 | 531,432 | 657,939 |
| ALV. 2 M 9.19 E2 | M | h | 222,899 | 0,015 | 0,049 | 0,028 | 0,004 | 1,887 | 447,338 | 590,735 |

Table A.8: Elements concentrations(mg/kg) in males hepatopancreas and muscle tissues.

| Sample Name | Sex | Tissue | Ga | K | Li | Mg | Mn | Na | Ni | P |
|---|---|---|---|---|---|---|---|---|---|---|
| ALV. 1 M 6.19 M1 | M | m | 0,0115 | 1930,844 | <DL | 352,618 | 7,497 | 1025,438 | 16,029 | 1948,250 |
| ALV. 1 M 6.19 M2 | M | m | 0,0030 | 2070,624 | <DL | 374,820 | 8,172 | 893,630 | 0,905 | 2030,047 |
| ALV. 1 M 6.19 M3 | M | m | 0,0095 | 1992,581 | <DL | 302,774 | 5,162 | 832,452 | 10,290 | 1512,067 |
| ALV. 1 M 7.19 M1 | M | m | 0,0003 | 26484,324 | <DL | 288,615 | 3,088 | 725,946 | 0,544 | 2114,099 |
| ALV. 1 M 7.19 M2 | M | m | 0,0021 | 24103,515 | 0,055 | 223,701 | 1,766 | 648,647 | 0,207 | 1659,500 |
| ALV. 1 M 7.19 M3 | M | m | 0,0044 | 22916,451 | <DL | 242,746 | 1,918 | 581,486 | 0,308 | 1810,191 |
| ALV. 1 M 8.19 M2 | M | m | 0,0021 | 24938,787 | <DL | 245,985 | 1,616 | 619,213 | 6,473 | 1543,033 |
| ALV. 1 M 8.19 M3 | M | m | 0,0004 | 22499,056 | 0,054 | 226,350 | 1,244 | 657,948 | 0,484 | 1292,870 |
| ALV. 1 M 8.19 M4 | M | m | <DL | 21273,248 | 0,001 | 238,034 | 1,456 | 851,891 | 0,801 | 1255,433 |
| ALV. 1 M 8.19 M5 | M | m | 0,0004 | 28701,959 | <DL | 238,726 | 1,220 | 790,189 | 1,707 | 1736,826 |
| ALV. 1 M 8.19 M6 | M | m | 0,0013 | 21245,986 | 0,020 | 279,538 | 2,063 | 704,917 | 2,542 | 1435,877 |
| ALV. 1 M 8.19 M7 | M | m | 0,0000 | 26143,549 | <DL | 277,415 | 2,102 | 760,831 | 1,278 | 1582,631 |
| ALV. 1 M 8.19 M8 | M | m | <DL | 20754,854 | <DL | 194,888 | 0,620 | 722,363 | 0,367 | 1257,376 |
| ALV. 1 M 8.19 M9 | M | m | 0,0004 | 27517,041 | <DL | 310,291 | 0,843 | 747,493 | 0,807 | 1961,857 |
| ALV. 1 M 8.19 M10 | M | m | 0,0008 | 20490,373 | 0,003 | 193,701 | 1,008 | 692,025 | 0,913 | 1273,700 |
| ALV. 1 M 8.19 M11 | M | m | 0,0011 | 24522,938 | <DL | 205,164 | 1,513 | 530,101 | 1,655 | 1523,999 |
| ALV. 1 M 8.19 M12 | M | m | <DL | 34108,881 | <DL | 341,080 | 1,224 | 683,483 | 0,924 | 2308,713 |
| ALV. 1 M 8.19 M13 | M | m | 0,0004 | 20110,438 | <DL | 218,529 | 1,400 | 518,369 | 2,623 | 1360,023 |
| ALV. 1 M 8.19 M14 | M | m | 0,0009 | 13382,165 | 0,214 | 114,321 | 0,463 | 542,670 | 0,328 | 673,824 |
| ALV. 1 M 8.19 M15 | M | m | 0,0004 | 22384,301 | 0,114 | 239,782 | 1,157 | 767,764 | 1,284 | 1654,788 |
| ALV. 1 M 9.19 M1 | M | m | 0,0007 | 18427,673 | 0,037 | 244,369 | 3,098 | 699,904 | 0,717 | 1410,236 |
| ALV. 1 M 9.19 M2 | M | m | 0,0009 | 21166,231 | 0,071 | 199,399 | 1,667 | 570,421 | 0,365 | 1350,076 |
| ALV. 1 M 9.19 M3 | M | m | 0,0018 | 26947,388 | 0,029 | 235,144 | 4,077 | 648,740 | 0,682 | 1971,204 |
| ALV. 2 M 7.19 M1 | M | m | 0,0051 | 36250,942 | 0,076 | 312,725 | 1,593 | 707,435 | 0,532 | 2519,197 |
| ALV. 2 M 7.19 M2 | M | m | 0,0059 | 1668,348 | <DL | 272,630 | 3,560 | 697,475 | 8,184 | 1669,853 |
| ALV. 2 M 7.19 M3 | M | m | 0,0014 | 1817,456 | <DL | 393,209 | 0,830 | 960,787 | 0,690 | 2044,775 |
| ALV. 2 M 8.19 M1 | M | m | 0,0009 | 27811,933 | 0,026 | 339,563 | 0,683 | 873,027 | 0,526 | 2111,100 |
| ALV. 2 M 9.19 M1 | M | m | 0,0026 | 22264,760 | 0,037 | 187,533 | 1,026 | 612,012 | 0,740 | 1328,331 |
| ALV. 2 M 9.19 M2 | M | m | 0,0015 | 23491,632 | 0,108 | 226,851 | 0,993 | 483,631 | 0,642 | 1658,444 |
| ALV. 1 M 6.19 E1 | M | h | 0,0009 | 1090,367 | 0,092 | 244,095 | 116,276 | 1028,673 | 1,486 | 1379,974 |
| ALV. 1 M 6.19 E2 | M | h | 0,0025 | 1177,756 | <DL | 184,856 | 98,173 | 1153,951 | 2,186 | 893,081 |
| ALV. 1 M 6.19 E3 | M | h | 0,0022 | 797,628 | <DL | 133,622 | 19,335 | 695,436 | 1,364 | 720,395 |
| ALV. 1 M 7.19 E1 | M | h | 0,0071 | 15964,831 | 0,131 | 266,610 | 50,341 | 868,612 | 1,984 | 1023,072 |
| ALV. 1 M 7.19 E2 | M | h | 0,0028 | 13041,395 | <DL | 164,635 | 26,206 | 1334,148 | 0,905 | 1423,571 |
| ALV. 1 M 7.19 E3 | M | h | 0,0041 | 9734,767 | 0,351 | 94,727 | 13,993 | 526,496 | 0,751 | 1012,922 |
| ALV. 1 M 8.19 E2 | M | h | 0,0012 | 12794,381 | 0,021 | 138,110 | 3,280 | 544,447 | 0,551 | 1084,304 |
| ALV. 1 M 8.19 E3 | M | h | 0,0000 | 8737,624 | 0,182 | 106,605 | 11,618 | 725,267 | 0,192 | 632,765 |
| ALV. 1 M 8.19 E4 | M | h | 0,0020 | 15145,349 | 0,067 | 131,527 | 24,887 | 1044,667 | 0,423 | 1096,941 |
| ALV. 1 M 8.19 E5 | M | h | <DL | 13517,268 | <DL | 118,191 | 43,913 | 824,487 | 0,400 | 1090,057 |
| ALV. 1 M 8.19 E6 | M | h | <DL | 15566,613 | 0,062 | 162,591 | 20,218 | 909,527 | 0,965 | 1029,571 |
| ALV. 1 M 8.19 E7 | M | h | 0,0020 | 12013,631 | 0,006 | 185,984 | 31,843 | 796,357 | 0,653 | 1014,866 |
| ALV. 1 M 8.19 E8 | M | h | <DL | 13366,723 | 0,099 | 158,579 | 25,643 | 1142,238 | 0,137 | 1430,492 |
| ALV. 1 M 8.19 E9 | M | h | <DL | 12922,351 | <DL | 129,442 | 6,481 | 593,322 | 0,355 | 541,303 |
| ALV. 1 M 8.19 E10 | M | h | <DL | 12514,487 | <DL | 137,759 | 8,021 | 598,975 | 0,761 | 915,765 |
| ALV. 1 M 8.19 E11 | M | h | 0,0007 | 16157,239 | <DL | 180,015 | 14,336 | 895,990 | 0,544 | 1816,865 |
| ALV. 1 M 8.19 E12 | M | h | 0,0003 | 7234,228 | 0,063 | 110,744 | 8,853 | 475,561 | 0,084 | 917,290 |
| ALV. 1 M 8.19 E13 | M | h | 0,0004 | 1581,914 | 0,095 | 22,572 | 2,469 | 111,015 | 0,089 | 148,567 |
| ALV. 1 M 8.19 E14 | M | h | 0,0001 | 9549,041 | 0,104 | 138,888 | 8,883 | 720,116 | 0,217 | 1023,140 |
| ALV. 1 M 8.19 E15 | M | h | <DL | 8901,047 | 0,038 | 105,135 | 8,925 | 400,159 | 0,875 | 714,887 |
| ALV. 2 M 7.19 E1 | M | h | 0,0017 | 10804,504 | 0,549 | 185,982 | 37,542 | 826,030 | 1,209 | 1517,007 |
| ALV. 2 M 7.19 E2 | M | h | 0,0024 | 863,355 | <DL | 213,898 | 6,372 | 699,845 | 1,564 | 692,729 |
| ALV. 2 M 7.19 E3 | M | h | 0,0033 | 802,341 | <DL | 239,706 | 1,946 | 821,204 | 1,811 | 863,412 |
| ALV. 2 M 8.19 E1 | M | h | 0,0001 | 9173,094 | 0,114 | 139,637 | 2,025 | 638,293 | 0,193 | 909,117 |
| ALV. 2 M 9.19 E1 | M | h | 0,0042 | 11097,147 | 0,110 | 167,451 | 9,715 | 663,015 | 0,238 | 1420,467 |
| ALV. 2 M 9.19 E2 | M | h | 0,0011 | 7982,929 | <DL | 112,131 | 3,283 | 361,490 | 0,093 | 759,345 |

Table A.9: Elements concentrations(mg/kg) in males hepatopancreas and muscle tissues.

| Sample Name | Sex | Tissue | Pb (206) | Pb (207) | Pb (208) | 32 –>68 S [O2] | 34 –>50 S [O2] | Si | Sr |
|---|---|---|---|---|---|---|---|---|---|
| ALV. 1 M 6.19 M1 | M | m | 0,081 | 0,073 | 0,070 | 1239,711171 | 1521,567438 | 25,172 | 1,556 |
| ALV. 1 M 6.19 M2 | M | m | 0,104 | 0,107 | 0,097 | 1324,611303 | 1594,082036 | 19,369 | 1,627 |
| ALV. 1 M 6.19 M3 | M | m | 0,045 | 0,056 | 0,046 | 1056,418476 | 1266,620286 | 32,433 | 1,413 |
| ALV. 1 M 7.19 M1 | M | m | 0,062 | 0,061 | 0,064 | 1353,607093 | 1478,621703 | 11,148 | 5,780 |
| ALV. 1 M 7.19 M2 | M | m | 0,095 | 0,103 | 0,098 | 1005,041077 | 1088,212692 | 7,352 | 2,638 |
| ALV. 1 M 7.19 M3 | M | m | 0,097 | 0,081 | 0,095 | 1286,270266 | 1407,421921 | 18,053 | 1,773 |
| ALV. 1 M 8.19 M2 | M | m | <DL | <DL | <DL | 1030,35723 | 1222,195308 | 10,637 | 2,198 |
| ALV. 1 M 8.19 M3 | M | m | 0,004 | 0,002 | 0,003 | 1012,418429 | 1171,598554 | 8,848 | 2,090 |
| ALV. 1 M 8.19 M4 | M | m | 0,007 | 0,003 | 0,003 | 899,3817749 | 1076,163673 | 6,625 | 2,767 |
| ALV. 1 M 8.19 M5 | M | m | 0,021 | 0,025 | 0,022 | 1393,106997 | 1618,851885 | 6,685 | 2,171 |
| ALV. 1 M 8.19 M6 | M | m | 0,012 | 0,016 | 0,012 | 1073,018934 | 1239,765157 | 11,724 | 4,472 |
| ALV. 1 M 8.19 M7 | M | m | 0,001 | 0,000 | 0,002 | 1275,225477 | 1477,210294 | 9,940 | 3,851 |
| ALV. 1 M 8.19 M8 | M | m | <DL | <DL | <DL | 933,7615494 | 1067,03716 | 5,000 | 2,081 |
| ALV. 1 M 8.19 M9 | M | m | 0,041 | 0,039 | 0,039 | 1182,186251 | 1336,937936 | 7,848 | 3,422 |
| ALV. 1 M 8.19 M10 | M | m | 0,004 | 0,010 | 0,005 | 992,8411619 | 1111,905003 | 11,101 | 3,184 |
| ALV. 1 M 8.19 M11 | M | m | 0,010 | 0,011 | 0,011 | 1097,448361 | 1209,671725 | 11,312 | 3,211 |
| ALV. 1 M 8.19 M12 | M | m | 0,041 | 0,032 | 0,040 | 1360,186641 | 1502,570049 | 18,856 | 4,088 |
| ALV. 1 M 8.19 M13 | M | m | 0,001 | 0,002 | 0,002 | 979,3712053 | 1061,763857 | 9,246 | 3,256 |
| ALV. 1 M 8.19 M14 | M | m | 0,025 | 0,034 | 0,031 | 430,1413605 | 481,5646308 | 1,292 | 1,114 |
| ALV. 1 M 8.19 M15 | M | m | 0,019 | 0,018 | 0,022 | 1185,782158 | 1322,978432 | 7,082 | 3,496 |
| ALV. 1 M 9.19 M1 | M | m | 0,087 | 0,068 | 0,082 | 1126,758123 | 1256,606299 | 7,887 | 4,348 |
| ALV. 1 M 9.19 M2 | M | m | 0,060 | 0,065 | 0,061 | 1123,815558 | 1225,876105 | 8,364 | 3,143 |
| ALV. 1 M 9.19 M3 | M | m | 0,004 | 0,005 | 0,005 | 1384,910834 | 1572,641231 | 8,060 | 3,450 |
| ALV. 2 M 7.19 M1 | M | m | 0,018 | 0,008 | 0,015 | 1705,698884 | 1835,103743 | 18,141 | 3,367 |
| ALV. 2 M 7.19 M2 | M | m | 0,046 | 0,034 | 0,035 | 1119,871749 | 1318,459394 | 15,729 | 1,703 |
| ALV. 2 M 7.19 M3 | M | m | 0,085 | 0,095 | 0,084 | 1265,770527 | 1480,022916 | 19,517 | 4,095 |
| ALV. 2 M 8.19 M1 | M | m | 0,054 | 0,059 | 0,058 | 1479,362044 | 1655,241694 | 18,841 | 2,978 |
| ALV. 2 M 9.19 M1 | M | m | 0,021 | 0,002 | 0,013 | 1089,326932 | 1193,758597 | 12,342 | 2,419 |
| ALV. 2 M 9.19 M2 | M | m | 0,023 | 0,016 | 0,022 | 1193,664829 | 1327,073055 | 10,854 | 5,055 |
| ALV. 1 M 6.19 E1 | M | h | 0,182 | 0,175 | 0,159 | 1041,540605 | 1215,011315 | 49,673 | 3,531 |
| ALV. 1 M 6.19 E2 | M | h | 0,089 | 0,081 | 0,078 | 1100,75118 | 1308,826938 | 18,597 | 2,203 |
| ALV. 1 M 6.19 E3 | M | h | 0,206 | 0,205 | 0,203 | 607,9007829 | 706,2941066 | 26,804 | 1,564 |
| ALV. 1 M 7.19 E1 | M | h | 0,103 | 0,113 | 0,114 | 1003,769377 | 1090,782799 | 37,499 | 10,452 |
| ALV. 1 M 7.19 E2 | M | h | 0,024 | 0,027 | 0,026 | 1064,736386 | 1162,650174 | 9,465 | 6,741 |
| ALV. 1 M 7.19 E3 | M | h | 0,032 | 0,036 | 0,035 | 678,2709989 | 621,5784742 | 21,237 | 2,715 |
| ALV. 1 M 8.19 E2 | M | h | 0,043 | 0,042 | 0,042 | 611,2195822 | 687,3096292 | 33,766 | 6,020 |
| ALV. 1 M 8.19 E3 | M | h | 0,027 | 0,020 | 0,038 | 395,2416563 | 368,4506298 | 8,139 | 5,859 |
| ALV. 1 M 8.19 E4 | M | h | 0,177 | 0,147 | 0,175 | 862,417305 | 791,1747028 | 35,196 | 8,897 |
| ALV. 1 M 8.19 E5 | M | h | 0,113 | 0,086 | 0,113 | 935,1494482 | 887,3233249 | 11,506 | 4,944 |
| ALV. 1 M 8.19 E6 | M | h | 0,147 | 0,110 | 0,126 | 862,783268 | 928,1584785 | 46,127 | 8,588 |
| ALV. 1 M 8.19 E7 | M | h | 0,057 | 0,033 | 0,053 | 815,4449536 | 854,8954555 | 35,555 | 9,955 |
| ALV. 1 M 8.19 E8 | M | h | 0,058 | 0,059 | 0,061 | 701,8139771 | 645,5823863 | 59,374 | 8,245 |
| ALV. 1 M 8.19 E9 | M | h | 0,010 | 0,009 | 0,007 | 474,4559086 | 529,6222659 | 23,341 | 3,614 |
| ALV. 1 M 8.19 E10 | M | h | 0,043 | 0,048 | 0,043 | 639,5731893 | 699,207147 | 38,759 | 4,900 |
| ALV. 1 M 8.19 E11 | M | h | 0,140 | 0,162 | 0,140 | 1239,510733 | 1180,738628 | 62,804 | 10,347 |
| ALV. 1 M 8.19 E12 | M | h | 0,052 | 0,067 | 0,053 | 524,2006045 | 480,3537623 | 26,001 | 5,784 |
| ALV. 1 M 8.19 E13 | M | h | 0,033 | 0,022 | 0,032 | 138,0793072 | 129,7628981 | 4,549 | 0,909 |
| ALV. 1 M 8.19 E14 | M | h | 0,066 | 0,067 | 0,079 | 648,7298412 | 610,1454286 | 23,148 | 7,744 |
| ALV. 1 M 8.19 E15 | M | h | 0,042 | 0,046 | 0,043 | 650,3174536 | 708,3433831 | 26,611 | 4,937 |
| ALV. 2 M 7.19 E1 | M | h | 0,276 | 0,196 | 0,211 | 1175,592838 | 1092,224226 | 23,839 | 10,251 |
| ALV. 2 M 7.19 E2 | M | h | 0,121 | 0,099 | 0,100 | 705,5008033 | 837,7401068 | 44,955 | 6,410 |
| ALV. 2 M 7.19 E3 | M | h | 0,115 | 0,119 | 0,116 | 592,1959971 | 703,8892645 | 72,935 | 4,773 |
| ALV. 2 M 8.19 E1 | M | h | 0,054 | 0,068 | 0,069 | 612,8391038 | 673,9857127 | 38,571 | 7,182 |
| ALV. 2 M 9.19 E1 | M | h | 0,114 | 0,103 | 0,119 | 883,2014642 | 964,4125123 | 45,147 | 11,553 |
| ALV. 2 M 9.19 E2 | M | h | 0,046 | 0,046 | 0,054 | 484,2155275 | 540,8159304 | 22,247 | 8,389 |

Table A.10: Elements concentrations(mg/kg) in males hepatopancreas and muscle tissues.

| Sample Name | Sex | Tissue | Tl | V | Zn |
|---|---|---|---|---|---|
| ALV. 1 M 6.19 M1 | M | m | <DL | 0,224 | 15,659 |
| ALV. 1 M 6.19 M2 | M | m | 0,0000 | 0,033 | 20,725 |
| ALV. 1 M 6.19 M3 | M | m | <DL | 0,150 | 12,461 |
| ALV. 1 M 7.19 M1 | M | m | <DL | 0,021 | 18,674 |
| ALV. 1 M 7.19 M2 | M | m | 0,0013 | 0,006 | 15,700 |
| ALV. 1 M 7.19 M3 | M | m | 0,0015 | 0,031 | 13,722 |
| ALV. 1 M 8.19 M2 | M | m | 0,0001 | 0,050 | 14,025 |
| ALV. 1 M 8.19 M3 | M | m | <DL | 0,018 | 10,650 |
| ALV. 1 M 8.19 M4 | M | m | <DL | 0,013 | 12,420 |
| ALV. 1 M 8.19 M5 | M | m | <DL | 0,018 | 16,667 |
| ALV. 1 M 8.19 M6 | M | m | <DL | 0,032 | 14,384 |
| ALV. 1 M 8.19 M7 | M | m | <DL | 0,018 | 13,489 |
| ALV. 1 M 8.19 M8 | M | m | <DL | 0,013 | 9,551 |
| ALV. 1 M 8.19 M9 | M | m | <DL | 0,016 | 18,204 |
| ALV. 1 M 8.19 M10 | M | m | <DL | 0,025 | 13,964 |
| ALV. 1 M 8.19 M11 | M | m | <DL | 0,026 | 12,372 |
| ALV. 1 M 8.19 M12 | M | m | <DL | 0,019 | 19,753 |
| ALV. 1 M 8.19 M13 | M | m | <DL | 0,023 | 11,780 |
| ALV. 1 M 8.19 M14 | M | m | 0,0093 | 0,005 | 6,811 |
| ALV. 1 M 8.19 M15 | M | m | 0,0013 | 0,011 | 17,339 |
| ALV. 1 M 9.19 M1 | M | m | 0,0002 | 0,015 | 14,150 |
| ALV. 1 M 9.19 M2 | M | m | 0,0004 | 0,014 | 11,786 |
| ALV. 1 M 9.19 M3 | M | m | 0,0001 | 0,017 | 13,924 |
| ALV. 2 M 7.19 M1 | M | m | 0,0016 | 0,023 | 20,475 |
| ALV. 2 M 7.19 M2 | M | m | <DL | 0,106 | 14,376 |
| ALV. 2 M 7.19 M3 | M | m | <DL | 0,017 | 17,943 |
| ALV. 2 M 8.19 M1 | M | m | 0,0006 | 0,013 | 17,819 |
| ALV. 2 M 9.19 M1 | M | m | <DL | 0,026 | 13,465 |
| ALV. 2 M 9.19 M2 | M | m | 0,0001 | 0,017 | 15,844 |
| ALV. 1 M 6.19 E1 | M | h | <DL | 0,101 | 58,650 |
| ALV. 1 M 6.19 E2 | M | h | <DL | 0,128 | 32,053 |
| ALV. 1 M 6.19 E3 | M | h | <DL | 0,052 | 7,705 |
| ALV. 1 M 7.19 E1 | M | h | 0,0026 | 0,097 | 11,156 |
| ALV. 1 M 7.19 E2 | M | h | 0,0041 | 0,012 | 15,479 |
| ALV. 1 M 7.19 E3 | M | h | 0,0050 | 0,022 | 11,797 |
| ALV. 1 M 8.19 E2 | M | h | 0,0004 | 0,031 | 12,551 |
| ALV. 1 M 8.19 E3 | M | h | 0,0008 | 0,014 | 6,174 |
| ALV. 1 M 8.19 E4 | M | h | 0,0014 | 0,057 | 12,313 |
| ALV. 1 M 8.19 E5 | M | h | 0,0007 | 0,018 | 25,083 |
| ALV. 1 M 8.19 E6 | M | h | 0,0009 | 0,058 | 13,003 |
| ALV. 1 M 8.19 E7 | M | h | 0,0010 | 0,068 | 8,555 |
| ALV. 1 M 8.19 E8 | M | h | 0,0006 | 0,072 | 10,215 |
| ALV. 1 M 8.19 E9 | M | h | 0,0000 | 0,023 | 5,547 |
| ALV. 1 M 8.19 E10 | M | h | 0,0004 | 0,034 | 15,316 |
| ALV. 1 M 8.19 E11 | M | h | 0,0009 | 0,040 | 10,713 |
| ALV. 1 M 8.19 E12 | M | h | 0,0006 | 0,038 | 6,073 |
| ALV. 1 M 8.19 E13 | M | h | 0,0004 | 0,006 | 2,012 |
| ALV. 1 M 8.19 E14 | M | h | 0,0002 | 0,026 | 6,811 |
| ALV. 1 M 8.19 E15 | M | h | 0,0001 | 0,034 | 7,779 |
| ALV. 2 M 7.19 E1 | M | h | 0,0079 | 0,010 | 29,163 |
| ALV. 2 M 7.19 E2 | M | h | <DL | 0,075 | 28,230 |
| ALV. 2 M 7.19 E3 | M | h | 0,0000 | 0,045 | 13,167 |
| ALV. 2 M 8.19 E1 | M | h | 0,0004 | 0,024 | 12,562 |
| ALV. 2 M 9.19 E1 | M | h | 0,0014 | 0,094 | 38,603 |
| ALV. 2 M 9.19 E2 | M | h | 0,0006 | 0,013 | 27,891 |

60

## A.3  Other Data

Table A.11: Blanck, LOD and BEC for every element detected.

| | blank | LOD | BEC |
|---|---|---|---|
| Hg | 2,0255E-11 | 1,83439E-06 | 3,37403E-06 |
| Ag | 2,95505E-11 | 9,98463E-07 | 1,81006E-06 |
| Al | 1,51094E-09 | 0,000119378 | 0,000273011 |
| As | 4,71745E-09 | 1,54377E-06 | 7,63991E-06 |
| B | 4,55306E-09 | 0,000184689 | 0,000235547 |
| Ba | 3,69905E-10 | 4,3823E-06 | 1,40202E-05 |
| Be [No Gas] | 8,2924E-12 | 0,0000009 | 2,17722E-07 |
| Be [He] | 7,34841E-11 | 2,09741E-05 | 4,03646E-06 |
| Ca | 2,82777E-09 | 0,000258511 | 0,000949723 |
| Cd | 3,38791E-13 | 8,46624E-07 | 1,62933E-07 |
| Co | 5,49521E-11 | 3,83485E-09 | 2,65009E-07 |
| Cr | 3,33669E-09 | 3,85381E-06 | 1,78237E-05 |
| Cs | 5,903E-11 | 5,57734E-07 | 2,30612E-06 |
| Cu | 6,7533E-09 | 5,00735E-06 | 1,73658E-05 |
| Fe [He] | 6,12649E-08 | 1,01971E-05 | 0,00044106 |
| Fe [O2] | 6,04217E-10 | 1,09523E-05 | 0,000212916 |
| Ga | 1,78266E-12 | 1,1125E-06 | 2,14101E-07 |
| K | 1,96735E-07 | 0,000885362 | 0,014044422 |
| Li [No Gas] | 1,28036E-07 | 0,000387188 | 0,001486685 |
| Li [He] | 1,00303E-07 | 0,000346815 | 0,001447383 |
| Mg | 1,12131E-09 | 4,35519E-05 | 0,000100657 |
| Mn | 4,42461E-10 | 1,96455E-06 | 2,34695E-06 |
| Na | 1,05499E-07 | 0,000757013 | 0,005738938 |
| Ni | 1,3811E-09 | 8,308E-06 | 1,18327E-05 |
| P | 3,31722E-10 | 8,77145E-06 | 0,000356353 |
| Pb [206 He] | 1,10289E-10 | 2,2422E-06 | 9,29442E-06 |
| Pb [207 He] | 1,09582E-10 | 3,34748E-06 | 1,05844E-05 |
| Pb [208 He] | 2,56475E-10 | 1,92498E-06 | 9,61753E-06 |
| Rb | 1,92E-10 | 1,70338E-06 | 1,74774E-06 |
| S [32–>48 O2] | 4,17977E-09 | 0,000103426 | 0,002567758 |
| S [34–>50 O2] | 3,38917E-10 | 3,41462E-05 | 0,004076492 |
| Si | 4,48981E-09 | 6,02674E-05 | 0,00152253 |
| Sr | 1,12715E-10 | 9,345832E-07 | 1,196012E-05 |
| TI | 1,11039E-11 | 4,93195E-08 | 2,45594E-07 |
| V | 3,70275E-11 | 8,43923E-09 | 2,57059E-07 |
| Zn | 7,59703E-09 | 2,70913E-05 | 8,75219E-05 |
| Sn | 1,3902E-11 | 0,021915541 | 0,016787822 |

Table A.12: Standard concentrations in every element detected.

| (ppm) | STD-FISH1 | STD-FISH2 | STD-FISH3 | STD-FISH4 | mean STD | SD |
|---|---|---|---|---|---|---|
| Hg | 0,490 | 0,525 | 0,475 | 0,420 | 0,478 | 0,043 |
| Ag | 0,003 | 0,003 | 0,006 | 0,007 | 0,005 | 0,002 |
| Al | 0,254 | 0,359 | 0,851 | 0,382 | 0,461 | 0,265 |
| As | 8,864 | 9,183 | 8,779 | 8,081 | 8,727 | 0,465 |
| B | 0,610 | 0,648 | 0,577 | 0,651 | 0,622 | 0,035 |
| Ba | 0,096 | 0,020 | 0,271 | 0,166 | 0,138 | 0,107 |
| Be [No Gas] | 0,005 | 0,004 | 0,004 | 0,005 | 0,005 | 0,001 |
| Be [He] | 0,000 | 0,003 | 0,003 | 0,000 | 0,001 | 0,002 |
| Ca | 65,042 | 70,720 | 65,194 | 53,804 | 63,690 | 7,100 |
| Cd | 0,008 | 0,009 | 0,007 | 0,004 | 0,007 | 0,002 |
| Co | 0,014 | 0,015 | 0,012 | 0,011 | 0,013 | 0,001 |
| Cr | 0,024 | 0,026 | 0,039 | 0,065 | 0,038 | 0,019 |
| Cs | 0,138 | 0,140 | 0,139 | 0,118 | 0,134 | 0,011 |
| Cu | 1,622 | 1,519 | 8,901 | 8,594 | 5,159 | 4,146 |
| Fe [He] | 5,964 | 7,019 | 6,750 | 5,748 | 6,370 | 0,610 |
| Fe [O2] | 4,908 | 5,767 | 5,499 | 5,178 | 5,338 | 0,374 |
| Ga | 0,001 | 0,001 | 0,000 | 0,001 | 0,001 | 0,000 |
| Li [He] | 0,099 | 0,073 | 0,000 | 0,062 | 0,058 | 0,042 |
| Mg | 804,898 | 849,897 | 798,827 | 696,948 | 787,642 | 64,612 |
| Mn | 0,244 | 0,273 | 0,259 | 0,219 | 0,249 | 0,023 |
| Na | 835,657 | 868,682 | 845,598 | 749,588 | 824,881 | 52,067 |
| Ni | 0,051 | 0,050 | 0,071 | 0,055 | 0,057 | 0,010 |
| P | 6997,818 | 7478,344 | 6704,825 | 6438,704 | 6904,923 | 445,287 |
| Pb [206 He] | 0,028 | 0,022 | 0,339 | 0,331 | 0,180 | 0,179 |
| Pb [207 He] | 0,028 | 0,028 | 0,349 | 0,311 | 0,179 | 0,175 |
| Pb [208 He] | 0,034 | 0,023 | 0,341 | 0,312 | 0,177 | 0,172 |
| Rb | 2,677 | 2,859 | 2,714 | 2,294 | 2,636 | 0,241 |
| S [32–>48 O2] | 6791,612 | 6782,419 | 6268,712 | 6103,476 | 6486,555 | 353,459 |
| S [34–>50 O2] | 7138,702 | 7363,642 | 6880,096 | 6748,210 | 7032,663 | 273,850 |
| Si | 7,465 | 5,729 | 14,012 | 12,206 | 9,853 | 3,896 |
| Sr | 0,926 | 0,994 | 0,962 | 0,803 | 0,922 | 0,083 |
| TI | 0,002 | 0,002 | 0,002 | 0,001 | 0,002 | 0,000 |
| V | 0,018 | 0,016 | 0,021 | 0,013 | 0,017 | 0,003 |
| Zn | 12,385 | 14,092 | 17,408 | 15,440 | 14,831 | 2,124 |
| Sn | 58,506 | 28,664 | 195,461 | 180,356 | 115,747 | 84,436 |

# Appendix B

# R Results

## B.1 Bartlett tests

Table B.1: Bartlett test tissue results for all the elements detected.

| Bartlett test | K - squared | df | P-value |
|---|---|---|---|
| *Hg* | 31.196 | 1 | <0.05 |
| *Ag* | 35.030 | 1 | <0.05 |
| *Al* | 0.024 | 1 | 0.877 |
| *As* | 63.755 | 1 | <0.05 |
| **B** | 0.589 | 1 | 0.443 |
| **Ba** | 50.383 | 1 | 0.000 |
| **Be (No gas)** | 26.084 | 1 | 0.000 |
| **Be (He)** | 35.485 | 1 | 0.000 |
| **Ca** | 32.886 | 1 | 0.000 |
| **Cd** | 222.510 | 1 | <0.05 |
| *Co* | 119.830 | 1 | <0.05 |
| **Cr** | 160.080 | 1 | <0.05 |
| **Cs** | 34.447 | 1 | <0.05 |
| **Cu** | 10.731 | 1 | 0.001 |
| **Fe (He)** | 175.700 | 1 | <0.05 |
| **Fe ($O_2$)** | 169.360 | 1 | <0.05 |
| **Ga** | 0.515 | 1 | 0.473 |
| **K** | 15.330 | 1 | <0.05 |
| **Li** | 29.930 | 1 | <0.05 |
| **Mg** | 0.848 | 1 | 0.357 |
| **Mn** | 165.190 | 1 | <0.05 |
| **Na** | 2.878 | 1 | 0.090 |
| **Ni** | 87.737 | 1 | <0.05 |
| **P** | 0.938 | 1 | 0.333 |
| **Pb (206 ->206)** | 80.228 | 1 | <0.05 |
| **Pb (207 ->207)** | 83.967 | 1 | <0.05 |
| **Pb (208 ->208)** | 81.764 | 1 | <0.05 |
| **S (32 ->48)** | 0.204 | 1 | 0.652 |
| **S (34 ->50)** | 0.175 | 1 | 0.675 |
| **Si** | 28.530 | 1 | <0.05 |
| **Sr** | 22.814 | 1 | <0.05 |
| **Tl** | 0.610 | 1 | 0.435 |
| **V** | 3.826 | 1 | 0.050 |
| **Zn** | 57.997 | 1 | <0.05 |

Table B.2: Bartlett test sex results for all the elements detected.

| Bartlett test | K - squared | df | P-value |
|---|---|---|---|
| *Hg* | 6.029 | 1 | 0.014 |
| *Ag* | 46.732 | 1 | <0.05 |
| *Al* | 11.475 | 1 | 0.001 |
| *As* | 2.510 | 1 | 0.113 |
| **B** | 4.256 | 1 | 0.039 |
| **Ba** | 3.184 | 1 | 0.074 |
| **Be (No gas)** | 1.538 | 1 | 0.215 |
| **Be (He)** | 0.002 | 1 | 0.968 |
| **Ca** | 0.017 | 1 | 0.895 |
| **Cd** | 0.262 | 1 | 0.609 |
| *Co* | 10.253 | 1 | 0.001 |
| **Cr** | 7.316 | 1 | 0.007 |
| **Cs** | 7.785 | 1 | 0.005 |
| **Cu** | 0.155 | 1 | 0.694 |
| **Fe (He)** | 3.213 | 1 | 0.073 |
| **Fe ($O_2$)** | 2.537 | 1 | 0.111 |
| **Ga** | 0.081 | 1 | 0.776 |
| **K** | 0.065 | 1 | 0.799 |
| **Li** | 6.973 | 1 | 0.008 |
| **Mg** | 0.757 | 1 | 0.384 |
| **Mn** | 22.429 | 1 | <0.05 |
| **Na** | 1.608 | 1 | 0.205 |
| **Ni** | 8.138 | 1 | 0.004 |
| **P** | 0.133 | 1 | 0.715 |
| **Pb (206 ->206)** | 127.800 | 1 | <0.05 |
| **Pb (207 ->207)** | 133.940 | 1 | <0.05 |
| **Pb (208 ->208)** | 133.490 | 1 | <0.05 |
| **S (32 ->48)** | 0.563 | 1 | 0.453 |
| **S (34 ->50)** | 0.284 | 1 | 0.594 |
| **Si** | 0.955 | 1 | 0.328 |
| **Sr** | 0.046 | 1 | 0.830 |
| **Tl** | 0.234 | 1 | 0.629 |
| **V** | 2.412 | 1 | 0.120 |
| **Zn** | 2.172 | 1 | 0.141 |

## B.2 Histograms
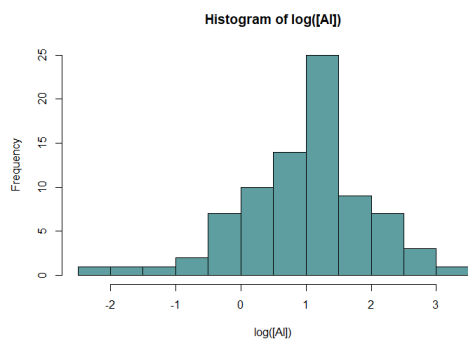


Figure B.1: Histogram of log([Al]).
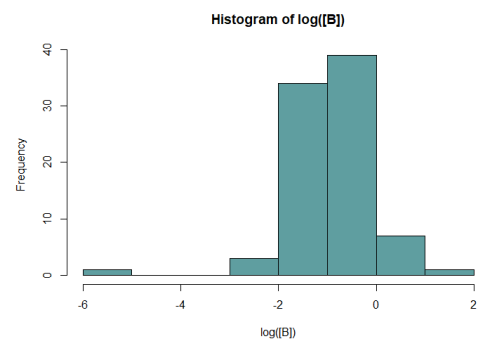


Figure B.4: Histogram of log([B]).
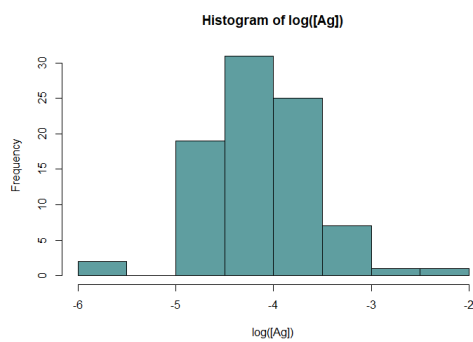


Figure B.2: Histogram of log([Ag]).
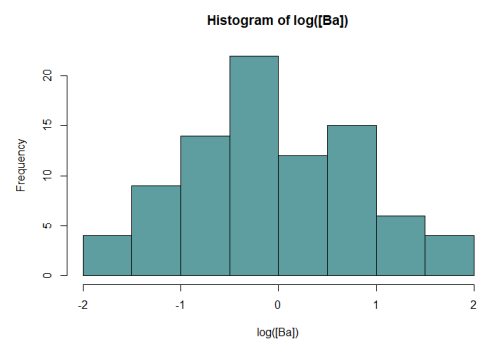


Figure B.5: Histogram of log([Ba]).
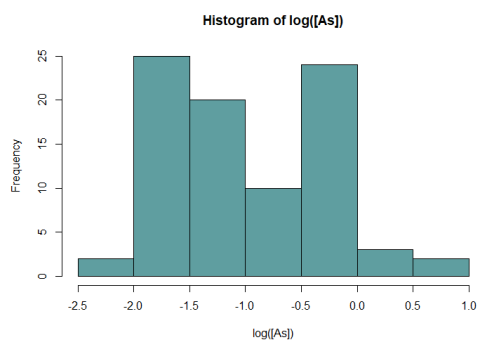


Figure B.3: Histogram of log([As]).
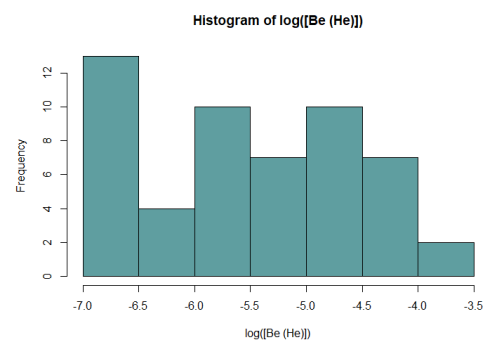


Figure B.6: Histogram of log([Be (He)]).
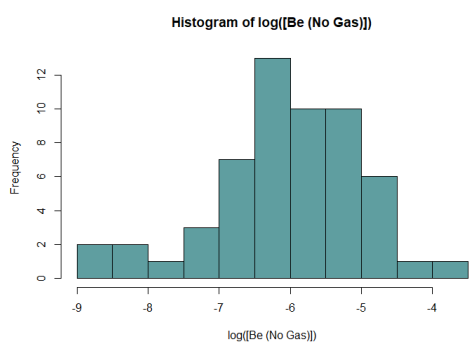
Figure B.7: Histogram of log([Be (No Gas)]).
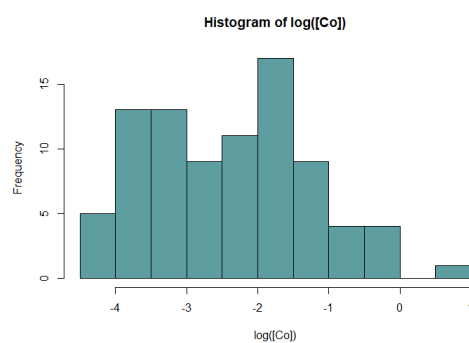


Figure B.10: Histogram of log([Co]).
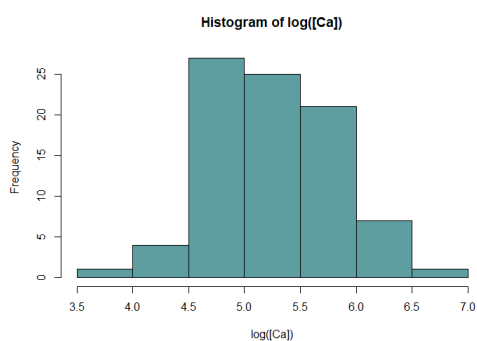


Figure B.8: Histogram of log([Ca]).
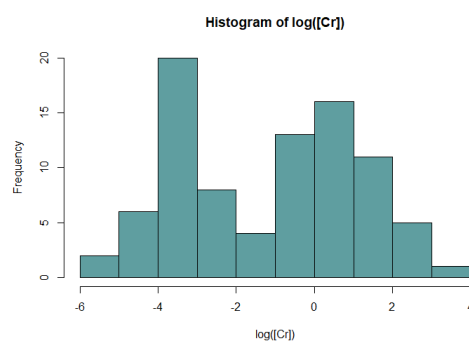


Figure B.11: Histogram of log([Cr]).
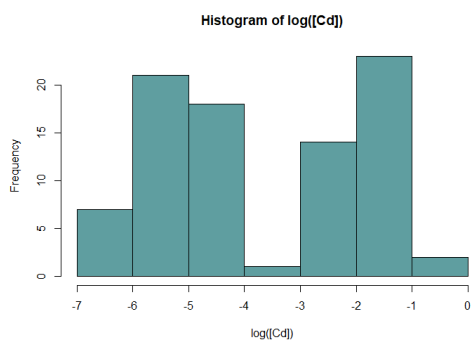


Figure B.9: Histogram of log([Cd]).
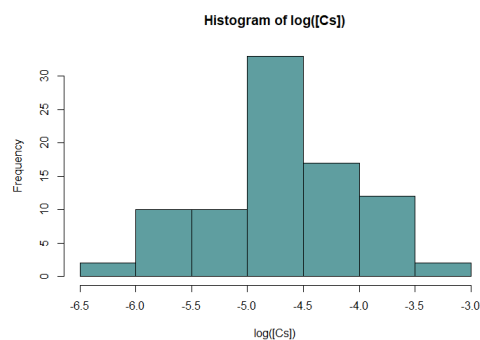


Figure B.12: Histogram of log([Cs]).

67
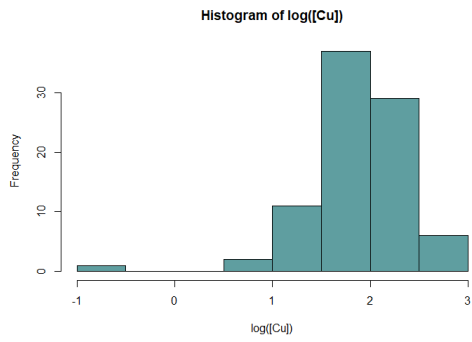
Figure B.13: Histogram of log([Cu]).
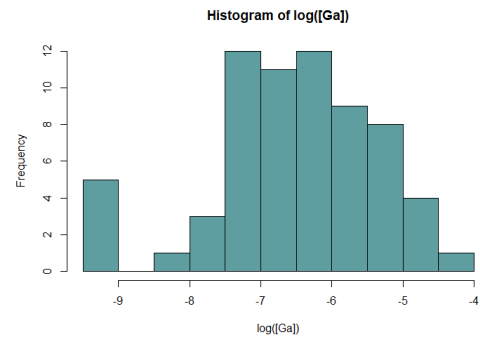


Figure B.16: Histogram of log([Ga]).
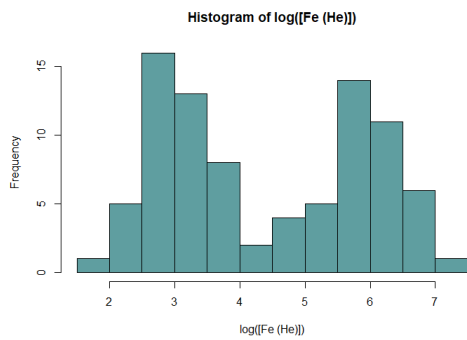


Figure B.14: Histogram of log([Fe (He)]).
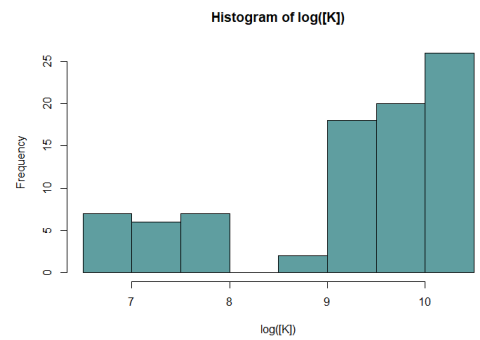


Figure B.17: Histogram of log([K]).
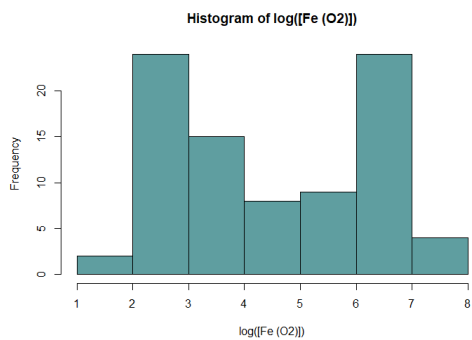


Figure B.15: Histogram of log([Fe $O_2$]).
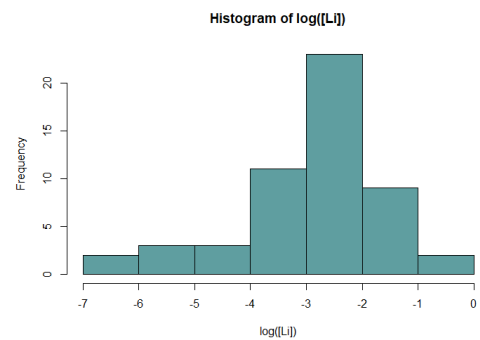


Figure B.18: Histogram of log([Li]).
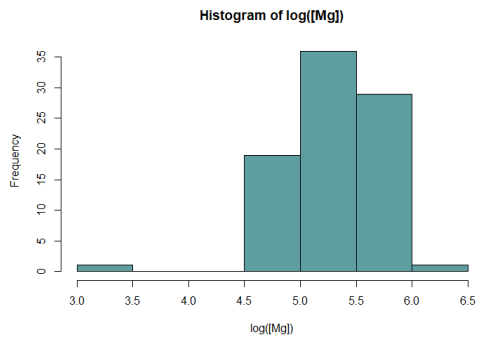
Figure B.19: Histogram of log([Mg]).
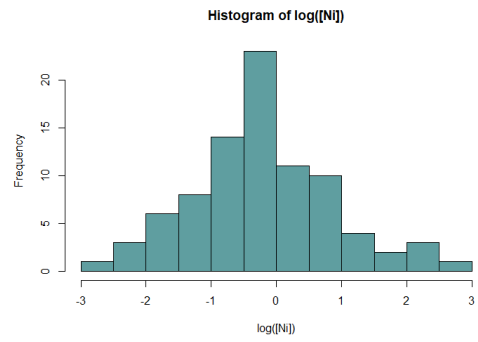


Figure B.22: Histogram of log([Ni]).
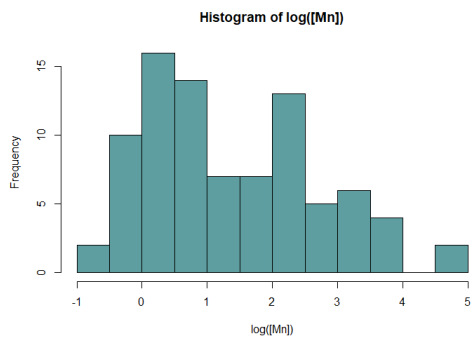


Figure B.20: Histogram of log([Mn]).
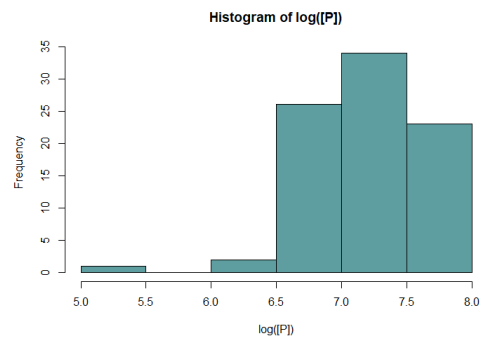


Figure B.23: Histogram of log([P]).
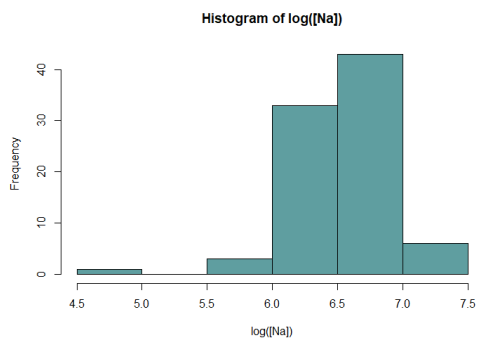


Figure B.21: Histogram of log([Na]).
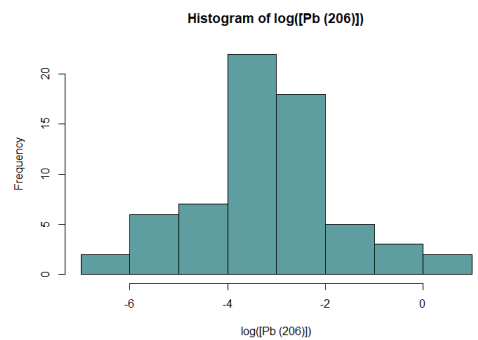


Figure B.24: Histogram of log([Pb (206)]).

69
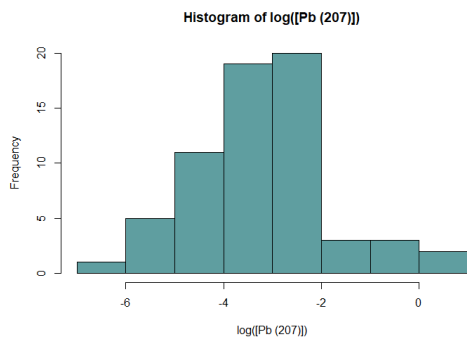
Figure B.25: Histogram of log([Pb (207)]).
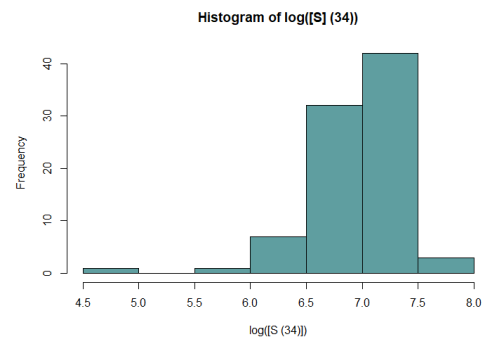


Figure B.28: Histogram of log([S (34)]).
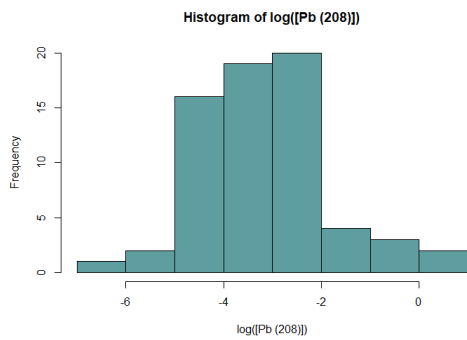


Figure B.26: Histogram of log([Pb (208)]).
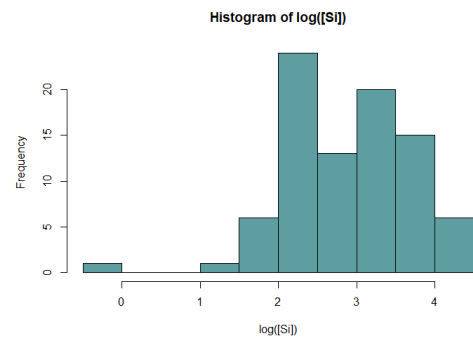


Figure B.29: Histogram of log([Si]).
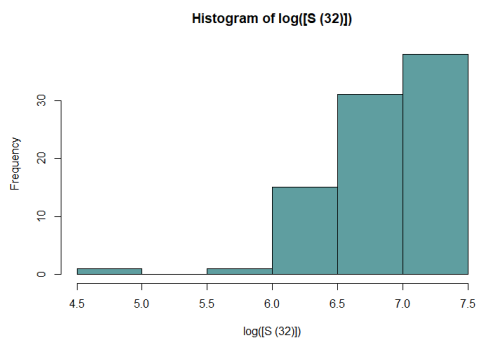


Figure B.27: Histogram of log([S (32)]).
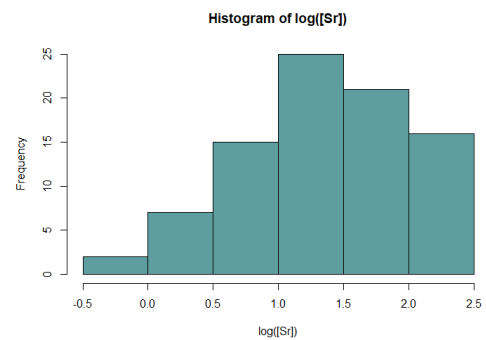


Figure B.30: Histogram of log([Sr]).

70
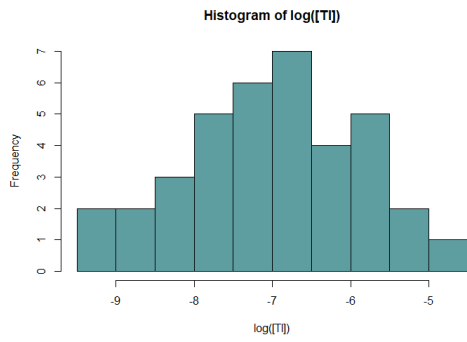
Figure B.31: Histogram of log([Tl]).
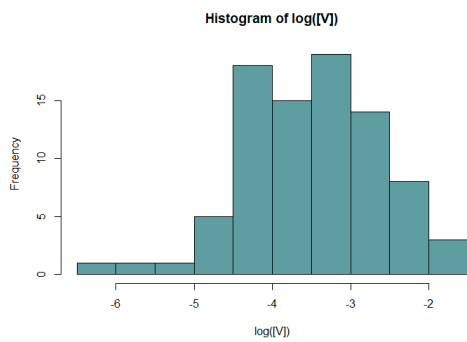


Figure B.32: Histogram of log([V]).
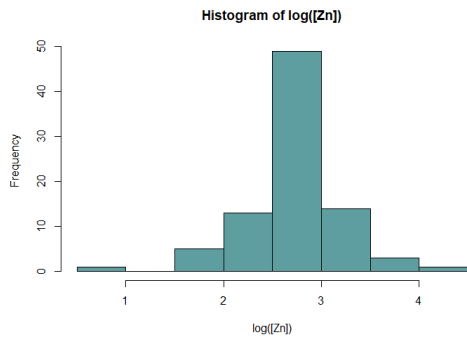


Figure B.33: Histogram of log([Zn]).

## B.3 Density plots
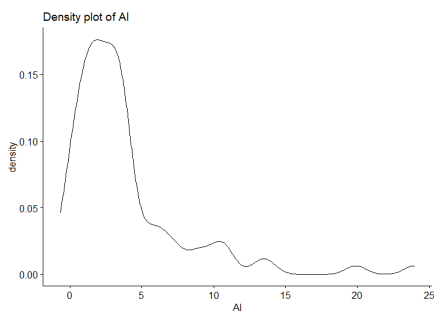
Figure B.34: Density plot of Al.
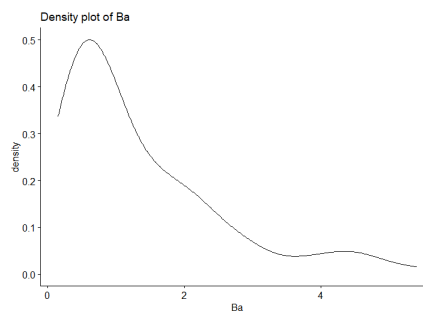
Figure B.38: Density plot of Ba.
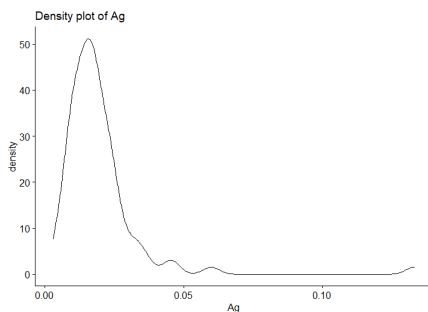
Figure B.35: Density plot of Ag.
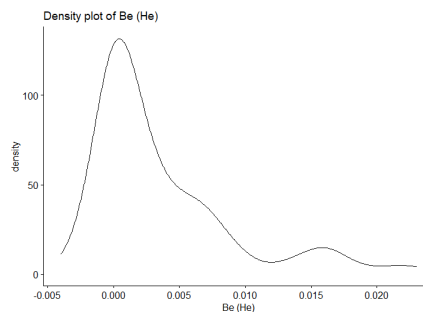
Figure B.39: Density plot of Be (He).
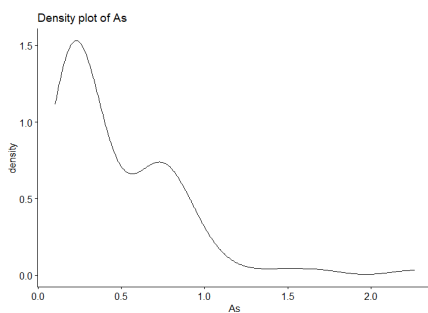
Figure B.36: Density plot of As.
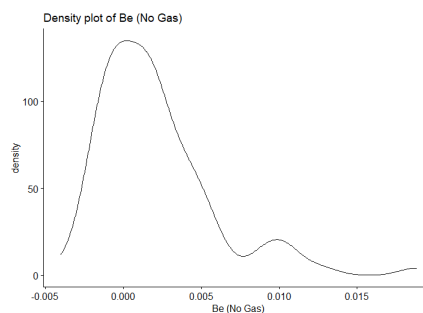
Figure B.40: Density plot of Be (No Gas).
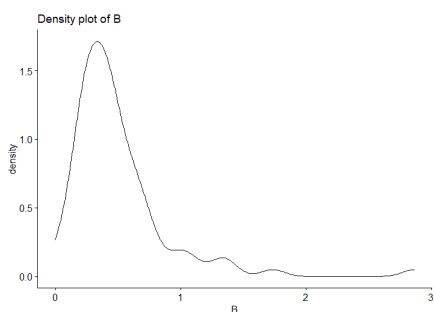
Figure B.37: Density plot of B.
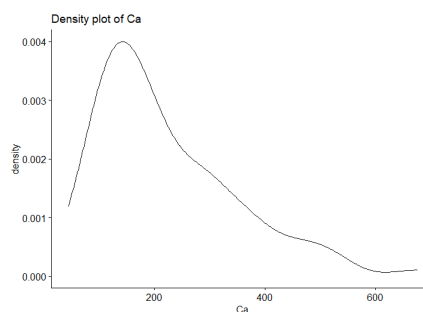
Figure B.41: Density plot of Ca.
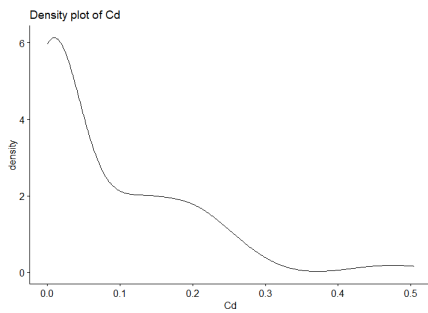
Figure B.42: Density plot of Cd.
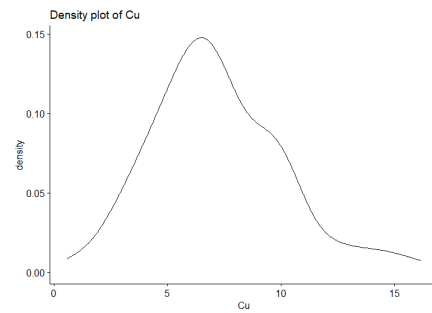


Figure B.46: Density plot of Cr.
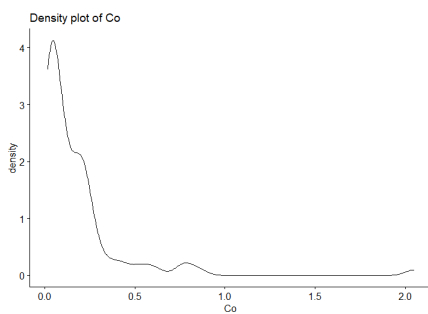


Figure B.43: Density plot of Co.
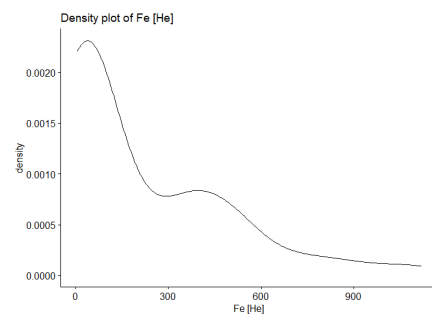


Figure B.47: Density plot of Fe (He).
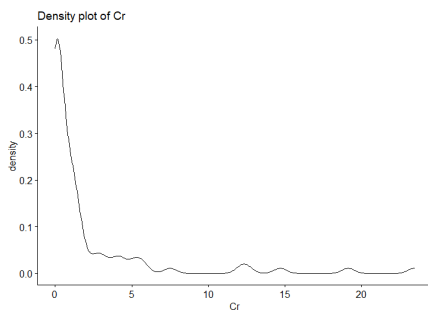


Figure B.44: Density plot of Cr.
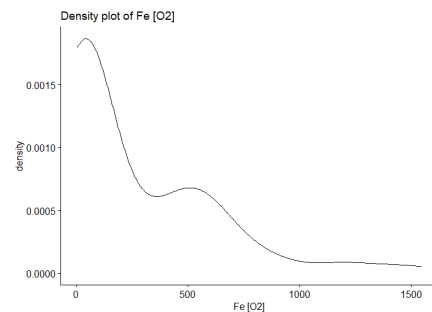


Figure B.48: Density plot of Fe (O$_2$).
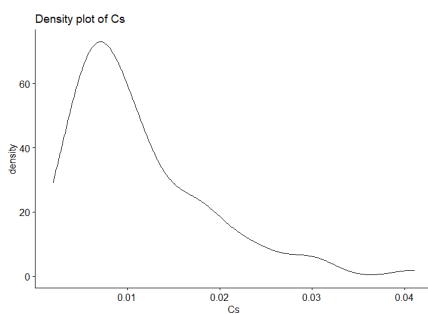


Figure B.45: Density plot of Cs.
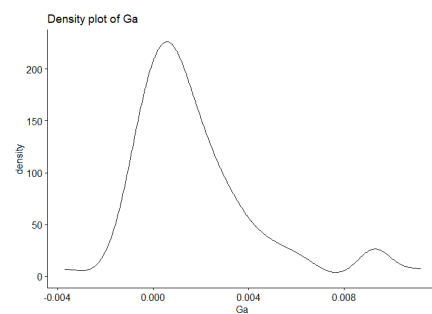


Figure B.49: Density plot of Ga.

73
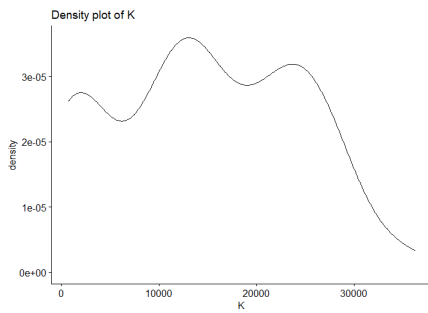
Figure B.50: Density plot of K.
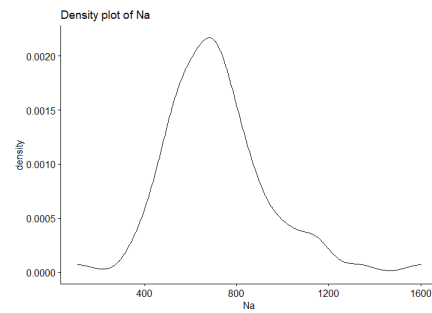


Figure B.54: Density plot of Na.
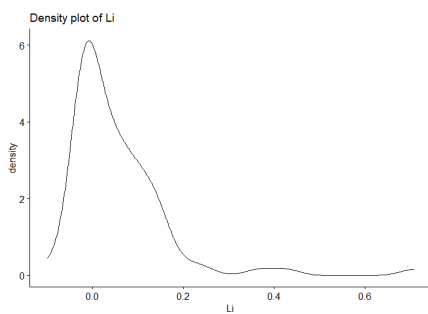


Figure B.51: Density plot of Li.
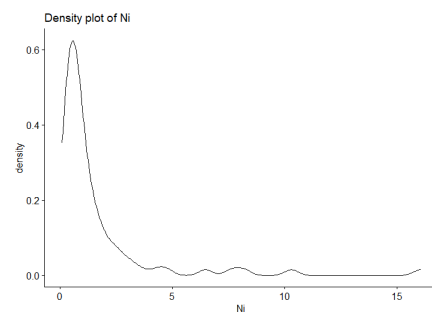


Figure B.55: Density plot of Ni.
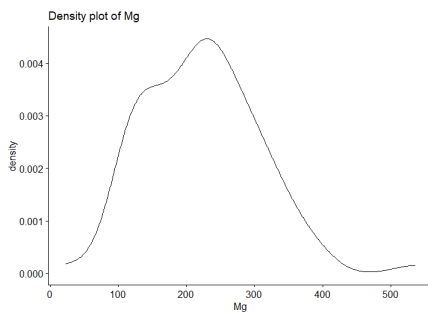


Figure B.52: Density plot of Mg.
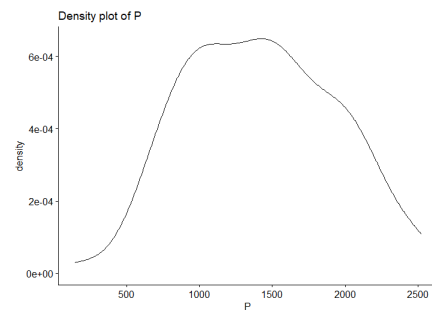


Figure B.56: Density plot of P.
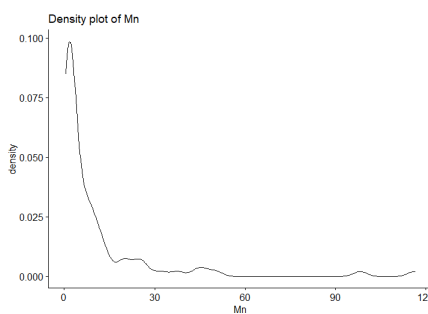


Figure B.53: Density plot of Mn.
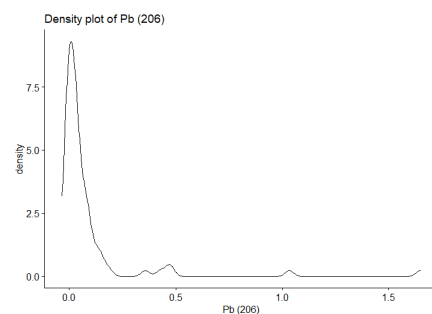


Figure B.57: Density plot of Pb (206).

74
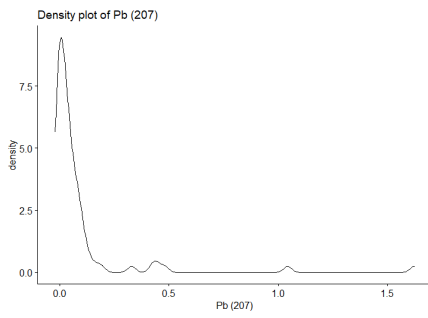
Figure B.58: Density plot of Pb (207).
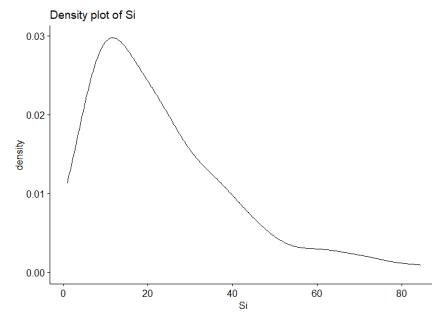


Figure B.62: Density plot of Si.
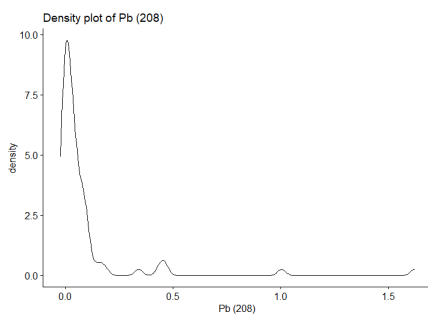


Figure B.59: Density plot of Pb (208).
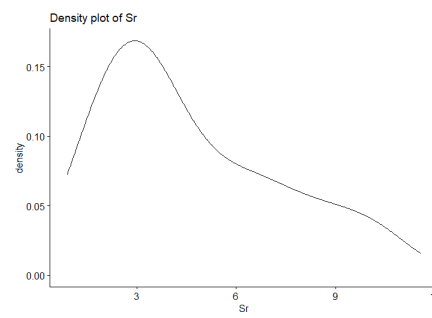


Figure B.63: Density plot of Sr.
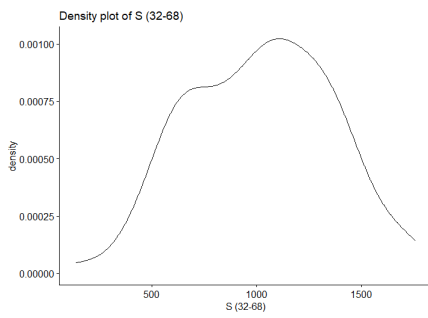


Figure B.60: Density plot of S (32 -> 68).
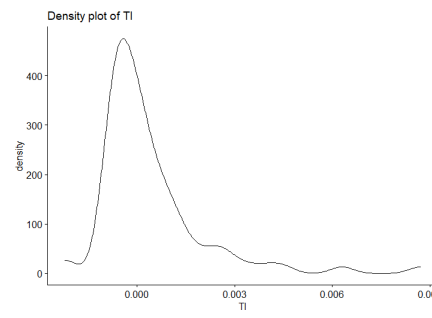


Figure B.64: Density plot of Tl.
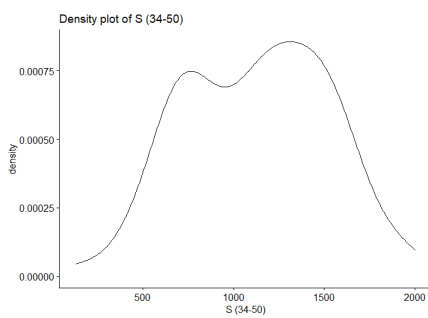


Figure B.61: Density plot of S (34 -> 50).
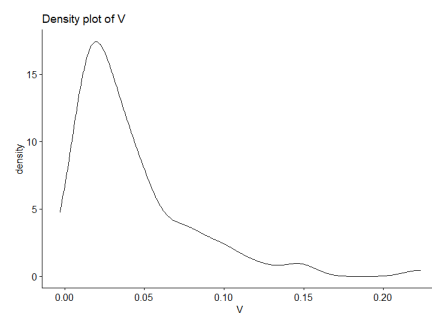


Figure B.65: Density plot of V.

75
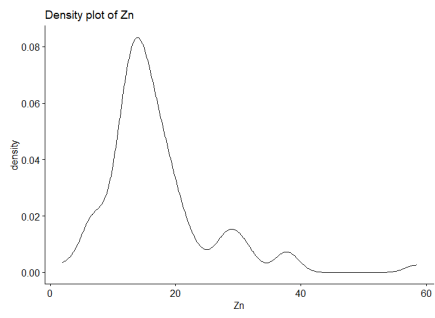
Figure B.66: Density plot of Zn.

# B.4 Quantile - Quantile plots
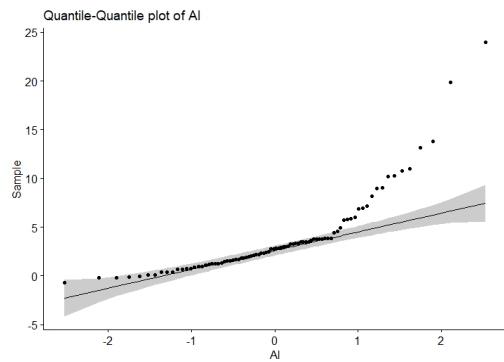


Figure B.67: Quantile - Quantile plot of Al.
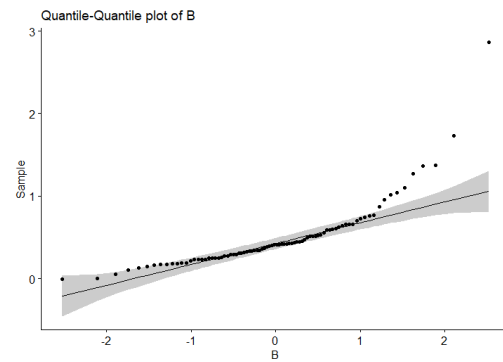
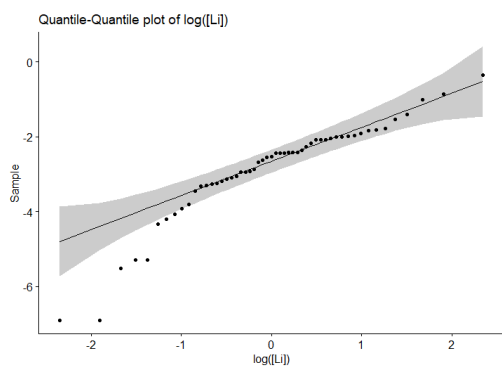

Figure B.70: Quantile - Quantile plot of B.
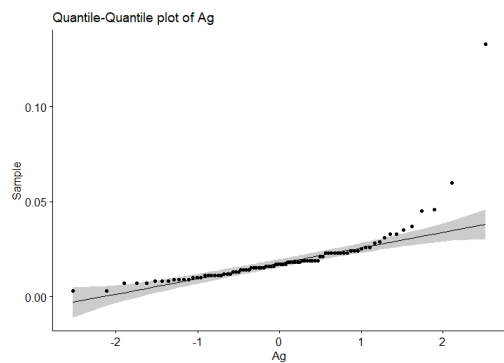


Figure B.68: Quantile - Quantile plot of Ag.
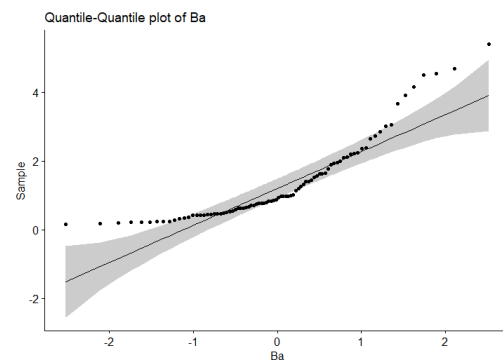


Figure B.71: Quantile - Quantile plot of Ba.
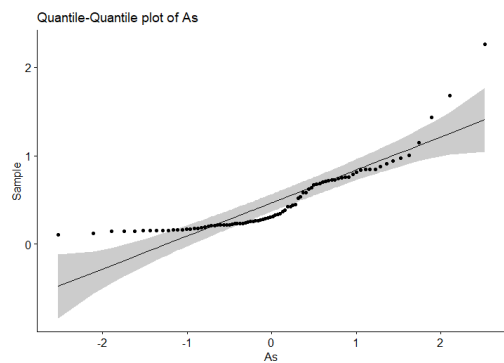


Figure B.69: Quantile - Quantile plot of As.
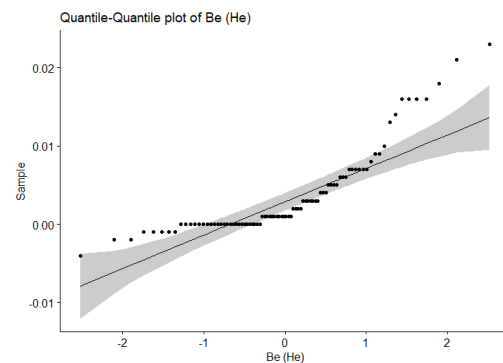


Figure B.72: Quantile - Quantile plot of Be (He).
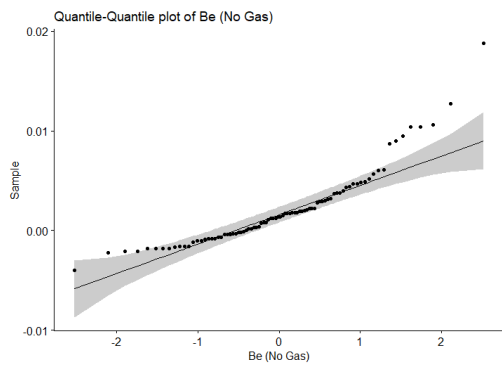
Figure B.73: Quantile - Quantile plot of Be (No Gas).



Figure B.74: Quantile - Quantile plot of Ca.



Figure B.75: Quantile - Quantile plot of Cd.



Figure B.76: Quantile - Quantile plot of Co.



Figure B.77: Quantile - Quantile plot of Cr.
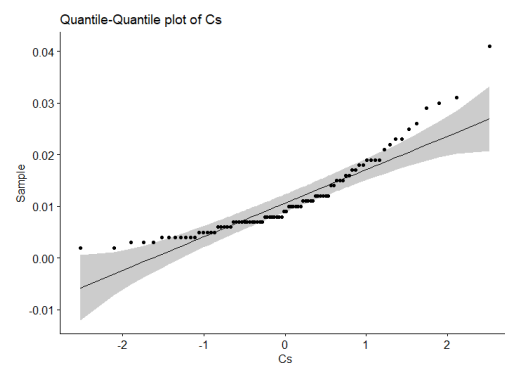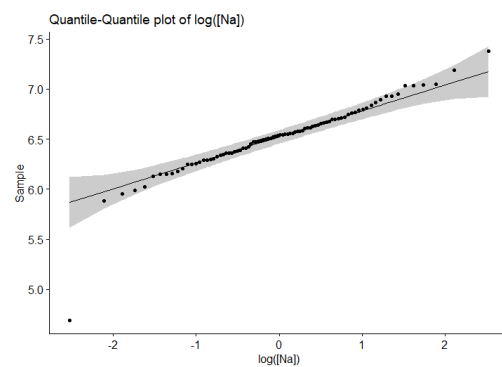


Figure B.78: Quantile - Quantile plot of Cs.

78
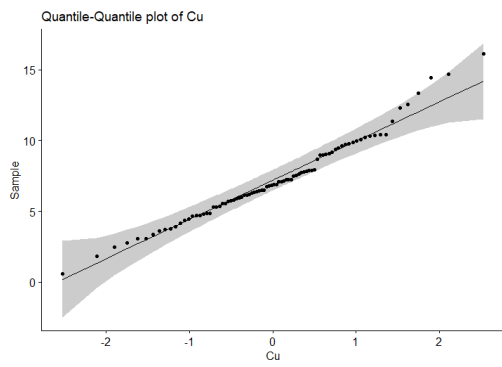
Figure B.79: Quantile - Quantile plot of Cr.
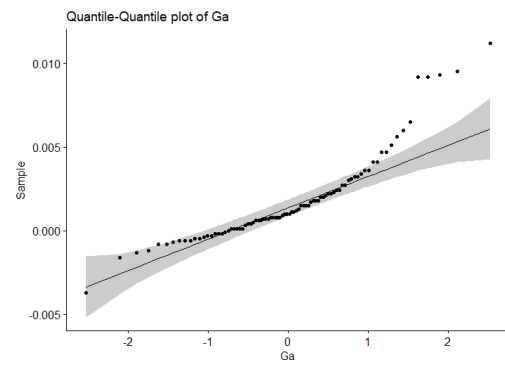


Figure B.82: Quantile - Quantile plot of Ga.
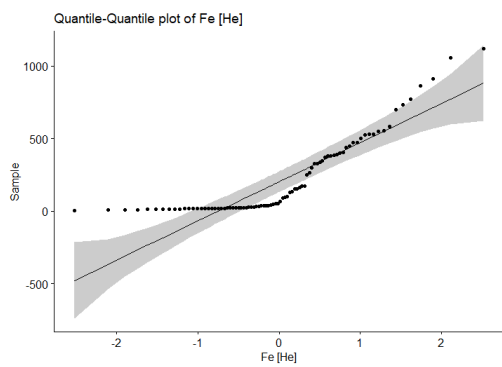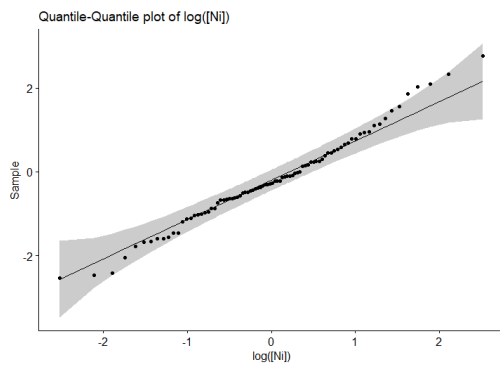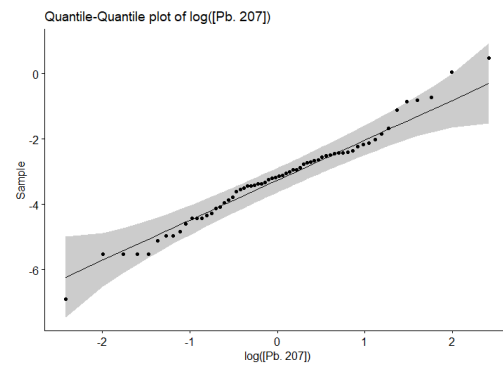


Figure B.80: Quantile - Quantile plot of Fe (He).
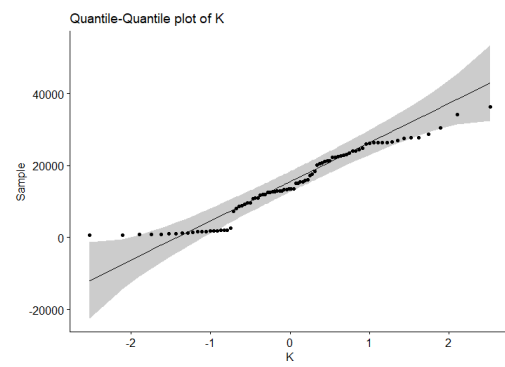


Figure B.83: Quantile - Quantile plot of K.
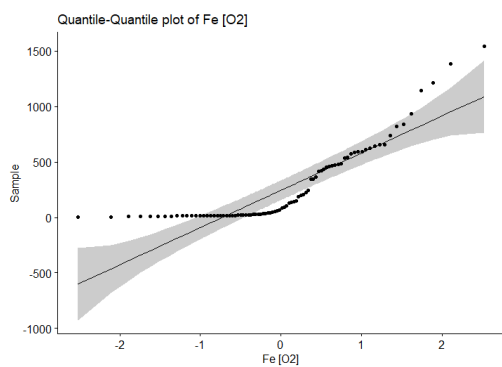


Figure B.81: Quantile - Quantile plot of Fe ($O_2$).
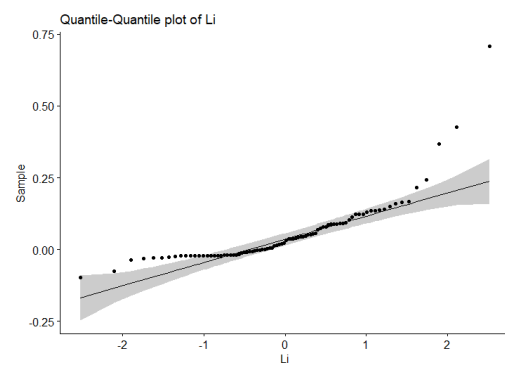


Figure B.84: Quantile - Quantile plot of Li.

79
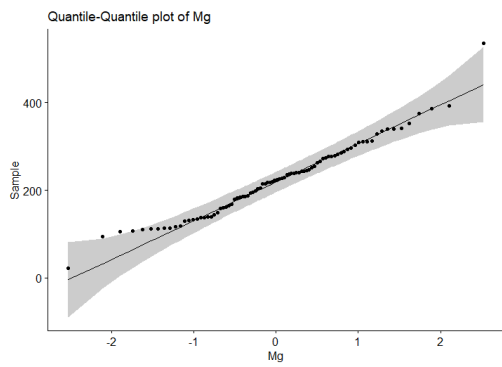
Figure B.85: Quantile - Quantile plot of Mg.
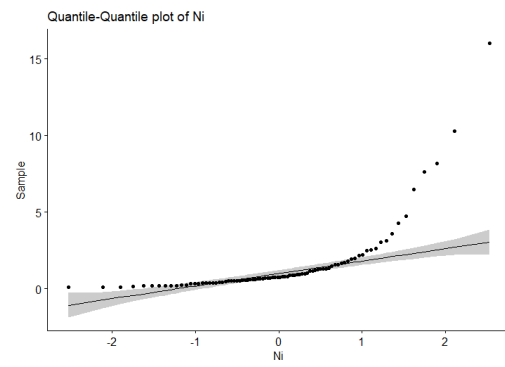


Figure B.88: Quantile - Quantile plot of Ni.
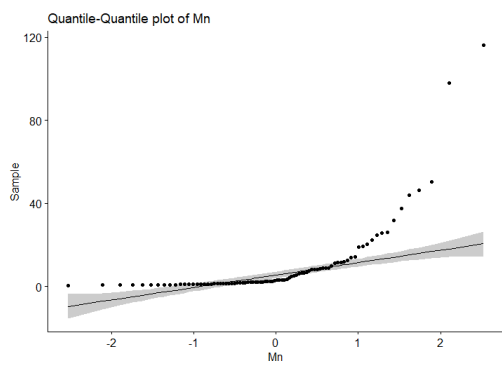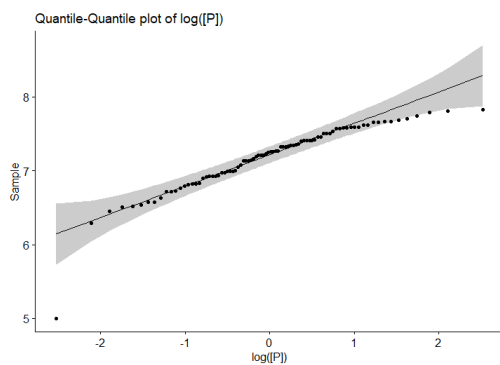


Figure B.86: Quantile - Quantile plot of Mn.
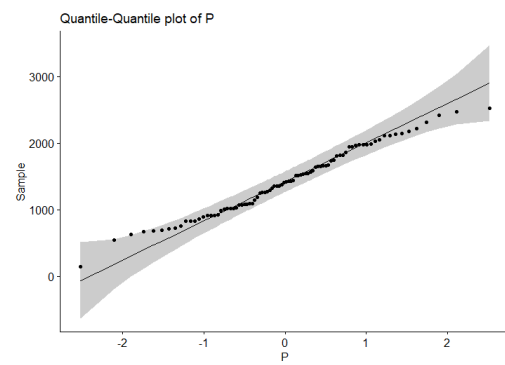


Figure B.89: Quantile - Quantile plot of P.
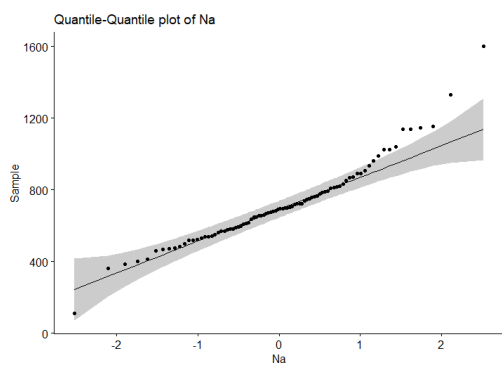


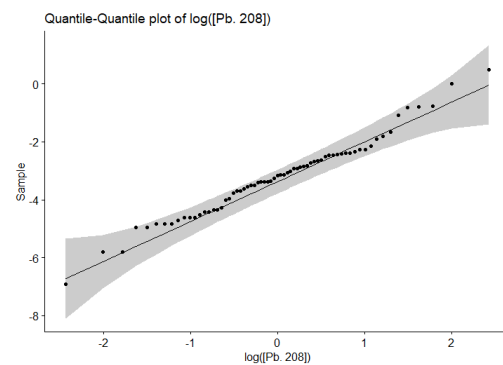Figure B.87: Quantile - Quantile plot of Na.
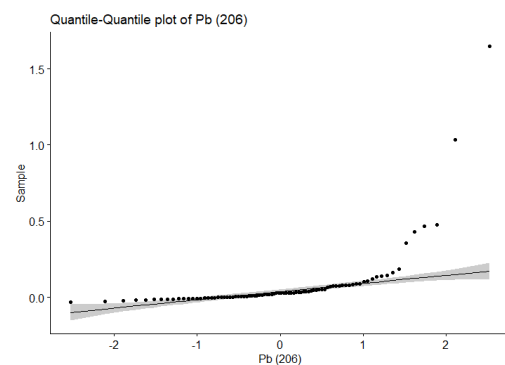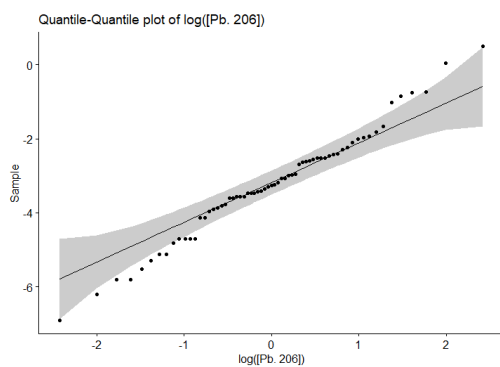


Figure B.90: Quantile - Quantile plot of Pb (206).

80
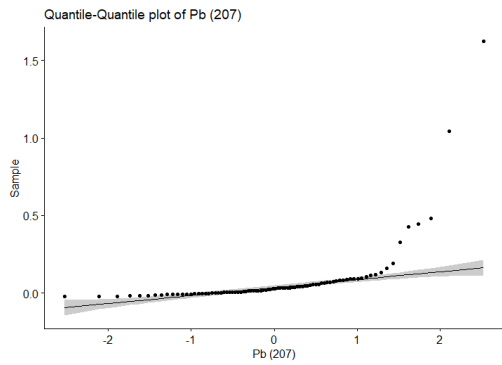
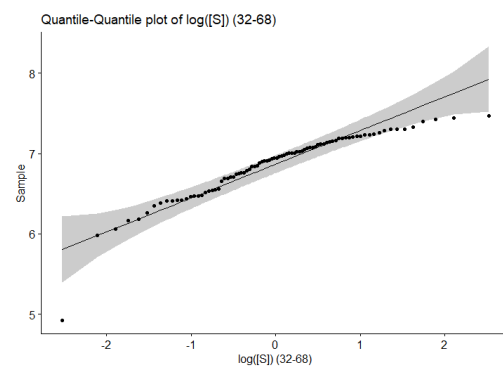Figure B.91: Quantile - Quantile plot of Pb (207).
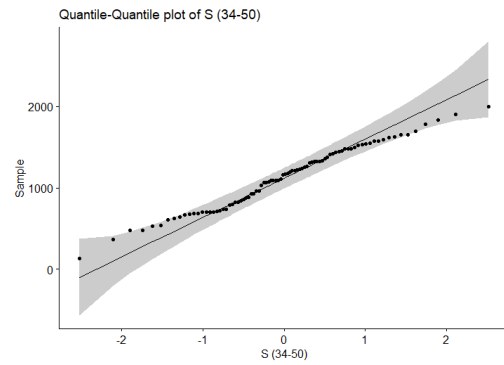


Figure B.94: Quantile - Quantile plot of S (34 -> 50).
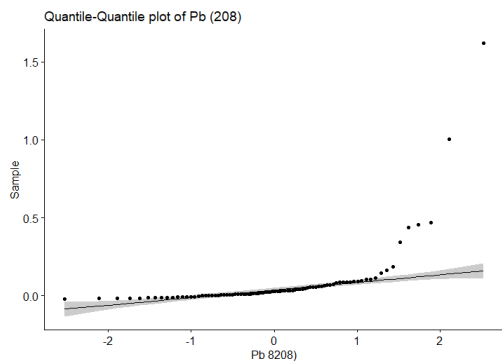


Figure B.92: Quantile - Quantile plot of Pb (208).
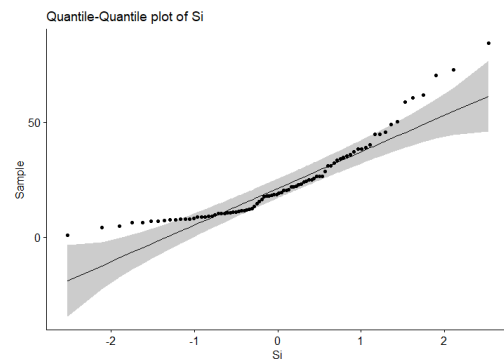


Figure B.95: Quantile - Quantile plot of Si.
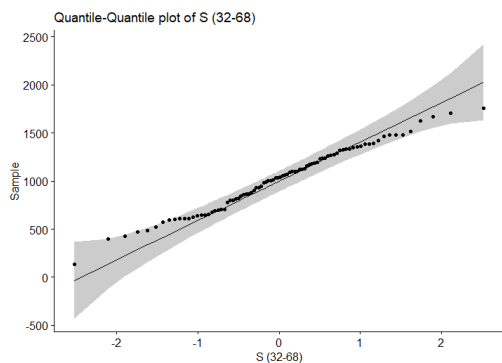


Figure B.93: Quantile - Quantile plot of S (32 -> 68).
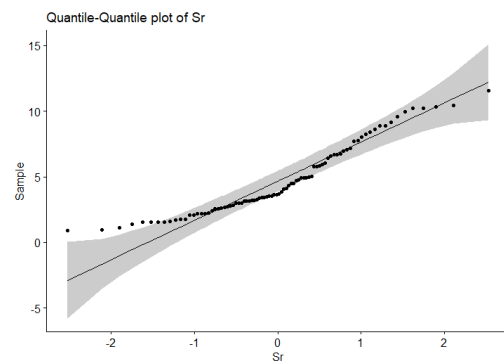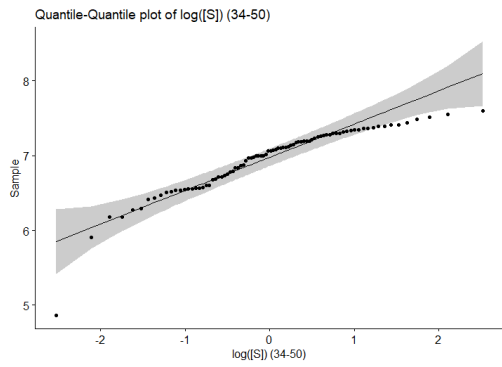


Figure B.96: Quantile - Quantile plot of Sr.

81
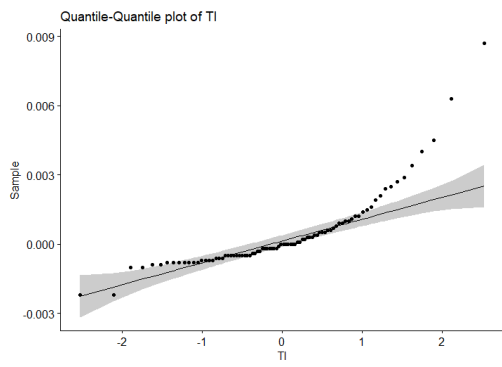
Figure B.97: Quantile - Quantile plot of Tl.
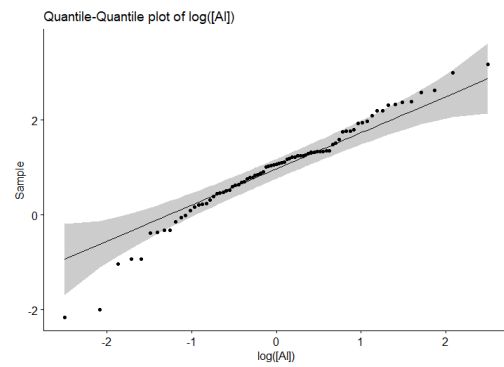


Figure B.100: Quantile - Quantile plot of log[Al].
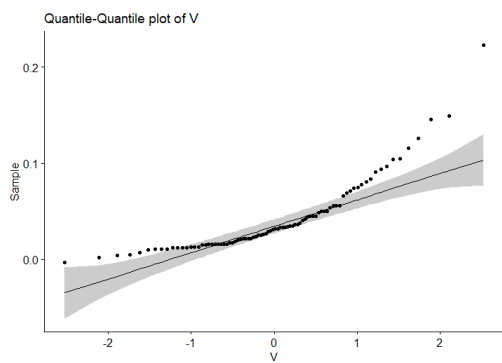


Figure B.98: Quantile - Quantile plot of V.
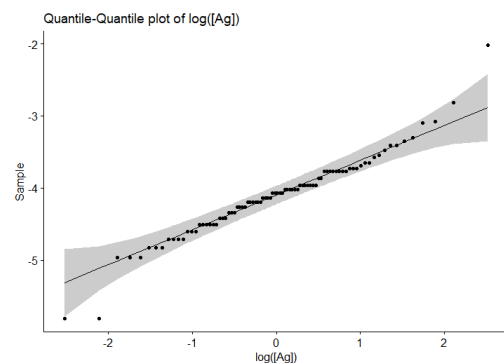


Figure B.101: Quantile - Quantile plot of log[Ag].
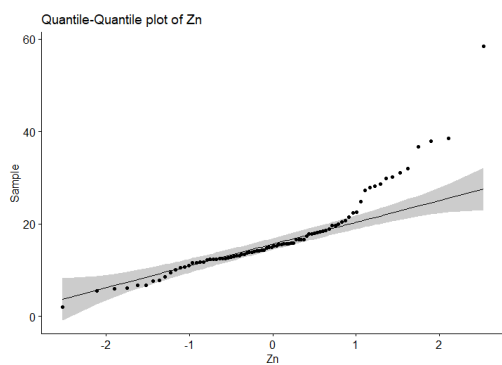
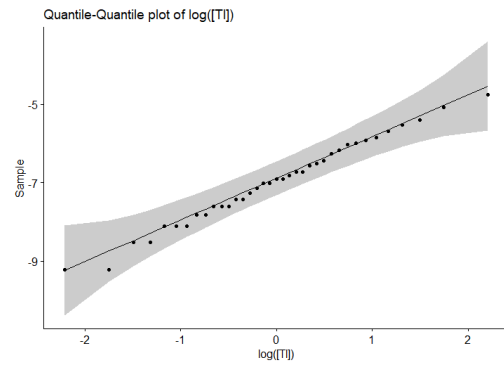

Figure B.99: Quantile - Quantile plot of Zn.
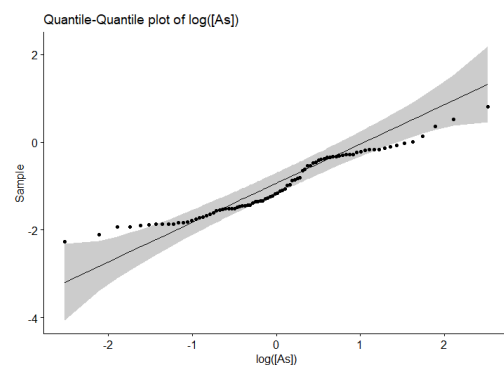


Figure B.102: Quantile - Quantile plot of log[As].

82
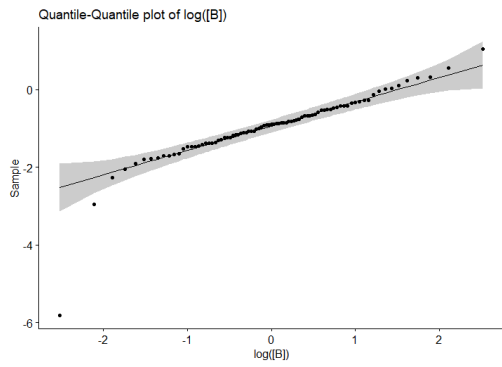
Figure B.103: Quantile - Quantile plot of log[B].
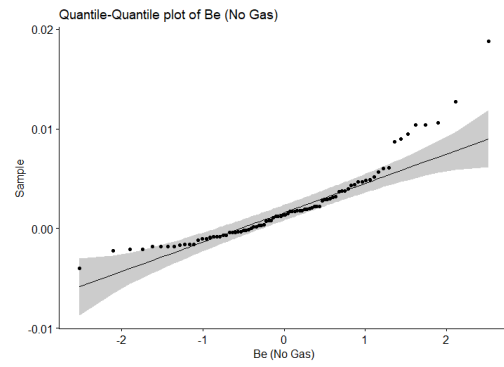


Figure B.106: Quantile - Quantile plot of log[Be. No.Gas].
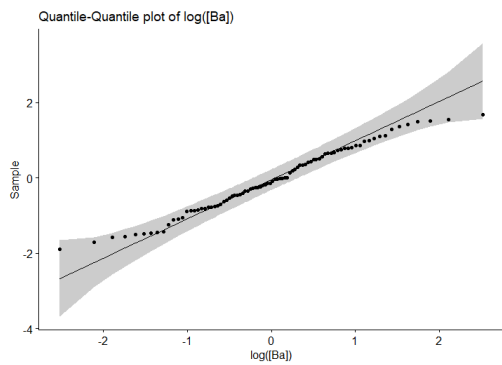


Figure B.104: Quantile - Quantile plot of log[Ba].
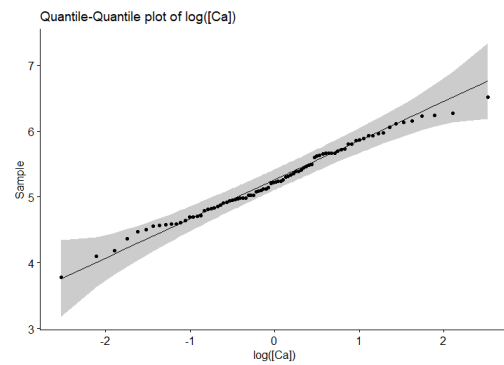


Figure B.107: Quantile - Quantile plot of log[Ca].
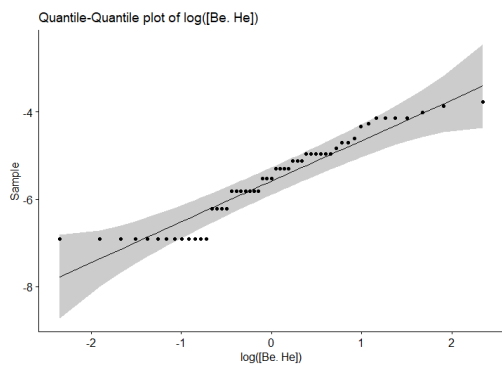


Figure B.105: Quantile - Quantile plot of log[Be. He].
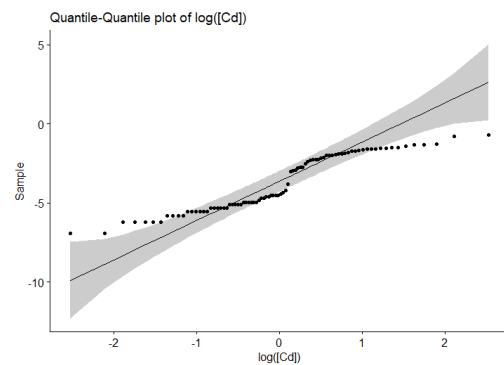


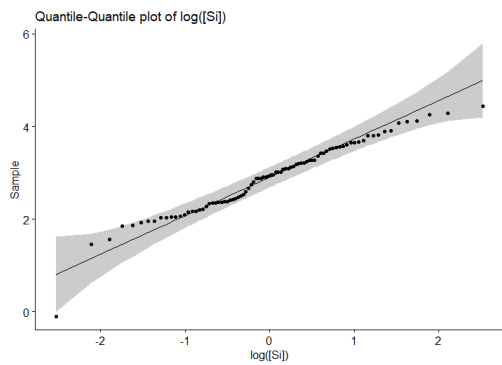Figure B.108: Quantile - Quantile plot of log[Cd] .

83
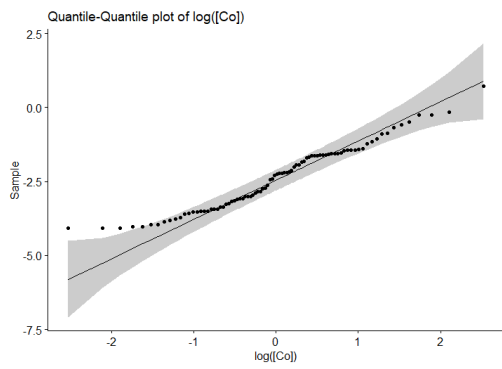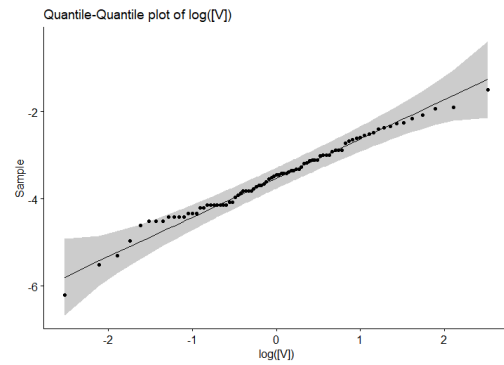
Figure B.109: Quantile - Quantile plot of log[Co].
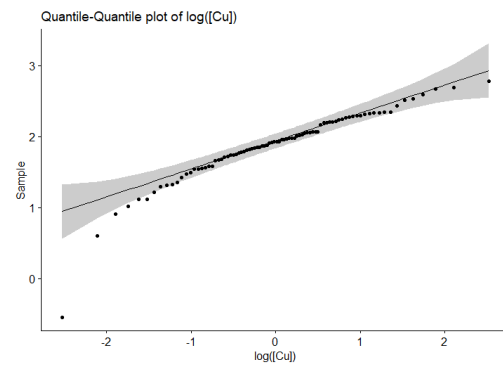


Figure B.112: Quantile - Quantile plot of log[Cr].
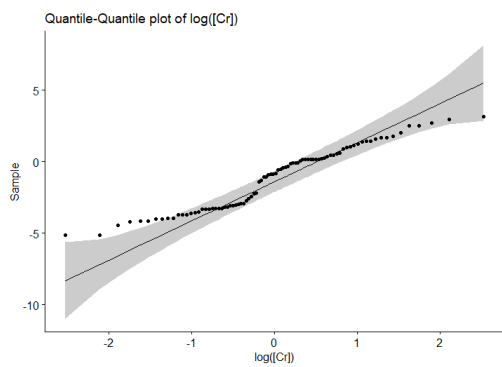


Figure B.110: Quantile - Quantile plot of log[Cr].
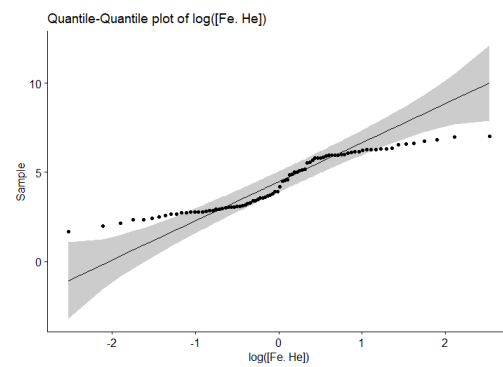


Figure B.113: Quantile - Quantile plot of log[Fe. He].
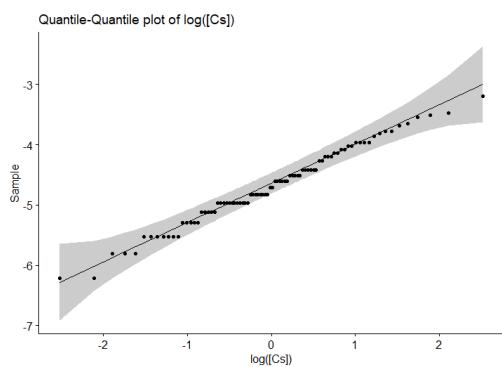


Figure B.111: Quantile - Quantile plot of log[Cs].
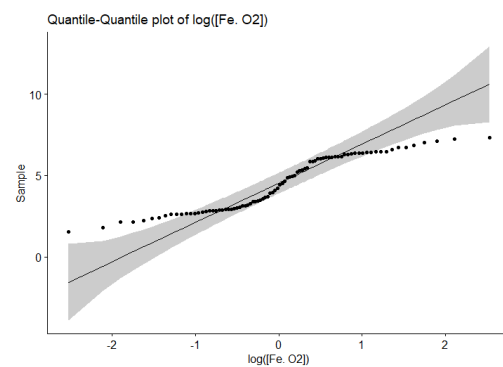


Figure B.114: Quantile - Quantile plot of log[Fe. $O_2$].

84
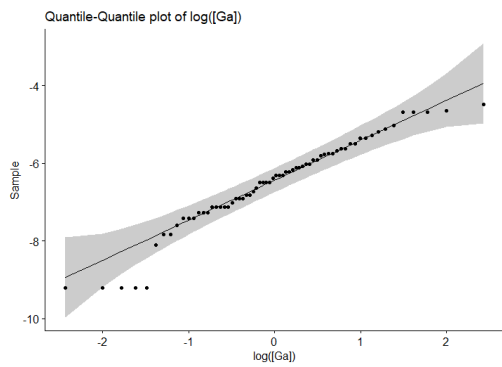
Figure B.115: Quantile - Quantile plot of log[Ga].
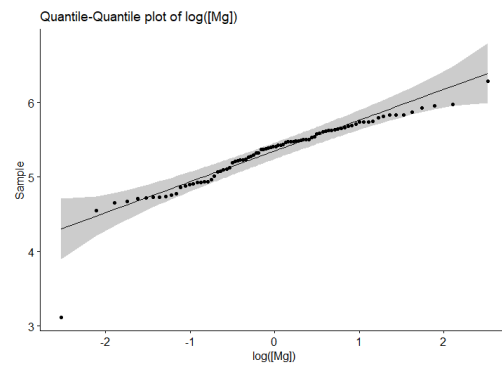


Figure B.118: Quantile - Quantile plot of log[Mg].
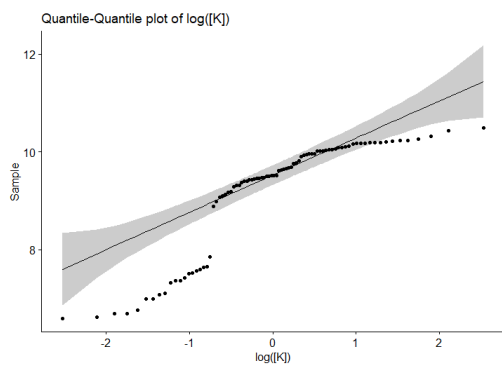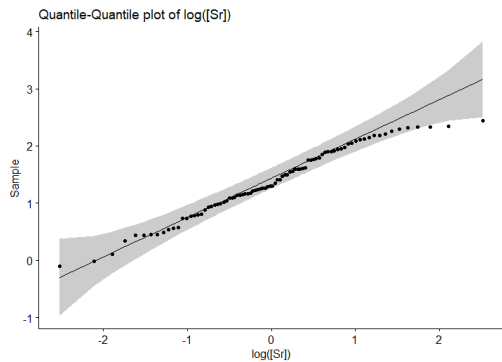


Figure B.116: Quantile - Quantile plot of log[K].
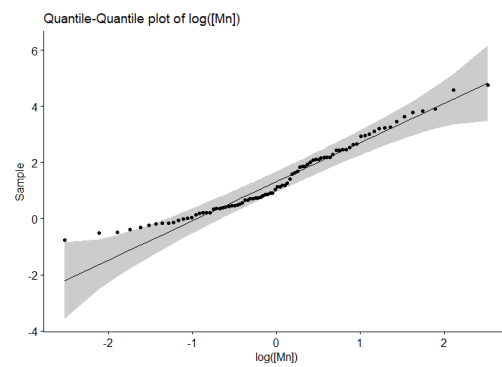


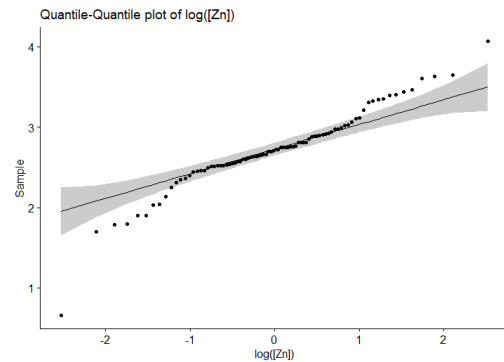Figure B.119: Quantile - Quantile plot of log[Mn].



Figure B.117: Quantile - Quantile plot of log[Li].



Figure B.120: Quantile - Quantile plot of log[Na].

85

Figure B.121: Quantile - Quantile plot of log[Ni].



Figure B.124: Quantile - Quantile plot of [Pb.207].



Figure B.122: Quantile - Quantile plot of log[P].



Figure B.125: Quantile - Quantile plot of [Pb.208].



Figure B.123: Quantile - Quantile plot of log[Pb.206].



Figure B.126: Quantile - Quantile plot of log[S] (32 -> 68).

86

Figure B.127: Quantile - Quantile plot of log [S] (34 -> 50).



Figure B.130: Quantile - Quantile plot of log[Tl].



Figure B.128: Quantile - Quantile plot of log[Si].



Figure B.131: Quantile - Quantile plot of log[V].



Figure B.132: Quantile - Quantile plot of log[Zn].



Figure B.129: Quantile - Quantile plot of log[Sr].

87

Table B.3: Shapiro - Wilk normality test results for the elements detected.

| Shapiro - Wilk test | W | P - value |
|---|---|---|
| **Hg** | 0.97025 | 0.0444 |
| **Ag** | 0.95689 | 0.005906 |
| **Al** | 0.97182 | 0.07091 |
| **As** | 0.94489 | 0.001114 |
| **B** | 0.84051 | 0.00003916 |
| **Ba** | 0.98184 | 0.269 |
| **Ca** | 0.98975 | 0.74 |
| **Cd** | 0.90096 | 0.006887 |
| **Co** | 0.95968 | 0.008889 |
| **Cr** | 0.94401 | 0.0009919 |
| **Cs** | 0.98845 | 0.6483 |
| **Cu** | 0.9017 | 0.007421 |
| **Fe (He)** | 0.90517 | 0.01059 |
| **Fe (O$_2$)** | 0.90584 | 0.01136 |
| **K** | 0.81149 | 4.12e-09 |
| **Li** | 0.89859 | 0.0002892 |
| **Mg** | 0.90507 | 0.01049 |
| **Mn** | 0.95285 | 0.003319 |
| **Na** | 0.89292 | 0.003103 |
| **Ni** | 0.98562 | 0.4594 |
| **P** | 0.89602 | 0.004204 |
| **S (32 ->48)** | 0.899 | 0.005653 |
| **S (34 ->50)** | 0.89024 | 0.002396 |
| **Si** | 0.9654 | 0.02098 |
| **Sr** | 0.97556 | 0.1021 |
| **V** | 0.98681 | 0.5435 |
| **Zn** | 0.94262 | 0.0008259 |

# B.5 Boxplots by tissue
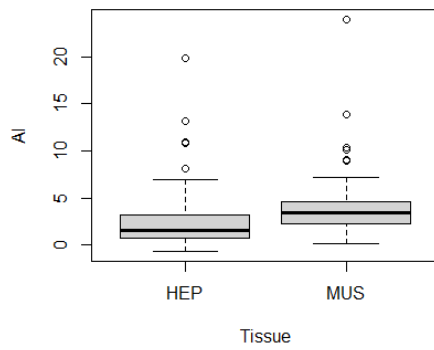


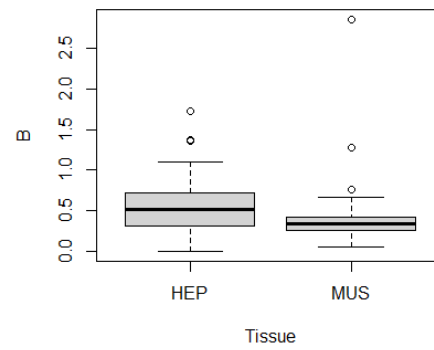Figure B.133: Boxplot of Al by tissue.


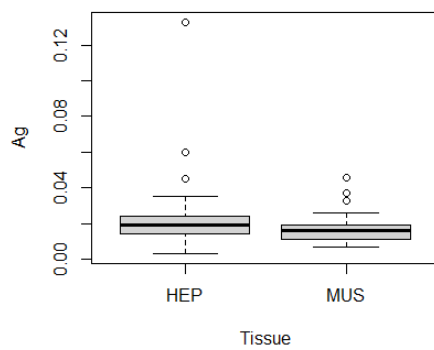
Figure B.136: Boxplot of B by tissue.



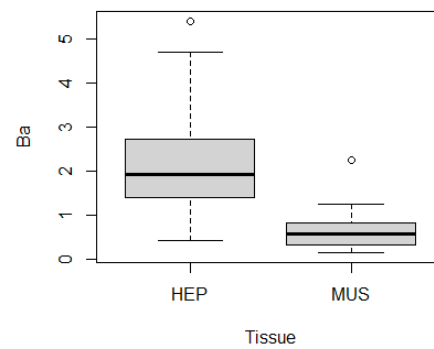Figure B.134: Boxplot of Ag by tissue.



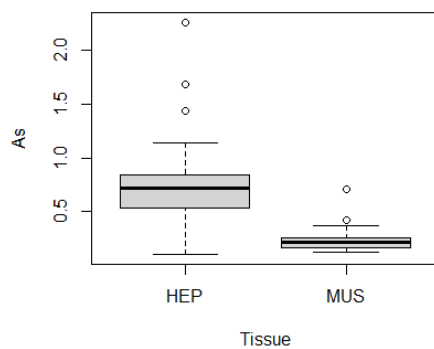Figure B.137: Boxplot of Ba by tissue.
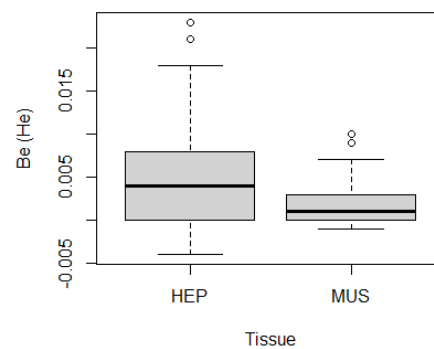


Figure B.135: Boxplot of As by tissue.



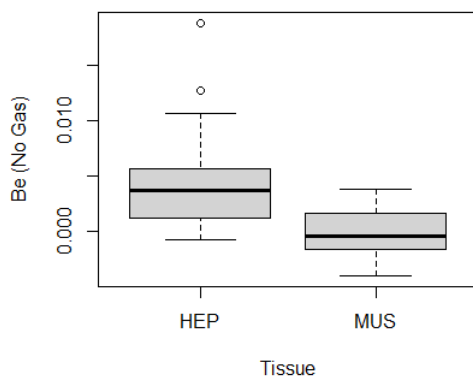Figure B.138: Boxplot of Be (He) by tissue.

Figure B.139: Boxplot of Be (No Gas) by tissue.



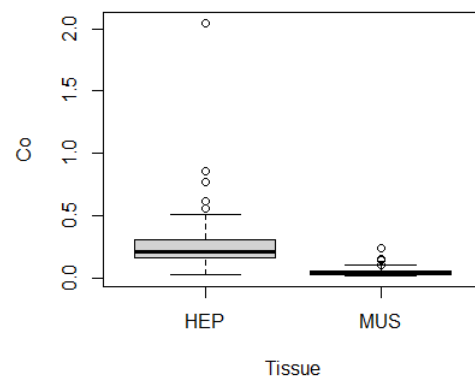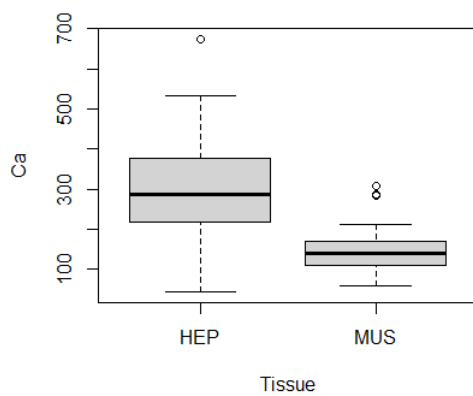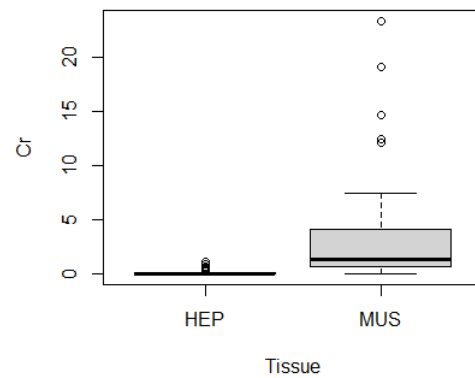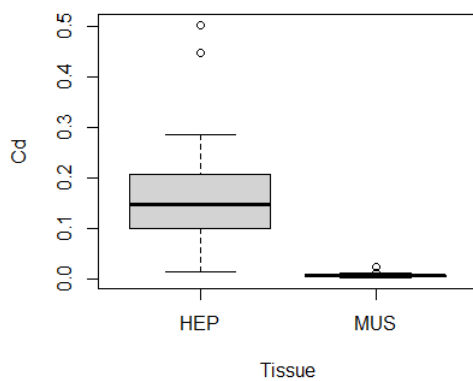Figure B.140: Boxplot of Ca by tissue.



Figure B.141: Boxplot of Cd by tissue.



Figure B.142: Boxplot of Co by tissue.



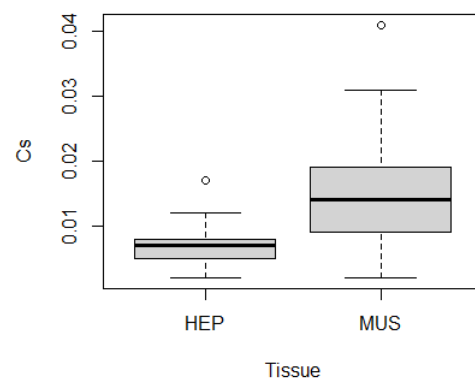Figure B.143: Boxplot of Cr by tissue.

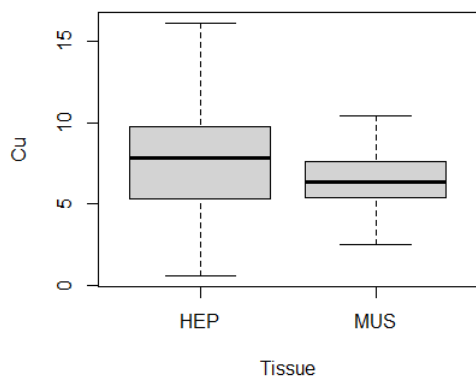

Figure B.144: Boxplot of Cs by tissue.

90

Figure B.145: Boxplot of Cu by tissue.



Figure B.148: Boxplot of Ga by tissue.



Figure B.146: Boxplot Fe (He) by tissue.



Figure B.149: Boxplot of K by tissue.
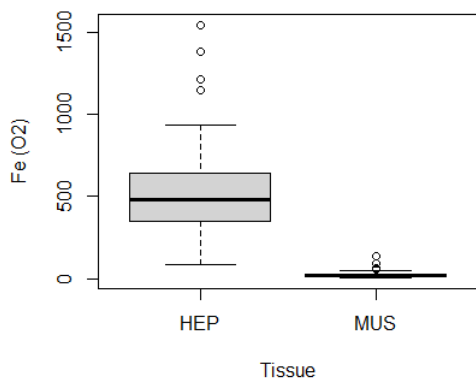


Figure B.147: Boxplot of Fe (O$_2$) by tissue.
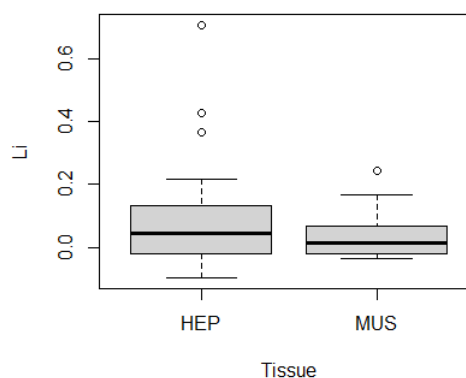


Figure B.150: Boxplot of Li by tissue.

91

Figure B.151: Boxplot of Mg by tissue.
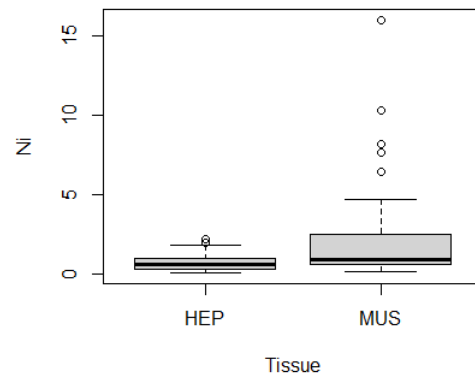


Figure B.154: Boxplot of Ni by tissue.
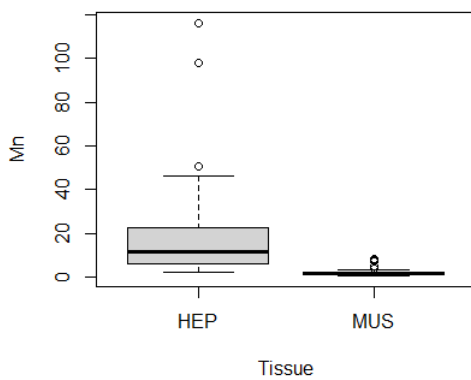


Figure B.152: Boxplot of Mn by tissue.
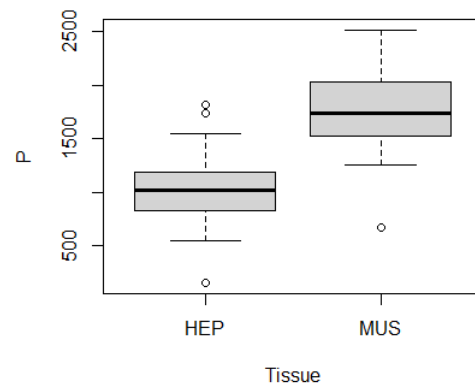


Figure B.155: Boxplot of P by tissue.
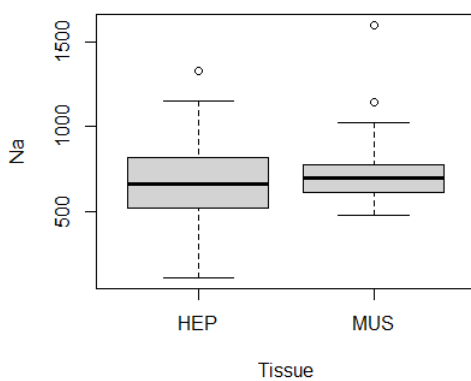


Figure B.153: Boxplot of Na by tissue.
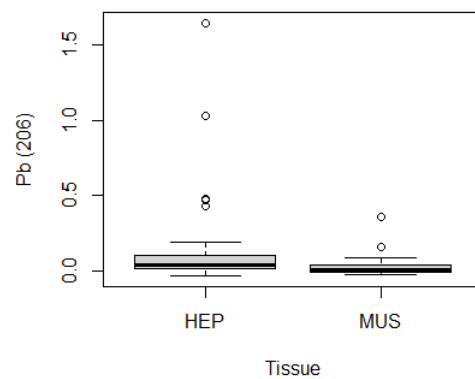


Figure B.156: Boxplot of Pb (206) by tissue.

92
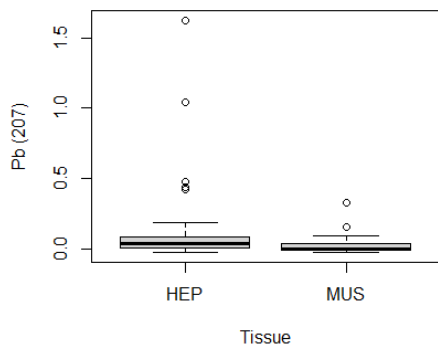
Figure B.157: Boxplot of Pb (207) by tissue.
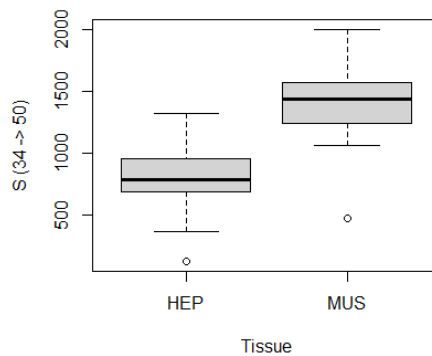


Figure B.160: Boxplot of S (34 -> 50) by tissue.
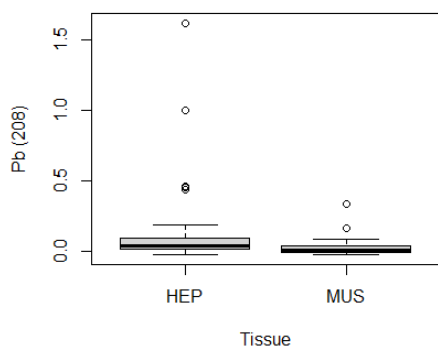


Figure B.158: Boxplot of Pb (208) by tissue.
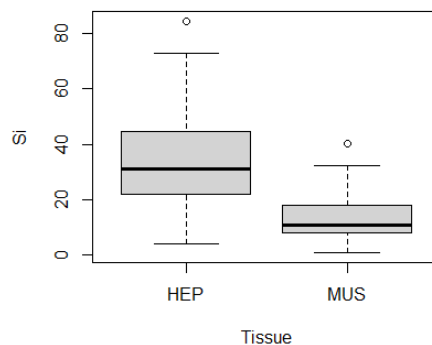


Figure B.161: Boxplot of Si by tissue.
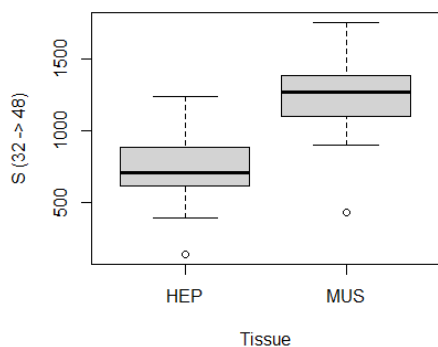


Figure B.159: Boxplot of S(32->68) by tissue.
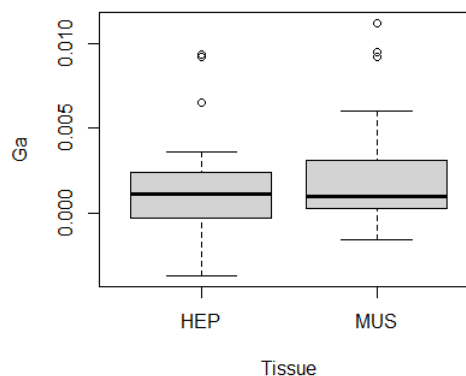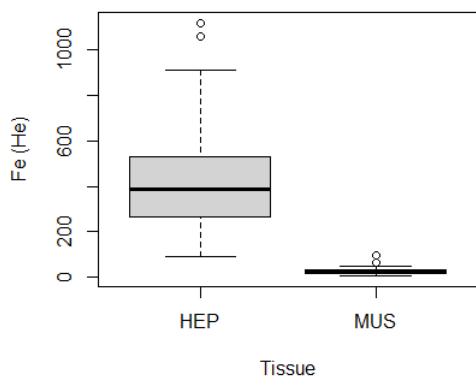


Figure B.162: Boxplot of Sr by tissue.

93
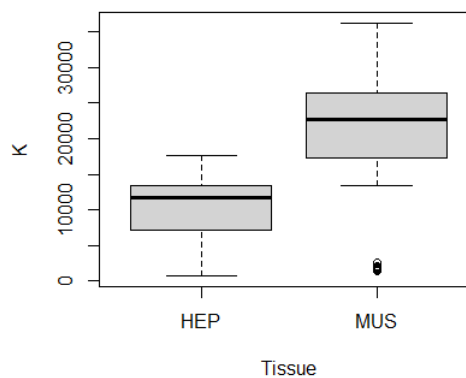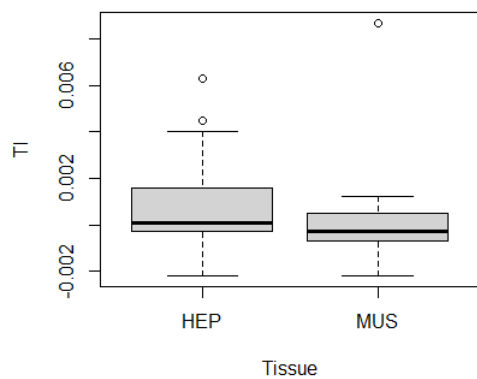
Figure B.163: Boxplot of Tl by tissue.
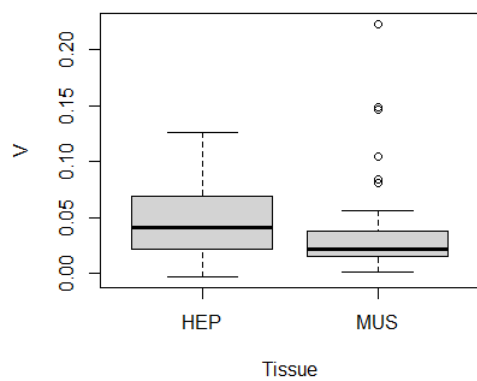


Figure B.164: Boxplot of V by tissue.
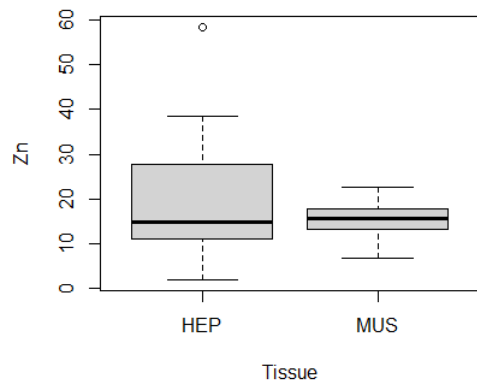


Figure B.165: Boxplot of Zn by tissue.

# B.6 Boxplots by sex



Figure B.166: Boxplot of Al by sex.
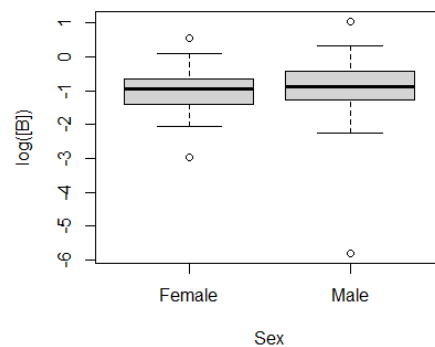


Figure B.169: Boxplot of B by sex.
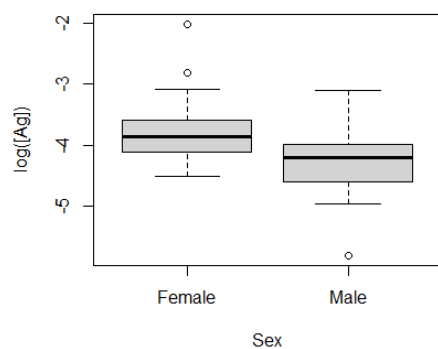


Figure B.167: Boxplot of Ag by sex.



Figure B.170: Boxplot of Ba by sex.



Figure B.168: Boxplot of As by sex.
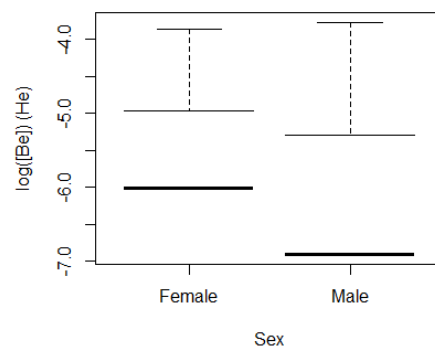


Figure B.171: Boxplot of Be (He) by sex.

Figure B.172: Boxplot of Be (No Gas) by sex.



Figure B.175: Boxplot of Co by sex.



Figure B.173: Boxplot of Ca by sex.
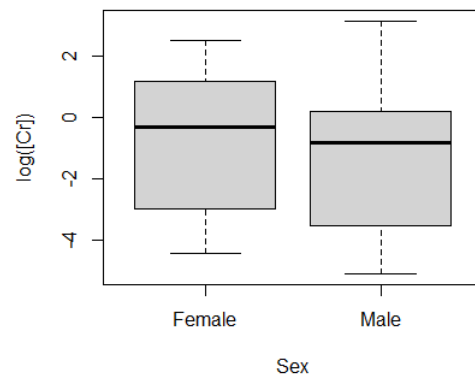


Figure B.176: Boxplot of Cr by sex.
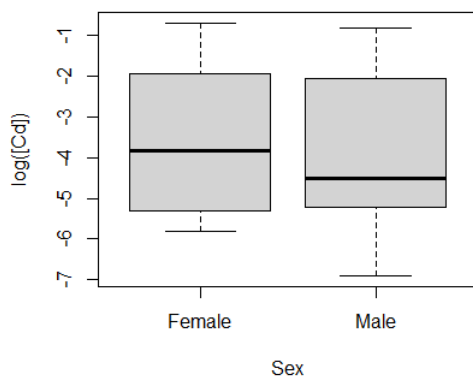


Figure B.174: Boxplot of Cd by sex.
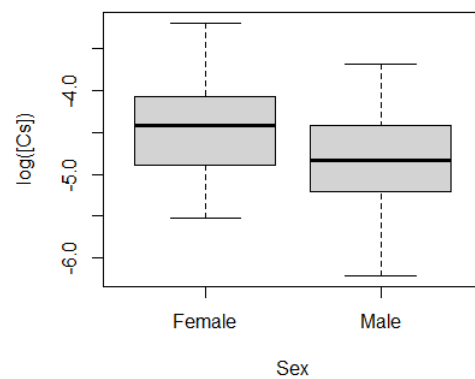


Figure B.177: Boxplot of Cs by sex.

96
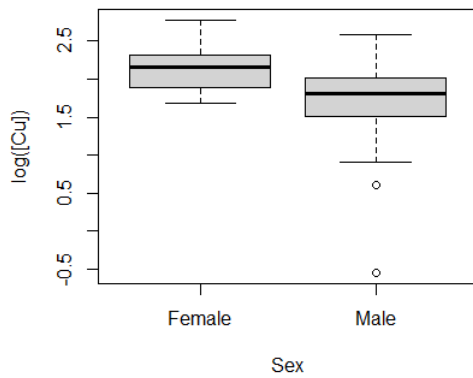
Figure B.178: Boxplot of Cu by sex.
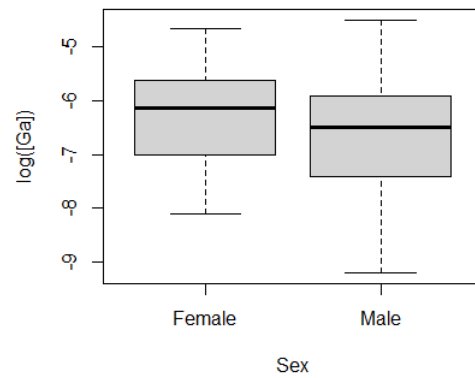


Figure B.181: Boxplot of Ga by sex.
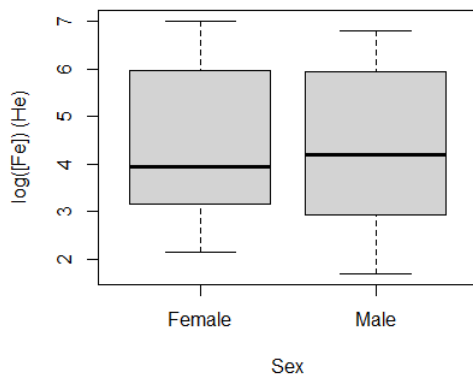


Figure B.179: Boxplot of Fe (He) by sex.
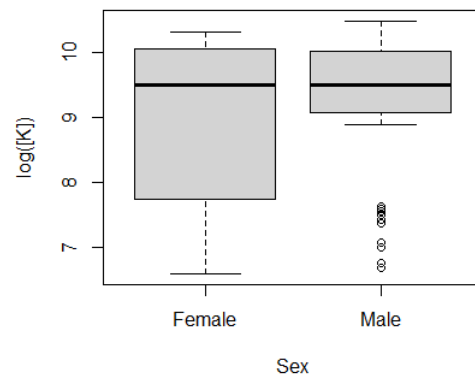


Figure B.182: Boxplot of K by sex.
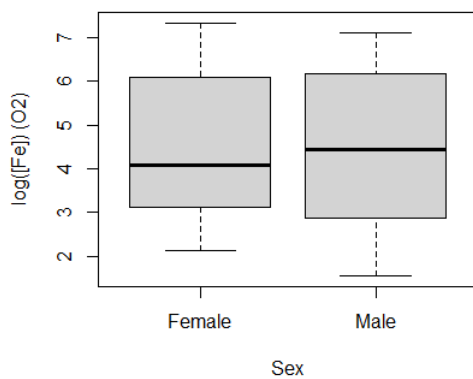


Figure B.180: Boxplot of Fe ($O_2$) by sex.
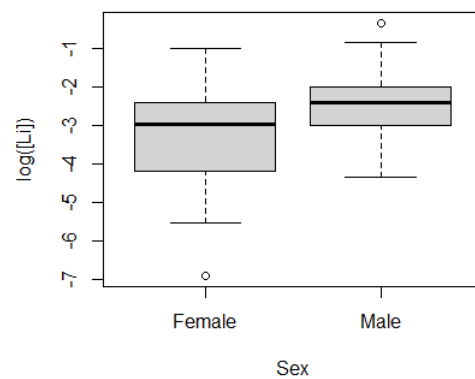


Figure B.183: Boxplot of Li by sex.

97
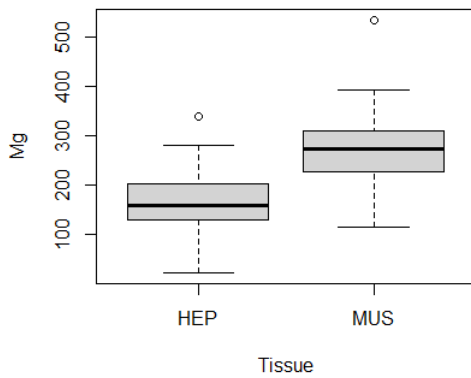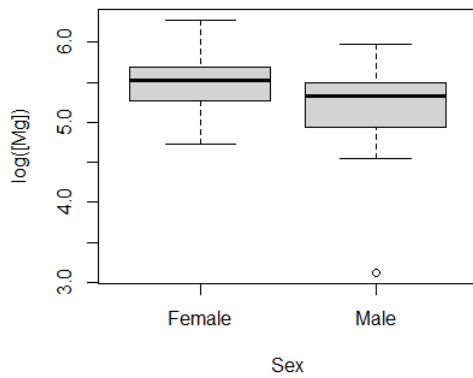
Figure B.184: Boxplot of Mg by sex.
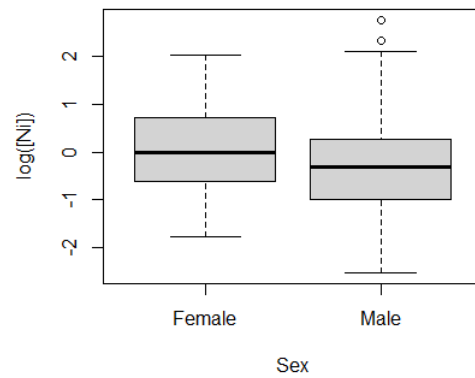


Figure B.187: Boxplot of Ni by sex.
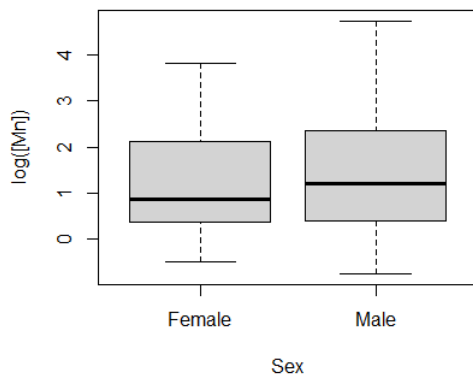


Figure B.185: Boxplot of Mn by sex.
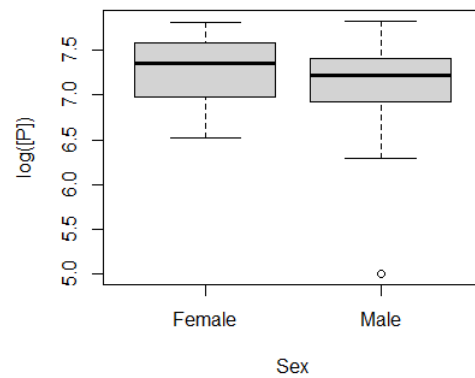


Figure B.188: Boxplot of P by sex.
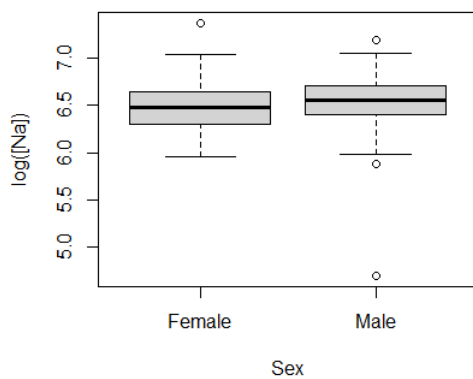


Figure B.186: Boxplot of Na by sex.
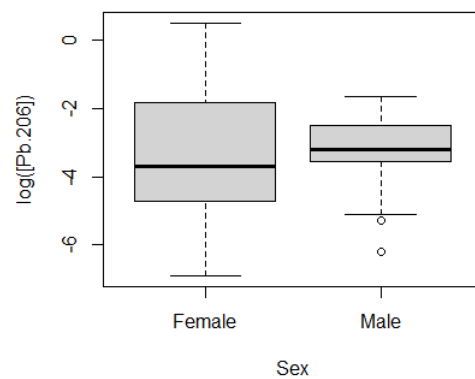


Figure B.189: Boxplot of Pb (206) by sex.

98
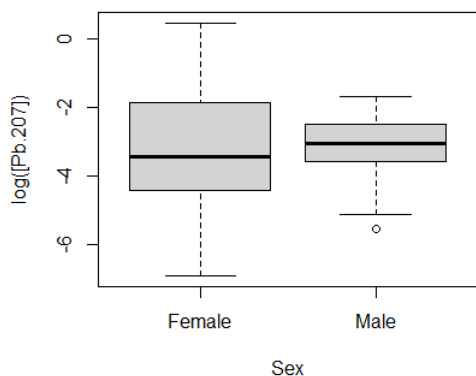
Figure B.190: Boxplot of Pb (207) by sex.
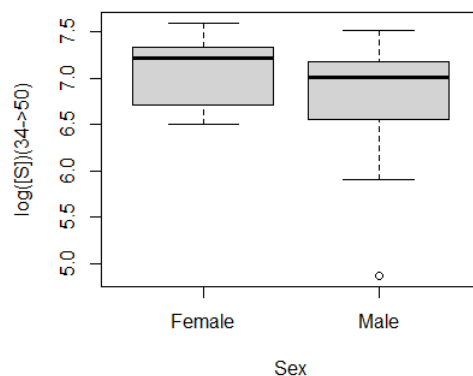


Figure B.193: Boxplot of S(34->50) by sex.
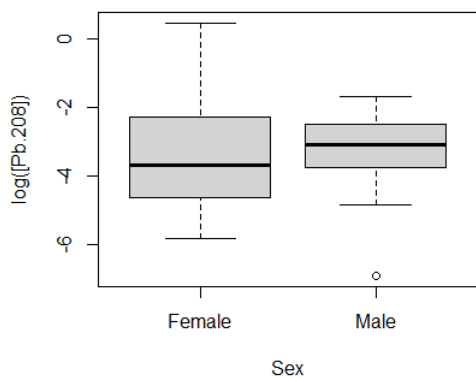


Figure B.191: Boxplot of Pb (208) by sex.
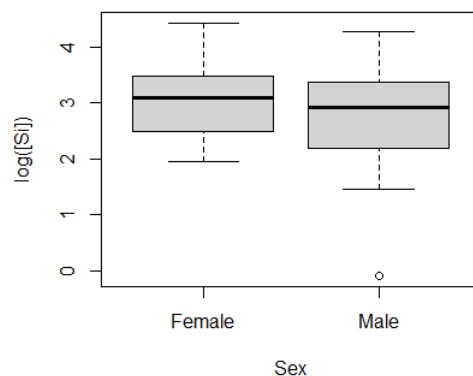


Figure B.194: Boxplot of Si by sex.
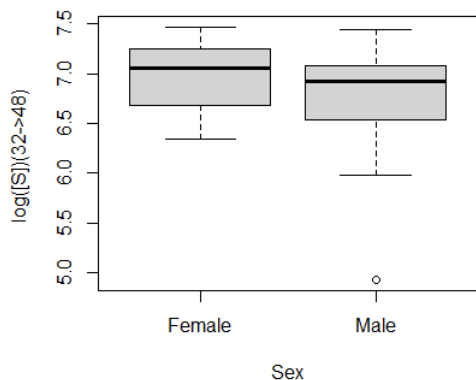


Figure B.192: Boxplot of S(32->68) bysex.
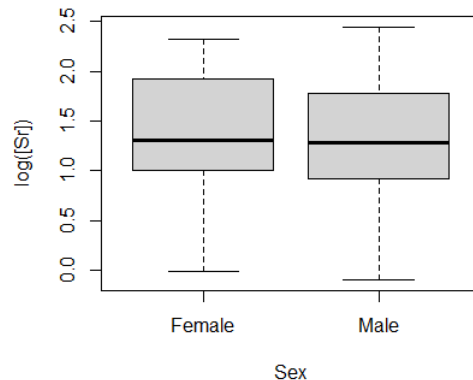


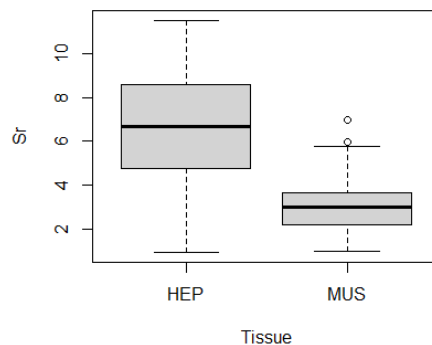Figure B.195: Boxplot of Sr by sex.

99
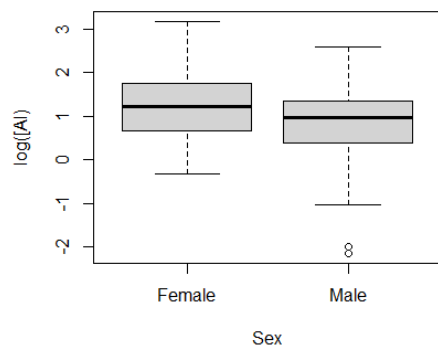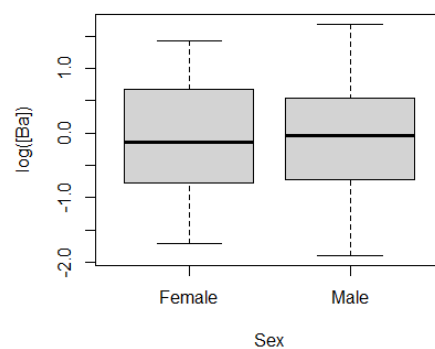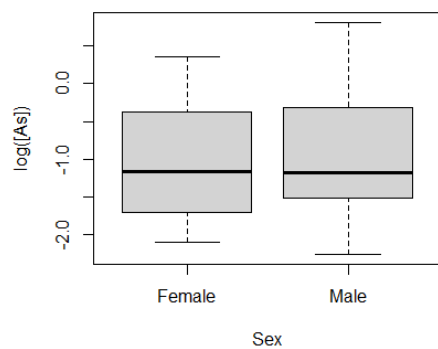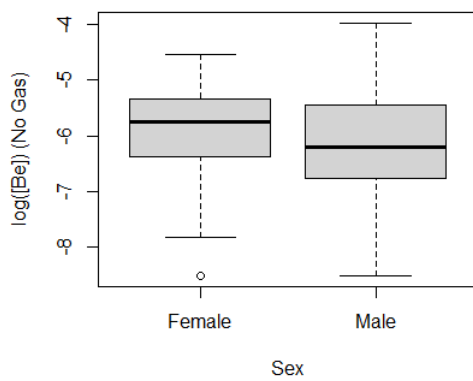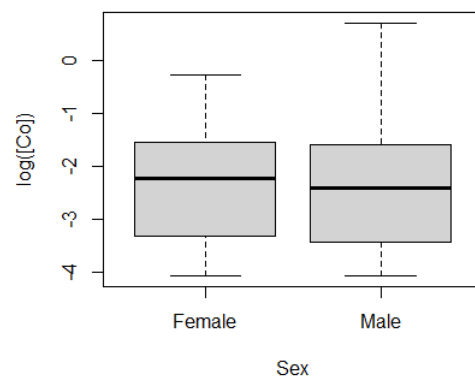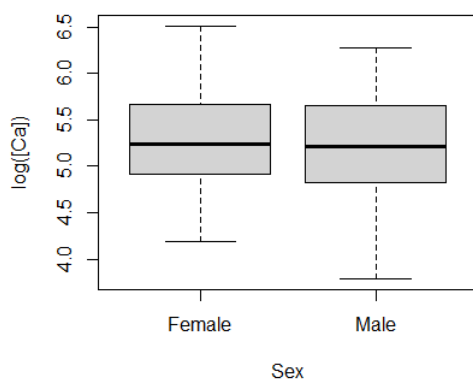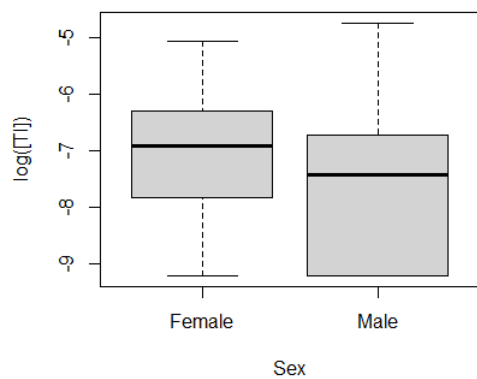
Figure B.196: Boxplot of Tl by sex.
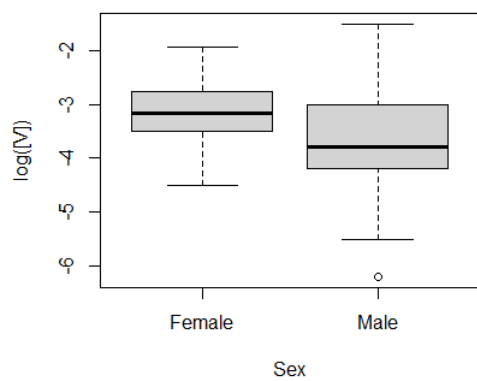


Figure B.197: Boxplot of V by sex.
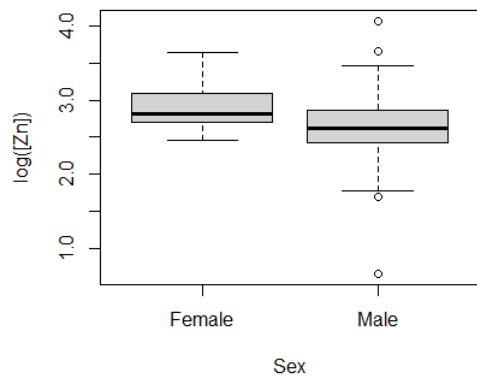


Figure B.198: Boxplot of Zn by sex.

## B.7  Correlation tests
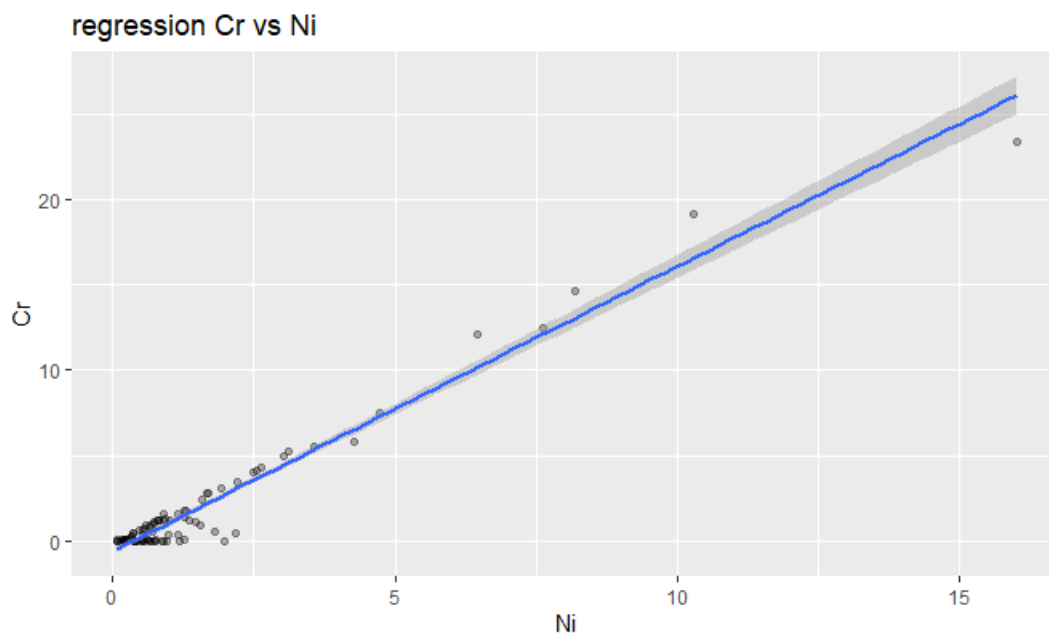


Figure B.199: Correlation test between Cr and Ni.
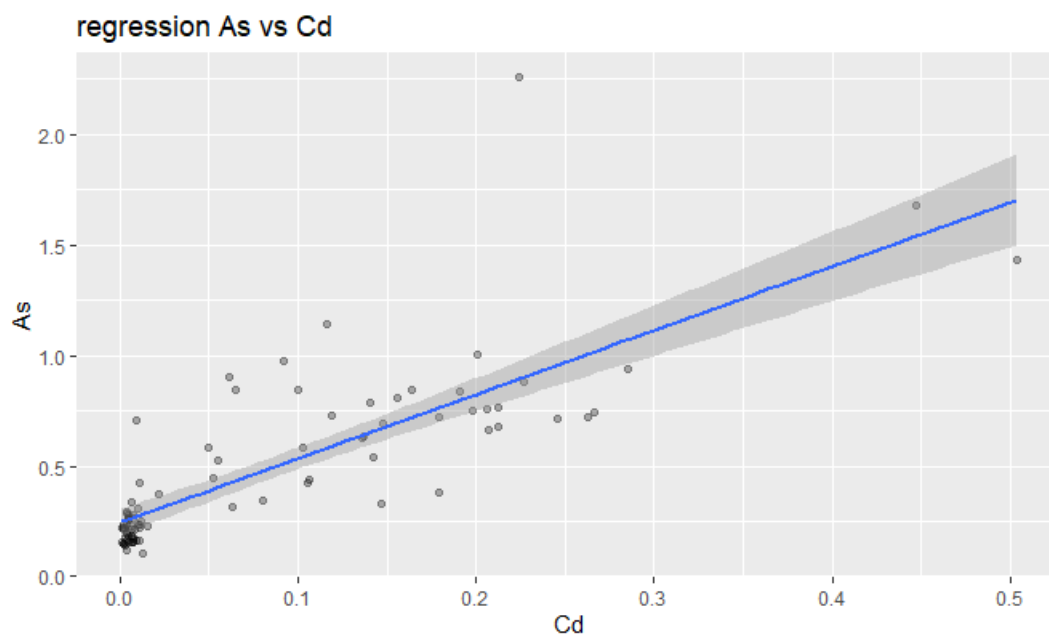


Figure B.200: Correlation test between As and Cd.

101
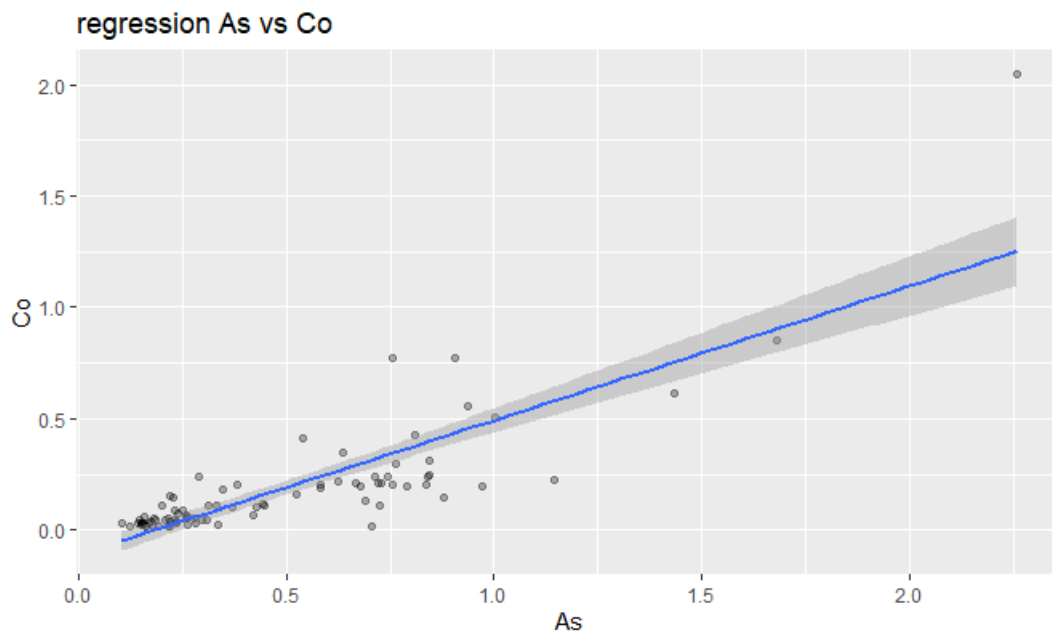
Figure B.201: Correlation test between As and Co.
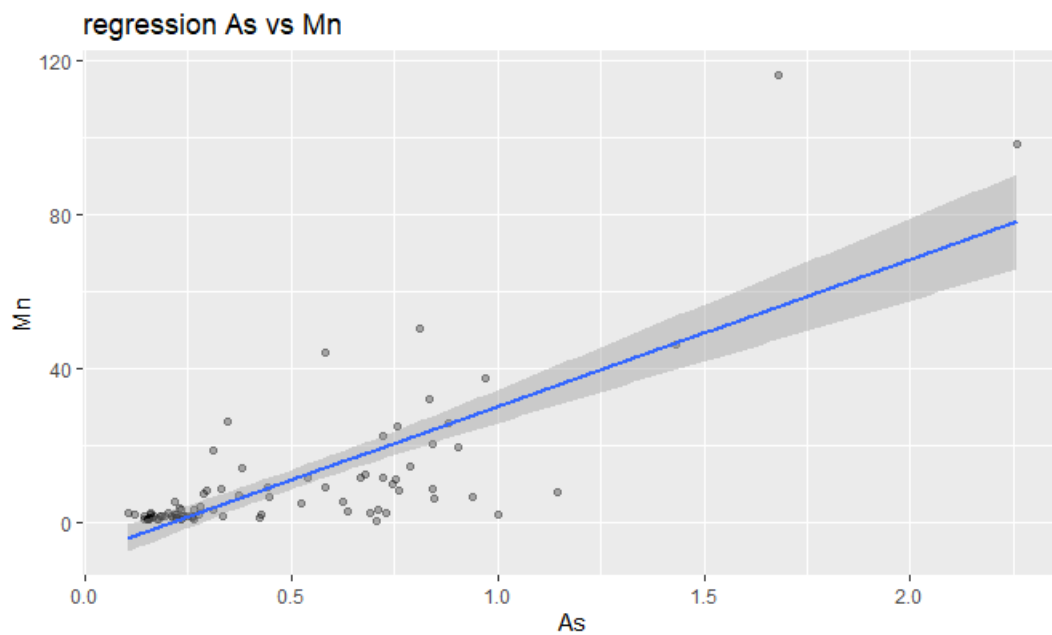


Figure B.202: Correlation test between As and Mn.

102

Table B.4: Two sample t-test by sex.

|  | t | df | p value | mean female | mean male |
|---|---|---|---|---|---|
| **Hg** | 1,906 | 84,000 | 0,060 | -2,738 | -3,166 |
| **Ag** | 4,354 | 84,000 | 0,000 | -3,787 | -4,287 |
| **Al** | 1,807 | 79,000 | 0,075 | 1,219 | 0,812 |
| **As** | -0,413 | 84,000 | 0,680 | -1,040 | -0,974 |
| **B** | -0,335 | 83,000 | 0,738 | -0,997 | -0,934 |
| **Ba** | -0,066 | 84,000 | 0,947 | -0,074 | -0,061 |
| **Be (He)** | 6,441 | 84,000 | 0,000 | 0,004 | 0,000 |
| **Ca** | 0,146 | 84,000 | 0,885 | 5,262 | 5,244 |
| **Cd** | 0,566 | 84,000 | 0,573 | -3,597 | -3,824 |
| **Co** | 0,558 | 84,000 | 0,578 | -2,286 | -2,426 |
| **Cr** | 1,271 | 84,000 | 0,207 | -0,752 | -1,376 |
| **Cs** | 2,934 | 84,000 | 0,004 | -4,423 | -4,827 |
| **Cu** | 4,127 | 84,000 | 0,000 | 2,141 | 1,724 |
| **Fe (He)** | 0,474 | 84,000 | 0,637 | 4,515 | 4,350 |
| **Fe ($O_2$)** | 0,397 | 84,000 | 0,693 | 4,582 | 4,432 |
| **K** | -0,674 | 84,000 | 0,502 | 9,060 | 9,236 |
| **Li** | -2,642 | 51,000 | 0,011 | -3,396 | -2,476 |
| **Mg** | 1,950 | 84,000 | 0,055 | 5,446 | 5,255 |
| **Mn** | -0,954 | 84,000 | 0,343 | 1,203 | 1,484 |
| **Na** | -0,532 | 84,000 | 0,596 | 6,492 | 6,533 |
| **Ni** | 1,266 | 84,000 | 0,209 | 0,001 | -0,301 |
| **P** | 1,686 | 84,000 | 0,095 | 7,284 | 7,120 |
| **S (32 ->48)** | 1,825 | 84,000 | 0,072 | 6,963 | 6,799 |
| **S (34 ->50)** | 1,826 | 84,000 | 0,071 | 7,061 | 6,886 |
| **Si** | 1,588 | 84,000 | 0,116 | 3,059 | 2,786 |
| **Sr** | 0,444 | 84,000 | 0,658 | 1,407 | 1,346 |
| **V** | 2,601 | 83,000 | 0,011 | -3,189 | -3,677 |
| **Zn** | 3,001 | 84,000 | 0,004 | 2,919 | 2,604 |

Table B.5: Two sample t-test by tissue.

|  | t | df | p value | mean hepato | mean muscle |
|---|---|---|---|---|---|
| **Hg** | -6,400 | 84,000 | 0,000 | 0,033 | 0,113 |
| **Ag** | 1,867 | 84,000 | 0,065 | 0,023 | 0,017 |
| **Al** | -1,623 | 84,000 | 0,108 | 3,047 | 4,494 |
| **As** | 8,772 | 84,000 | 0,000 | 0,747 | 0,230 |
| **B** | 1,814 | 84,000 | 0,073 | 0,577 | 0,419 |
| **Ba** | 7,703 | 84,000 | 0,000 | 2,144 | 0,622 |
| **Be (He)** | 3,575 | 84,000 | 0,001 | 0,006 | 0,002 |
| **Ca** | 7,001 | 84,000 | 0,000 | 302,230 | 148,864 |
| **Cd** | 10,357 | 84,000 | <2.2e-16 | 0,161 | 0,006 |
| **Co** | 5,173 | 84,000 | 0,000 | 0,315 | 0,051 |
| **Cr** | -4,208 | 84,000 | 0,000 | 0,200 | 3,574 |
| **Cs** | -6,116 | 84,000 | 0,000 | 0,007 | 0,015 |
| **Cu** | 2,097 | 84,000 | 0,039 | 7,868 | 6,568 |
| **Fe (He)** | 10,900 | 84,000 | <2.2e-16 | 435,645 | 25,012 |
| **Fe ($O_2$)** | 10,161 | 84,000 | 0,000 | 538,340 | 26,657 |
| **K** | -5,470 | 84,000 | 0,000 | 9621,147 | 19425,988 |
| **Li** | 2,032 | 84,000 | 0,045 | 0,080 | 0,032 |
| **Mg** | -7,515 | 84,000 | 0,000 | 166,925 | 273,937 |
| **Mn** | 4,766 | 84,000 | 0,000 | 19,023 | 2,018 |
| **Na** | -0,621 | 84,000 | 0,536 | 697,661 | 727,802 |
| **Ni** | -3,153 | 84,000 | 0,002 | 0,727 | 2,272 |
| **P** | -9,425 | 84,000 | 0,000 | 1038,484 | 1766,585 |
| **S (32 ->48)** | -9,670 | 84,000 | 0,000 | 762,224 | 1252,642 |
| **S (34 ->50)** | -10,737 | 84,000 | <2.2e-16 | 812,882 | 1410,656 |
| **Si** | 6,839 | 84,000 | 0,000 | 34,036 | 13,562 |
| **Sr** | 7,307 | 84,000 | 0,000 | 6,450 | 3,074 |
| **V** | 1,080 | 84,000 | 0,283 | 0,047 | 0,038 |
| **Zn** | 2,008 | 84,000 | 0,048 | 18,843 | 15,206 |

103

# Appendix C

# R Codes

```r
1  library(tidyverse)
2  library(ggplot2)
3  library(corrgram)
4  library(corrplot)
5  library(qwraps2)
6  library(dplyr)
7  library(ggpubr)
8  library(corrgram)
9  library(corrplot)
10 library(lubridate)
11
12 #load the data
13 gmb <-read.csv("Tables_.csv",
14 sep=";",na.strings=c(""," ","NA"))
15 gmb<-as_tibble(gmb)
16 View(gmb) # click on data on environment table
17 str(gmb)
18 attach(gmb)
19
20
21
22 # transform Sex and Tissue in factors
23
24 gmb$Sex <- as.factor(gmb$Sex)
25 levels(gmb$Sex) <- c("F","M")
26 gmb$Tissue <- as.factor(gmb$Tissue)
27 levels(gmb$Tissue)<-c("H","M")
28
29 # exploratory analysis
30
31 hist(log(gmb$Hg), col='cadetblue', xlab = 'log([Hg])', ylab = 'Frequency', ...
       main = 'Histogram of log([Hg])')
32 hist(log(gmb$Ag), col='cadetblue', xlab = 'log([Ag])', ylab = 'Frequency', ...
       main = 'Histogram of log([Ag])')
33 hist(log(gmb$Al),col='cadetblue', xlab = 'log([Al])', ylab = 'Frequency', ...
       main = 'Histogram of log([Al])')
34 hist(log(gmb$As), col='cadetblue', xlab = 'log([As])', ylab = 'Frequency', ...
       main = 'Histogram of log([As])')
35 hist(log(gmb$B),col='cadetblue', xlab = 'log([B])', ylab = 'Frequency', main ...
       = 'Histogram of log([B])')
36 hist(log(gmb$Ba), col='cadetblue', xlab = 'log([Ba])', ylab = 'Frequency', ...
       main = 'Histogram of log([Ba])')
```

105

```r
37  hist(log(gmb$Be..No.Gas.), col='cadetblue', xlab = 'log([Be (No Gas)])', ...
       ylab = 'Frequency', main = 'Histogram of log([Be (No Gas)])')
38  hist(log(gmb$Be..He.), col='cadetblue', xlab = 'log([Be (He)])', ylab = ...
       'Frequency', main = 'Histogram of log([Be (He)])')
39  hist(log(gmb$Ca), col='cadetblue', xlab = 'log([Ca])', ylab = 'Frequency', ...
       main = 'Histogram of log([Ca])')
40  hist(log(gmb$Cd), col='cadetblue', xlab = 'log([Cd])', ylab = 'Frequency', ...
       main = 'Histogram of log([Cd])')
41  hist(log(gmb$Co), col='cadetblue', xlab = 'log([Co])', ylab = 'Frequency', ...
       main = 'Histogram of log([Co])')
42  hist(log(gmb$Cr), col='cadetblue', xlab = 'log([Cr])', ylab = 'Frequency', ...
       main = 'Histogram of log([Cr])')
43  hist(log(gmb$Cs), col='cadetblue', xlab = 'log([Cs])', ylab = 'Frequency', ...
       main = 'Histogram of log([Cs])')
44  hist(log(gmb$Cu), col='cadetblue', xlab = 'log([Cu])', ylab = 'Frequency', ...
       main = 'Histogram of log([Cu])')
45  hist(log(gmb$Fe..He.), col='cadetblue', xlab = 'log([Fe (He)])', ylab = ...
       'Frequency', main = 'Histogram of log([Fe (He)])')
46  hist(log(gmb$Fe..O2.), col='cadetblue', xlab = 'log([Fe (O2)])', ylab = ...
       'Frequency', main = 'Histogram of log([Fe (O2)])')
47  hist(log(gmb$Ga), col='cadetblue', xlab = 'log([Ga])', ylab = 'Frequency', ...
       main = 'Histogram of log([Ga])')
48  hist(log(gmb$K), col='cadetblue', xlab = 'log([K])', ylab = 'Frequency', ...
       main = 'Histogram of log([K])')
49  hist(log(gmb$Li), col='cadetblue', xlab = 'log([Li])', ylab = 'Frequency', ...
       main = 'Histogram of log([Li])')
50  hist(log(gmb$Mg), col='cadetblue', xlab = 'log([Mg])', ylab = 'Frequency', ...
       main = 'Histogram of log([Mg])')
51  hist(log(gmb$Mn), col='cadetblue', xlab = 'log([Mn])', ylab = 'Frequency', ...
       main = 'Histogram of log([Mn])')
52  hist(log(gmb$Na), col='cadetblue', xlab = 'log([Na])', ylab = 'Frequency', ...
       main = 'Histogram of log([Na])')
53  hist(log(gmb$Ni), col='cadetblue', xlab = 'log([Ni])', ylab = 'Frequency', ...
       main = 'Histogram of log([Ni])')
54  hist(log(gmb$P), col='cadetblue', xlab = 'log([P])', ylab = 'Frequency', ...
       main = 'Histogram of log([P])')
55  hist(log(gmb$Pb..He.), col='cadetblue', xlab = 'log([Pb (206)])', ylab = ...
       'Frequency', main = 'Histogram of log([Pb (206)])')
56  hist(log(gmb$X207Pb), col='cadetblue', xlab = 'log([Pb (207)])', ylab = ...
       'Frequency', main = 'Histogram of log([Pb (207)])')
57  hist(log(gmb$X208Pb), col='cadetblue', xlab = 'log([Pb (208)])', ylab = ...
       'Frequency', main = 'Histogram of log([Pb (208)])')
58  hist(log(gmb$X32S), col='cadetblue', xlab = 'log([S (32)])', ylab = ...
       'Frequency', main = 'Histogram of log([S (32)])')
59  hist(log(gmb$X34S), col='cadetblue', xlab = 'log([S (34)])', ylab = ...
       'Frequency', main = 'Histogram of log([S] (34))')
60  hist(log(gmb$Si), col='cadetblue', xlab = 'log([Si])', ylab = 'Frequency', ...
       main = 'Histogram of log([Si])')
61  hist(log(gmb$Sr), col='cadetblue', xlab = 'log([Sr])', ylab = 'Frequency', ...
       main = 'Histogram of log([Sr])')
62  hist(log(gmb$Tl), col='cadetblue', xlab = 'log([Tl])', ylab = 'Frequency', ...
       main = 'Histogram of log([Tl])')
63  hist(log(gmb$V), col='cadetblue', xlab = 'log([V])', ylab = 'Frequency', ...
       main = 'Histogram of log([V])')
64  hist(log(gmb$Zn),col='cadetblue', xlab = 'log([Zn])', ylab = 'Frequency', ...
       main = 'Histogram of log([Zn])')
65
66  # bartlett test gender
67
68  bartlett.test(Hg ¬ Sex, data=gmb)
69  bartlett.test(Ag ¬ Sex, data=gmb)
```

106

```
70  bartlett.test(Al ¬ Sex, data=gmb)
71  bartlett.test(As ¬ Sex, data=gmb)
72  bartlett.test(B ¬ Sex, data=gmb)
73  bartlett.test(Ba ¬ Sex, data=gmb)
74  bartlett.test(Be..No.Gas. ¬ Sex, data=gmb)
75  bartlett.test(Be..He. ¬ Sex, data=gmb)
76  bartlett.test(Ca ¬ Sex, data=gmb)
77  bartlett.test(Cd ¬ Sex, data=gmb)
78  bartlett.test(Co ¬ Sex, data=gmb)
79  bartlett.test(Cr ¬ Sex, data=gmb)
80  bartlett.test(Cs ¬ Sex, data=gmb)
81  bartlett.test(Cu ¬ Sex, data=gmb)
82  bartlett.test(Fe..He. ¬ Sex, data=gmb)
83  bartlett.test(Fe..O2. ¬ Sex, data=gmb)
84  bartlett.test(Ga ¬ Sex, data=gmb)
85  bartlett.test(K ¬ Sex, data=gmb)
86  bartlett.test(Li ¬ Sex, data=gmb)
87  bartlett.test(Mg ¬ Sex, data=gmb)
88  bartlett.test(Mn ¬ Sex, data=gmb)
89  bartlett.test(Na ¬ Sex, data=gmb)
90  bartlett.test(Ni ¬ Sex, data=gmb)
91  bartlett.test(P ¬ Sex, data=gmb)
92  bartlett.test(Pb..He. ¬ Sex, data=gmb)
93  bartlett.test(X207Pb ¬ Sex, data=gmb)
94  bartlett.test(X208Pb ¬ Sex, data=gmb)
95  bartlett.test(X32S ¬ Sex, data=gmb)
96  bartlett.test(X34S ¬ Sex, data=gmb)
97  bartlett.test(Si ¬ Sex, data=gmb)
98  bartlett.test(Sr ¬ Sex, data=gmb)
99  bartlett.test(Tl ¬ Sex, data=gmb)
100 bartlett.test(V ¬ Sex, data=gmb)
101 bartlett.test(Zn ¬ Sex, data=gmb)
102
103
104 # test for normality
105
106 ggdensity(gmb$Hg,
107 main = "Density plot of Hg",
108 xlab = "Hg")
109 ggqqplot(gmb$Hg, main = "Quantile-Quantile plot of Hg",
110 xlab = "Hg")
111 ggqqplot(log(gmb$Hg),
112 main = "Quantile-Quantile plot of log([Hg])",
113 xlab = "log(gmb$Hg)")
114 shapiro.test(log(gmb$Hg))
115
116
117
118 ggdensity(gmb$Ag,
119 main = "Density plot of Ag",
120 xlab = "Ag")
121 ggqqplot(gmb$Ag,
122 main = "Quantile-Quantile plot of Ag",
123 xlab = "Ag")
124 ggqqplot(log(gmb$Ag),
125 main = "Quantile-Quantile plot of log([Ag])",
126 xlab = "log([Ag])")
127 shapiro.test(log(gmb$Ag))
128
129 ggdensity(gmb$Al,
130 main = "Density plot of Al",
```

107

```r
131  xlab = "Al")
132  ggqqplot(gmb$Al,
133  main = "Quantile-Quantile plot of Al",
134  xlab = "Al")
135  ggqqplot(log(gmb$Al),
136  main = "Quantile-Quantile plot of log([Al])",
137  xlab = "log([Al])")
138  shapiro.test(log(gmb$Al))
139
140
141  ggdensity(gmb$As,
142  main = "Density plot of As",
143  xlab = "As")
144  ggqqplot(gmb$As,
145  main = "Quantile-Quantile plot of As",
146  xlab = "As")
147  ggqqplot(log(gmb$As),
148  main = "Quantile-Quantile plot of log([As])",
149  xlab = "log([As])")
150  shapiro.test(log(gmb$As))
151
152
153  ggdensity(gmb$B,
154  main = "Density plot of B",
155  xlab = "B")
156  ggqqplot(gmb$B,
157  main = "Quantile-Quantile plot of B",
158  xlab = "B")
159  ggqqplot(log(gmb$B),
160  main = "Quantile-Quantile plot of log([B])",
161  xlab = "log([B])")
162  shapiro.test(log(gmb$B))
163
164
165  ggdensity(gmb$Ba,
166  main = "Density plot of Ba",
167  xlab = "Ba")
168  ggqqplot(gmb$Ba,
169  main = "Quantile-Quantile plot of Ba",
170  xlab = "Ba")
171  ggqqplot(log(gmb$Ba),
172  main = "Quantile-Quantile plot of log([Ba])",
173  xlab = "log([Ba])")
174  shapiro.test(log(gmb$Ba))
175
176
177  ggdensity(gmb$Be..No.Gas.,
178  main = "Density plot of Be (No Gas)",
179  xlab = "Be (No Gas)")
180  ggqqplot(gmb$Be..No.Gas.,
181  main = "Quantile-Quantile plot of Be (No Gas)",
182  xlab = "Be (No Gas)")
183  ggqqplot(log(gmb$Be..No.Gas.),
184  main = "Quantile-Quantile plot of log([Be. No Gas])",
185  xlab = "log([Be. No Gas])")
186  shapiro.test(log(gmb$Be..No.Gas.))
187
188
189  ggdensity(gmb$Be..He.,
190  main = "Density plot of Be (He)",
191  xlab = "Be (He)")
```

108

```
192  ggqqplot(gmb$Be..He.,
193  main = "Quantile-Quantile plot of Be (He)",
194  xlab = "Be (He)")
195  ggqqplot(log(gmb$Be..He.),
196  main = "Quantile-Quantile plot of log([Be. He])",
197  xlab = "log([Be. He])")
198  shapiro.test(log(gmb$Be..He.))
199
200
201  ggdensity(gmb$Ca,
202  main = "Density plot of Ca",
203  xlab = "Ca")
204  ggqqplot(gmb$Ca,
205  main = "Quantile-Quantile plot of Ca",
206  xlab = "Ca")
207  ggqqplot(log(gmb$Ca),
208  main = "Quantile-Quantile plot of log([Ca])",
209  xlab = "log([Ca])")
210  shapiro.test(log(gmb$Ca))
211
212
213  ggdensity(gmb$Cd,
214  main = "Density plot of Cd",
215  xlab = "Cd")
216  ggqqplot(gmb$Cd,
217  main = "Quantile-Quantile plot of Cd",
218  xlab = "Cd")
219  ggqqplot(log(gmb$Cd),
220  main = "Quantile-Quantile plot of log([Cd])",
221  xlab = "log([Cd])")
222  shapiro.test(log(gmb$Cd))
223
224
225  ggdensity(gmb$Co,
226  main = "Density plot of Co",
227  xlab = "Co")
228  ggqqplot(gmb$Co,
229  main = "Quantile-Quantile plot of Co",
230  xlab = "Co")
231  ggqqplot(log(gmb$Co),
232  main = "Quantile-Quantile plot of log([Co])",
233  xlab = "log([Co])")
234  shapiro.test(log(gmb$Co))
235
236
237  ggdensity(gmb$Cr,
238  main = "Density plot of Cr",
239  xlab = "Cr")
240  ggqqplot(gmb$Cr,
241  main = "Quantile-Quantile plot of Cr",
242  xlab = "Cr")
243  ggqqplot(log(gmb$Cr),
244  main = "Quantile-Quantile plot of log([Cr])",
245  xlab = "log([Cr])")
246  shapiro.test(log(gmb$Cr))
247
248
249  ggdensity(gmb$Cs,
250  main = "Density plot of Cs",
251  xlab = "Cs")
252  ggqqplot(gmb$Cs,
```

109

```
253  main = "Quantile-Quantile plot of Cs",
254  xlab = "Cs")
255  ggqqplot(log(gmb$Cs),
256  main = "Quantile-Quantile plot of log([Cs])",
257  xlab = "log([Cs])")
258  shapiro.test(log(gmb$Cs))
259
260
261  ggdensity(gmb$Cu,
262  main = "Density plot of Cu",
263  xlab = "Cu")
264  ggqqplot(gmb$Cu,
265  main = "Quantile-Quantile plot of Cu",
266  xlab = "Cu")
267  ggqqplot(log(gmb$Cu),
268  main = "Quantile-Quantile plot of log([Cu])",
269  xlab = "log([Cu])")
270  shapiro.test(log(gmb$Cu))
271
272
273  ggdensity(gmb$Fe..He.,
274  main = "Density plot of Fe [He]",
275  xlab = "Fe [He]")
276  ggqqplot(gmb$Fe..He.,
277  main = "Quantile-Quantile plot of Fe [He]",
278  xlab = "Fe [He]")
279  ggqqplot(log(gmb$Fe..He.),
280  main = "Quantile-Quantile plot of log([Fe. He])",
281  xlab = "log([Fe. He])")
282  shapiro.test(log(gmb$Fe..He.))
283
284
285  ggdensity(gmb$Fe..O2.,
286  main = "Density plot of Fe [O2]",
287  xlab = "Fe [O2]")
288  ggqqplot(gmb$Fe..O2.,
289  main = "Quantile-Quantile plot of Fe [O2]",
290  xlab = "Fe [O2]")
291  ggqqplot(log(gmb$Fe..O2.),
292  main = "Quantile-Quantile plot of log([Fe. O2])",
293  xlab = "log([Fe. O2])")
294  shapiro.test(log(gmb$Fe..O2.))
295
296
297  ggdensity(gmb$Ga,
298  main = "Density plot of Ga",
299  xlab = "Ga")
300  ggqqplot(gmb$Ga,
301  main = "Quantile-Quantile plot of Ga",
302  xlab = "Ga")
303  ggqqplot(log(gmb$Ga),
304  main = "Quantile-Quantile plot of log([Ga])",
305  xlab = "log([Ga])")
306  shapiro.test(log(gmb$Ga))
307
308
309  ggdensity(gmb$K,
310  main = "Density plot of K",
311  xlab = "K")
312  ggqqplot(gmb$K,
313  main = "Quantile-Quantile plot of K",
```

110

```
314  xlab = "K")
315  ggqqplot(log(gmb$K),
316  main = "Quantile-Quantile plot of log([K])",
317  xlab = "log([K])")
318  shapiro.test(log(gmb$K))
319
320
321  ggdensity(gmb$Li,
322  main = "Density plot of Li",
323  xlab = "Li")
324  ggqqplot(gmb$Li,
325  main = "Quantile-Quantile plot of Li",
326  xlab = "Li")
327  ggqqplot(log(gmb$Li),
328  main = "Quantile-Quantile plot of log([Li])",
329  xlab = "log([Li])")
330  shapiro.test(log(gmb$Li))
331
332
333  ggdensity(gmb$Mg,
334  main = "Density plot of Mg",
335  xlab = "Mg")
336  ggqqplot(gmb$Mg,
337  main = "Quantile-Quantile plot of Mg",
338  xlab = "Mg")
339  ggqqplot(log(gmb$Mg),
340  main = "Quantile-Quantile plot of log([Mg])",
341  xlab = "log([Mg])")
342  shapiro.test(log(gmb$Mg))
343
344
345  ggdensity(gmb$Mn,
346  main = "Density plot of Mn",
347  xlab = "Mn")
348  ggqqplot(gmb$Mn,
349  main = "Quantile-Quantile plot of Mn",
350  xlab = "Mn")
351  ggqqplot(log(gmb$Mn),
352  main = "Quantile-Quantile plot of log([Mn])",
353  xlab = "log([Mn])")
354  shapiro.test(log(gmb$Mn))
355
356
357  ggdensity(gmb$Na,
358  main = "Density plot of Na",
359  xlab = "Na")
360  ggqqplot(gmb$Na,
361  main = "Quantile-Quantile plot of Na",
362  xlab = "Na")
363  ggqqplot(log(gmb$Na),
364  main = "Quantile-Quantile plot of log([Na])",
365  xlab = "log([Na])")
366  shapiro.test(log(gmb$Na))
367
368
369  ggdensity(gmb$Ni,
370  main = "Density plot of Ni",
371  xlab = "Ni")
372  ggqqplot(gmb$Ni,
373  main = "Quantile-Quantile plot of Ni",
374  xlab = "Ni")
```

111

```
375  ggqqplot(log(gmb$Ni),
376  main = "Quantile-Quantile plot of log([Ni])",
377  xlab = "log([Ni])")
378  shapiro.test(log(gmb$Ni))
379
380
381  ggdensity(gmb$P,
382  main = "Density plot of P",
383  xlab = "P")
384  ggqqplot(gmb$P,
385  main = "Quantile-Quantile plot of P",
386  xlab = "P")
387  ggqqplot(log(gmb$P),
388  main = "Quantile-Quantile plot of log([P])",
389  xlab = "log([P])")
390  shapiro.test(log(gmb$P))
391
392
393  ggdensity(gmb$Pb..He.,
394  main = "Density plot of Pb (206)",
395  xlab = "Pb (206)")
396  ggqqplot(gmb$Pb..He.,
397  main = "Quantile-Quantile plot of Pb (206)",
398  xlab = "Pb (206)")
399  ggqqplot(log(gmb$Pb..He.),
400  main = "Quantile-Quantile plot of log([Pb. 206])",
401  xlab = "log([Pb. 206])")
402  shapiro.test(log(gmb$Pb..He.))
403
404
405  ggdensity(gmb$X207Pb,
406  main = "Density plot of Pb (207)",
407  xlab = "Pb (207)")
408  ggqqplot(gmb$X207Pb,
409  main = "Quantile-Quantile plot of Pb (207)",
410  xlab = "Pb (207)")
411  ggqqplot(log(gmb$X207Pb),
412  main = "Quantile-Quantile plot of log([Pb. 207])",
413  xlab = "log([Pb. 207])")
414  shapiro.test(log(gmb$X207Pb))
415
416
417  ggdensity(gmb$X208Pb,
418  main = "Density plot of Pb (208)",
419  xlab = "Pb (208)")
420  ggqqplot(gmb$X208Pb,
421  main = "Quantile-Quantile plot of Pb (208)",
422  xlab = "Pb 8208)")
423  ggqqplot(log(gmb$X208Pb),
424  main = "Quantile-Quantile plot of log([Pb. 208])",
425  xlab = "log([Pb. 208])")
426  shapiro.test(log(gmb$X208Pb))
427
428
429  ggdensity(gmb$X32S,
430  main = "Density plot of S (32-68)",
431  xlab = "S (32-68)")
432  ggqqplot(gmb$X32S,
433  main = "Quantile-Quantile plot of S (32-68)",
434  xlab = "S (32-68)")
435  ggqqplot(log(gmb$X32S),
```

112

```
436  main = "Quantile-Quantile plot of log([S]) (32-68)",
437  xlab = "log([S]) (32-68)")
438  shapiro.test(log(gmb$X32S))
439
440
441  ggdensity(gmb$X34S,
442  main = "Density plot of S (34-50)",
443  xlab = "S (34-50)")
444  ggqqplot(gmb$X34S,
445  main = "Quantile-Quantile plot of S (34-50)",
446  xlab = "S (34-50)")
447  ggqqplot(log(gmb$X34S),
448  main = "Quantile-Quantile plot of log([S]) (34-50)",
449  xlab = "log([S]) (34-50)")
450  shapiro.test(log(gmb$X34S))
451
452
453  ggdensity(gmb$Si,
454  main = "Density plot of Si",
455  xlab = "Si")
456  ggqqplot(gmb$Si,
457  main = "Quantile-Quantile plot of Si",
458  xlab = "Si")
459  ggqqplot(log(gmb$Si),
460  main = "Quantile-Quantile plot of log([Si])",
461  xlab = "log([Si])")
462  shapiro.test(log(gmb$Si))
463
464
465  ggdensity(gmb$Sr,
466  main = "Density plot of Sr",
467  xlab = "Sr")
468  ggqqplot(gmb$Sr,
469  main = "Quantile-Quantile plot of Sr",
470  xlab = "Sr")
471  ggqqplot(log(gmb$Sr),
472  main = "Quantile-Quantile plot of log([Sr])",
473  xlab = "log([Sr])")
474  shapiro.test(log(gmb$Sr))
475
476
477  ggdensity(gmb$Tl,
478  main = "Density plot of Tl",
479  xlab = "Tl")
480  ggqqplot(gmb$Tl,
481  main = "Quantile-Quantile plot of Tl",
482  xlab = "Tl")
483  ggqqplot(log(gmb$Tl),
484  main = "Quantile-Quantile plot of log([Tl])",
485  xlab = "log([Tl])")
486  shapiro.test(log(gmb$Tl))
487
488
489  ggdensity(gmb$V,
490  main = "Density plot of V",
491  xlab = "V")
492  ggqqplot(gmb$V,
493  main = "Quantile-Quantile plot of V",
494  xlab = "V")
495  ggqqplot(log(gmb$V),
496  main = "Quantile-Quantile plot of log([V])",
```

113

```r
497  xlab = "log([V])")
498  shapiro.test(log(gmb$V))
499
500
501  ggdensity(gmb$Zn,
502  main = "Density plot of Zn",
503  xlab = "Zn")
504  ggqqplot(gmb$Zn,
505  main = "Quantile-Quantile plot of Zn",
506  xlab = "Zn")
507  ggqqplot(log(gmb$Zn),
508  main = "Quantile-Quantile plot of log([Zn])",
509  xlab = "log([Zn])")
510  shapiro.test(log(gmb$Zn))
511
512
513
514
515  # bartlett test tissue
516
517  bartlett.test(Hg ¬ Tissue, data=gmb)
518  boxplot(Hg ¬ Tissue,
519  data = gmb,
520  names=c("HEP","MUS"),
521  ylab="Hg")
522
523  bartlett.test(Ag ¬ Tissue, data=gmb)
524  boxplot(Ag ¬ Tissue,
525  data = gmb,
526  names=c("HEP","MUS"),
527  ylab="Ag")
528
529  bartlett.test(Al ¬ Tissue, data=gmb)
530  boxplot(Al ¬ Tissue,
531  data = gmb,
532  names=c("HEP","MUS"),
533  ylab="Al")
534
535  bartlett.test(As ¬ Tissue, data=gmb)
536  boxplot(As ¬ Tissue,
537  data = gmb,
538  names=c("HEP","MUS"),
539  ylab="As")
540
541  bartlett.test(B ¬ Tissue, data=gmb)
542  boxplot(B ¬ Tissue,
543  data = gmb,
544  names=c("HEP","MUS"),
545  ylab="B")
546
547  bartlett.test(Ba ¬ Tissue, data=gmb)
548  boxplot(Ba ¬ Tissue,
549  data = gmb,
550  names=c("HEP","MUS"),
551  ylab="Ba")
552
553  bartlett.test(Be..No.Gas. ¬ Tissue, data=gmb)
554  boxplot(Be..No.Gas.¬ Tissue,
555  data = gmb,
556  names=c("HEP","MUS"),
557  ylab="Be (No Gas)")
```

114

```
558
559  bartlett.test(Be..He. ¬ Tissue, data=gmb)
560  boxplot(Be..He. ¬ Tissue,
561  data = gmb,
562  names=c("HEP","MUS"),
563  ylab="Be (He)")
564
565  bartlett.test(Ca ¬ Tissue, data=gmb)
566  boxplot(Ca ¬ Tissue,
567  data = gmb,
568  names=c("HEP","MUS"),
569  ylab="Ca")
570
571  bartlett.test(Cd ¬ Tissue, data=gmb)
572  boxplot(Cd ¬ Tissue,
573  data = gmb,
574  names=c("HEP","MUS"),
575  ylab="Cd")
576
577  bartlett.test(Co ¬ Tissue, data=gmb)
578  boxplot(Co ¬ Tissue,
579  data = gmb,
580  names=c("HEP","MUS"),
581  ylab="Co")
582
583  bartlett.test(Cr ¬ Tissue, data=gmb)
584  boxplot(Cr ¬ Tissue,
585  data = gmb,
586  names=c("HEP","MUS"),
587  ylab="Cr")
588
589  bartlett.test(Cs ¬ Tissue, data=gmb)
590  boxplot(Cs ¬ Tissue,
591  data = gmb,
592  names=c("HEP","MUS"),
593  ylab="Cs")
594
595  bartlett.test(Cu ¬ Tissue, data=gmb)
596  boxplot(Cu ¬ Tissue,
597  data = gmb,
598  names=c("HEP","MUS"),
599  ylab="Cu")
600
601  bartlett.test(Fe..He. ¬ Tissue, data=gmb)
602  boxplot(Fe..He. ¬ Tissue,
603  data = gmb,
604  names=c("HEP","MUS"),
605  ylab="Fe (He)")
606
607  bartlett.test(Fe..O2. ¬ Tissue, data=gmb)
608  boxplot(Fe..O2. ¬ Tissue,
609  data = gmb,
610  names=c("HEP","MUS"),
611  ylab="Fe (O2)")
612
613  bartlett.test(Ga ¬ Tissue, data=gmb)
614  boxplot(Ga ¬ Tissue,
615  data = gmb,
616  names=c("HEP","MUS"),
617  ylab="Ga")
618
```

115

```
619  bartlett.test(K ¬ Tissue, data=gmb)
620  boxplot(K ¬ Tissue,
621  data = gmb,
622  names=c("HEP","MUS"),
623  ylab="K")
624
625  bartlett.test(Li ¬ Tissue, data=gmb)
626  boxplot(Li ¬ Tissue,
627  data = gmb,
628  names=c("HEP","MUS"),
629  ylab="Li")
630
631  bartlett.test(Mg ¬ Tissue, data=gmb)
632  boxplot(Mg ¬ Tissue,
633  data = gmb,
634  names=c("HEP","MUS"),
635  ylab="Mg")
636
637  bartlett.test(Mn ¬ Tissue, data=gmb)
638  boxplot(Mn ¬ Tissue,
639  data = gmb,
640  names=c("HEP","MUS"),
641  ylab="Mn")
642
643  bartlett.test(Na ¬ Tissue, data=gmb)
644  boxplot(Na ¬ Tissue,
645  data = gmb,
646  names=c("HEP","MUS"),
647  ylab="Na")
648
649  bartlett.test(Ni ¬ Tissue, data=gmb)
650  boxplot(Ni ¬ Tissue,
651  data = gmb,
652  names=c("HEP","MUS"),
653  ylab="Ni")
654
655  bartlett.test(P ¬ Tissue, data=gmb)
656  boxplot(P ¬ Tissue,
657  data = gmb,
658  names=c("HEP","MUS"),
659  ylab="P")
660
661  bartlett.test(Pb..He. ¬ Tissue, data=gmb)
662  boxplot(Pb..He. ¬ Tissue,
663  data = gmb,
664  names=c("HEP","MUS"),
665  ylab="Pb (206)")
666
667  bartlett.test(X207Pb ¬ Tissue, data=gmb)
668  boxplot(X207Pb ¬ Tissue,
669  data = gmb,
670  names=c("HEP","MUS"),
671  ylab="Pb (207)")
672
673  bartlett.test(X208Pb ¬ Tissue, data=gmb)
674  boxplot(X208Pb ¬ Tissue,
675  data = gmb,
676  names=c("HEP","MUS"),
677  ylab="Pb (208)")
678
679  bartlett.test(X32S ¬ Tissue, data=gmb)
```

116

```
680  boxplot(X32S ¬ Tissue,
681  data = gmb,
682  names=c("HEP","MUS"),
683  ylab="S (32 -> 48)")
684
685  bartlett.test(X34S ¬ Tissue, data=gmb)
686  boxplot(X34S ¬ Tissue,
687  data = gmb,
688  names=c("HEP","MUS"),
689  ylab="S (34 -> 50)")
690
691  bartlett.test(Si ¬ Tissue, data=gmb)
692  boxplot(Si ¬ Tissue,
693  data = gmb,
694  names=c("HEP","MUS"),
695  ylab="Si")
696
697  bartlett.test(Sr ¬ Tissue, data=gmb)
698  boxplot(Sr ¬ Tissue,
699  data = gmb,
700  names=c("HEP","MUS"),
701  ylab="Sr")
702
703  bartlett.test(Tl ¬ Tissue, data=gmb)
704  boxplot(Tl ¬ Tissue,
705  data = gmb,
706  names=c("HEP","MUS"),
707  ylab="Tl")
708
709  bartlett.test(V ¬ Tissue, data=gmb)
710  boxplot(V ¬ Tissue,
711  data = gmb,
712  names=c("HEP","MUS"),
713  ylab="V")
714
715  bartlett.test(Zn ¬ Tissue, data=gmb)
716  boxplot(Zn ¬ Tissue,
717  data = gmb,
718  names=c("HEP","MUS"),
719  ylab="Zn")
720
721
722  # bartlett test sex
723
724  bartlett.test(Hg ¬ Tissue, data=gmb)
725  boxplot(log(Hg) ¬ Sex,
726  data = gmb,
727  names=c("Female","Male"),
728  ylab="log([Hg])")
729
730  bartlett.test(Ag ¬ Sex, data=gmb)
731  boxplot(log(Ag) ¬ Sex,
732  data = gmb,
733  names=c("Female","Male"),
734  ylab="log([Ag])")
735
736  bartlett.test(Al ¬ Sex, data=gmb)
737  boxplot(log(Al) ¬ Sex,
738  data = gmb,
739  names=c("Female","Male"),
740  ylab="log([Al])")
```

117

```
741
742  bartlett.test(As ¬ Sex, data=gmb)
743  boxplot(log(As) ¬ Sex,
744  data = gmb,
745  names=c("Female","Male"),
746  ylab="log([As])")
747
748  bartlett.test(B ¬ Sex, data=gmb)
749  boxplot(log(B) ¬ Sex,
750  data = gmb,
751  names=c("Female","Male"),
752  ylab="log([B])")
753
754  bartlett.test(Ba ¬ Sex, data=gmb)
755  boxplot(log(Ba) ¬ Sex,
756  data = gmb,
757  names=c("Female","Male"),
758  ylab="log([Ba])")
759
760  bartlett.test(Be..No.Gas. ¬ Sex, data=gmb)
761  boxplot(log(Be..No.Gas.) ¬ Sex,
762  data = gmb,
763  names=c("Female","Male"),
764  ylab="log([Be) (No Gas)")
765
766  bartlett.test(Be..He. ¬ Sex, data=gmb)
767  boxplot(log(Be..He.) ¬ Sex,
768  data = gmb,
769  names=c("Female","Male"),
770  ylab="log([Be) (He)")
771
772  bartlett.test(Ca ¬ Sex, data=gmb)
773  boxplot(log(Ca) ¬ Sex,
774  data = gmb,
775  names=c("Female","Male"),
776  ylab="log([Ca])")
777
778  bartlett.test(Cd ¬ Sex, data=gmb)
779  boxplot(log(Cd) ¬ Sex,
780  data = gmb,
781  names=c("Female","Male"),
782  ylab="log([Cd])")
783
784  bartlett.test(Co ¬ Sex, data=gmb)
785  boxplot(log(Co) ¬ Sex,
786  data = gmb,
787  names=c("Female","Male"),
788  ylab="log([Co])")
789
790  bartlett.test(Cr ¬ Sex, data=gmb)
791  boxplot(log(Cr) ¬ Sex,
792  data = gmb,
793  names=c("Female","Male"),
794  ylab="log([Cr])")
795
796  bartlett.test(Cs ¬ Sex, data=gmb)
797  boxplot(log(Cs) ¬ Sex,
798  data = gmb,
799  names=c("Female","Male"),
800  ylab="log([Cs])")
801
```

118

```
802  bartlett.test(Cu ¬ Sex, data=gmb)
803  boxplot(log(Cu) ¬ Sex,
804  data = gmb,
805  names=c("Female","Male"),
806  ylab="log([Cu])")
807
808  bartlett.test(Fe..He. ¬ Sex, data=gmb)
809  boxplot(log(Fe..He.) ¬ Sex,
810  data = gmb,
811  names=c("Female","Male"),
812  ylab="log([Fe]) (He)")
813
814  bartlett.test(Fe..O2. ¬ Sex, data=gmb)
815  boxplot(log(Fe..O2.) ¬ Sex,
816  data = gmb,
817  names=c("Female","Male"),
818  ylab="log([Fe]) (O2)")
819
820  bartlett.test(Ga ¬ Sex, data=gmb)
821  boxplot(log(Ga) ¬ Sex,
822  data = gmb,
823  names=c("Female","Male"),
824  ylab="log([Ga])")
825
826  bartlett.test(K ¬ Sex, data=gmb)
827  boxplot(log(K) ¬ Sex,
828  data = gmb,
829  names=c("Female","Male"),
830  ylab="log([K])")
831
832  bartlett.test(Li ¬ Sex, data=gmb)
833  boxplot(log(Li) ¬ Sex,
834  data = gmb,
835  names=c("Female","Male"),
836  ylab="log([Li])")
837
838  bartlett.test(Mg ¬ Sex, data=gmb)
839  boxplot(log(Mg) ¬ Sex,
840  data = gmb,
841  names=c("Female","Male"),
842  ylab="log([Mg])")
843
844  bartlett.test(Mn ¬ Sex, data=gmb)
845  boxplot(log(Mn) ¬ Sex,
846  data = gmb,
847  names=c("Female","Male"),
848  ylab="log([Mn])")
849
850  bartlett.test(Na ¬ Sex, data=gmb)
851  boxplot(log(Na) ¬ Sex,
852  data = gmb,
853  names=c("Female","Male"),
854  ylab="log([Na])")
855
856  bartlett.test(Ni ¬ Sex, data=gmb)
857  boxplot(log(Ni) ¬ Sex,
858  data = gmb,
859  names=c("Female","Male"),
860  ylab="log([Ni])")
861
862  bartlett.test(P ¬ Sex, data=gmb)
```

119

```
863  boxplot(log(P) ¬ Sex,
864  data = gmb,
865  names=c("Female","Male"),
866  ylab="log([P])")
867
868  bartlett.test(Pb..He. ¬ Sex, data=gmb)
869  boxplot(log(Pb..He.) ¬ Sex,
870  data = gmb,
871  names=c("Female","Male"),
872  ylab="log([Pb.206])")
873
874  bartlett.test(X207Pb ¬ Sex, data=gmb)
875  boxplot(log(X207Pb) ¬ Sex,
876  data = gmb,
877  names=c("Female","Male"),
878  ylab="log([Pb.207])")
879
880  bartlett.test(X208Pb ¬ Sex, data=gmb)
881  boxplot(log(X208Pb) ¬ Sex,
882  data = gmb,
883  names=c("Female","Male"),
884  ylab="log([Pb.208])")
885
886  bartlett.test(X32S ¬ Sex, data=gmb)
887  boxplot(log(X32S) ¬ Sex,
888  data = gmb,
889  names=c("Female","Male"),
890  ylab="log([S])(32->48) ")
891
892  bartlett.test(X34S ¬ Sex, data=gmb)
893  boxplot(log(X34S) ¬ Sex,
894  data = gmb,
895  names=c("Female","Male"),
896  ylab="log([S])(34->50)")
897
898  bartlett.test(Si ¬ Sex, data=gmb)
899  boxplot(log(Si) ¬ Sex,
900  data = gmb,
901  names=c("Female","Male"),
902  ylab="log([Si])")
903
904  bartlett.test(Sr ¬ Sex, data=gmb)
905  boxplot(log(Sr) ¬ Sex,
906  data = gmb,
907  names=c("Female","Male"),
908  ylab="log([Sr])")
909
910  bartlett.test(Tl ¬ Sex, data=gmb)
911  boxplot(log(Tl) ¬ Sex,
912  data = gmb,
913  names=c("Female","Male"),
914  ylab="log([Tl])")
915
916  bartlett.test(V ¬ Sex, data=gmb)
917  boxplot(log(V) ¬ Sex,
918  data = gmb,
919  names=c("Female","Male"),
920  ylab="log([V])")
921
922  bartlett.test(Zn ¬ Sex, data=gmb)
923  boxplot(log(Zn) ¬ Sex,
```

120

```
924  data = gmb,
925  names=c("Female","Male"),
926  ylab="log([Zn])")
927
928
929
930  # t test
931
932  t.test(log(Hg) ¬ Sex, data=gmb,
933  var.equal=TRUE,
934  conf.level=0.95)
935
936  t.test(Hg ¬ Tissue, data=gmb,
937  var.equal=TRUE,
938  conf.level=0.95)
939
940  t.test(log(Ag) ¬ Sex, data=gmb,
941  var.equal=TRUE,
942  conf.level=0.95)
943
944  t.test(Ag ¬ Tissue, data=gmb,
945  var.equal=TRUE,
946  conf.level=0.95)
947
948  t.test(log(Al) ¬ Sex, data=gmb,
949  var.equal=TRUE,
950  conf.level=0.95)
951
952  t.test(Al ¬ Tissue, data=gmb,
953  var.equal=TRUE,
954  conf.level=0.95)
955
956  t.test(log(As) ¬ Sex, data=gmb,
957  var.equal=TRUE,
958  conf.level=0.95)
959
960  t.test(As ¬ Tissue, data=gmb,
961  var.equal=TRUE,
962  conf.level=0.95)
963
964  t.test(log(B) ¬ Sex, data=gmb,
965  var.equal=TRUE,
966  conf.level=0.95)
967
968  t.test(B ¬ Tissue, data=gmb,
969  var.equal=TRUE,
970  conf.level=0.95)
971
972  t.test(log(Ba) ¬ Sex, data=gmb,
973  var.equal=TRUE,
974  conf.level=0.95)
975
976  t.test(Ba ¬ Tissue, data=gmb,
977  var.equal=TRUE,
978  conf.level=0.95)
979
980  t.test(log(Be..He.) ¬ Sex, data=gmb,
981  var.equal=TRUE,
982  conf.level=0.95)
983
984  t.test(Be..He. ¬ Tissue, data=gmb,
```

121

```
985  var.equal=TRUE,
986  conf.level=0.95)
987
988  t.test(log(Be..No.Gas) ¬ Sex, data=gmb,
989  var.equal=TRUE,
990  conf.level=0.95)
991
992  t.test(Be..No.Gas.¬ Tissue, data=gmb,
993  var.equal=TRUE,
994  conf.level=0.95)
995
996  t.test(log(Ca) ¬ Sex, data=gmb,
997  var.equal=TRUE,
998  conf.level=0.95)
999
1000 t.test(Ca ¬ Tissue, data=gmb,
1001 var.equal=TRUE,
1002 conf.level=0.95)
1003
1004 t.test(log(Cd) ¬ Sex, data=gmb,
1005 var.equal=TRUE,
1006 conf.level=0.95)
1007
1008 t.test(Cd ¬ Tissue, data=gmb,
1009 var.equal=TRUE,
1010 conf.level=0.95)
1011
1012 t.test(log(Co) ¬ Sex, data=gmb,
1013 var.equal=TRUE,
1014 conf.level=0.95)
1015
1016 t.test(Co ¬ Tissue, data=gmb,
1017 var.equal=TRUE,
1018 conf.level=0.95)
1019
1020 t.test(log(Cr) ¬ Sex, data=gmb,
1021 var.equal=TRUE,
1022 conf.level=0.95)
1023
1024 t.test(Cr ¬ Tissue, data=gmb,
1025 var.equal=TRUE,
1026 conf.level=0.95)
1027
1028 t.test(log(Cs) ¬ Sex, data=gmb,
1029 var.equal=TRUE,
1030 conf.level=0.95)
1031
1032 t.test(Cs ¬ Tissue, data=gmb,
1033 var.equal=TRUE,
1034 conf.level=0.95)
1035
1036 t.test(log(Cu) ¬ Sex, data=gmb,
1037 var.equal=TRUE,
1038 conf.level=0.95)
1039
1040 t.test(Cu ¬ Tissue, data=gmb,
1041 var.equal=TRUE,
1042 conf.level=0.95)
1043
1044 t.test(log(Fe..He.) ¬ Sex, data=gmb,
1045 var.equal=TRUE,
```

122

```
1046  conf.level=0.95)
1047
1048  t.test(Fe..He. ¬ Tissue, data=gmb,
1049  var.equal=TRUE,
1050  conf.level=0.95)
1051
1052  t.test(log(Fe..O2.) ¬ Sex, data=gmb,
1053  var.equal=TRUE,
1054  conf.level=0.95)
1055
1056  t.test(Fe..O2. ¬ Tissue, data=gmb,
1057  var.equal=TRUE,
1058  conf.level=0.95)
1059
1060  t.test(na.exclude(log(Ga) ¬ Sex), data=gmb,
1061  var.equal=TRUE,
1062  conf.level=0.95)
1063
1064  t.test(Ga ¬ Tissue, data=gmb,
1065  var.equal=TRUE,
1066  conf.level=0.95)
1067
1068  t.test(log(K) ¬ Sex, data=gmb,
1069  var.equal=TRUE,
1070  conf.level=0.95)
1071
1072  t.test(K ¬ Tissue, data=gmb,
1073  var.equal=TRUE,
1074  conf.level=0.95)
1075
1076  t.test(log(Li) ¬ Sex, data=gmb,
1077  var.equal=TRUE,
1078  conf.level=0.95)
1079
1080  t.test(Li ¬ Tissue, data=gmb,
1081  var.equal=TRUE,
1082  conf.level=0.95)
1083
1084  t.test(log(Mg) ¬ Sex, data=gmb,
1085  var.equal=TRUE,
1086  conf.level=0.95)
1087
1088  t.test(Mg ¬ Tissue, data=gmb,
1089  var.equal=TRUE,
1090  conf.level=0.95)
1091
1092  t.test(log(Mn) ¬ Sex, data=gmb,
1093  var.equal=TRUE,
1094  conf.level=0.95)
1095
1096  t.test(Mn ¬ Tissue, data=gmb,
1097  var.equal=TRUE,
1098  conf.level=0.95)
1099
1100  t.test(log(Na) ¬ Sex, data=gmb,
1101  var.equal=TRUE,
1102  conf.level=0.95)
1103
1104  t.test(Na ¬ Tissue, data=gmb,
1105  var.equal=TRUE,
1106  conf.level=0.95)
```

123

```
1107
1108   t.test(log(Ni) ¬ Sex, data=gmb,
1109   var.equal=TRUE,
1110   conf.level=0.95)
1111
1112   t.test(Ni ¬ Tissue, data=gmb,
1113   var.equal=TRUE,
1114   conf.level=0.95)
1115
1116   t.test(log(P) ¬ Sex, data=gmb,
1117   var.equal=TRUE,
1118   conf.level=0.95)
1119
1120   t.test(P ¬ Tissue, data=gmb,
1121   var.equal=TRUE,
1122   conf.level=0.95)
1123
1124   t.test(log(Pb..He) ¬ Sex, data=gmb,
1125   var.equal=TRUE,
1126   conf.level=0.95)
1127
1128   t.test(Pb..He ¬ Tissue, data=gmb,
1129   var.equal=TRUE,
1130   conf.level=0.95)
1131
1132   t.test(log(Si) ¬ Sex, data=gmb,
1133   var.equal=TRUE,
1134   conf.level=0.95)
1135
1136   t.test(Si ¬ Tissue, data=gmb,
1137   var.equal=TRUE,
1138   conf.level=0.95)
1139
1140   t.test(log(Sr) ¬ Sex, data=gmb,
1141   var.equal=TRUE,
1142   conf.level=0.95)
1143
1144   t.test(Sr ¬ Tissue, data=gmb,
1145   var.equal=TRUE,
1146   conf.level=0.95)
1147
1148   t.test(log(Tl) ¬ Sex, data=gmb,
1149   var.equal=TRUE,
1150   conf.level=0.95)
1151
1152   t.test(Tl ¬ Tissue, data=gmb,
1153   var.equal=TRUE,
1154   conf.level=0.95)
1155
1156   t.test(log(V) ¬ Sex, data=gmb,
1157   var.equal=TRUE,
1158   conf.level=0.95)
1159
1160   t.test(V ¬ Tissue, data=gmb,
1161   var.equal=TRUE,
1162   conf.level=0.95)
1163
1164   t.test(log(X207Pb) ¬ Sex, data=gmb,
1165   var.equal=TRUE,
1166   conf.level=0.95)
1167
```

124

```
1168  t.test(X207Pb ¬ Tissue, data=gmb,
1169  var.equal=TRUE,
1170  conf.level=0.95)
1171
1172  t.test(log(X208Pb) ¬ Sex, data=gmb,
1173  var.equal=TRUE,
1174  conf.level=0.95)
1175
1176  t.test(X208Pb ¬ Tissue, data=gmb,
1177  var.equal=TRUE,
1178  conf.level=0.95)
1179
1180  t.test(log(X32S) ¬ Sex, data=gmb,
1181  var.equal=TRUE,
1182  conf.level=0.95)
1183
1184  t.test(X32S ¬ Tissue, data=gmb,
1185  var.equal=TRUE,
1186  conf.level=0.95)
1187
1188  t.test(log(X34S) ¬ Sex, data=gmb,
1189  var.equal=TRUE,
1190  conf.level=0.95)
1191
1192  t.test(X34S ¬ Tissue, data=gmb,
1193  var.equal=TRUE,
1194  conf.level=0.95)
1195
1196  t.test(log(Zn) ¬ Sex, data=gmb,
1197  var.equal=TRUE,
1198  conf.level=0.95)
1199
1200
1201  t.test(Zn ¬ Tissue, data=gmb,
1202  var.equal=TRUE,
1203  conf.level=0.95)
1204
1205
1206
1207  # correlations
1208  num.cols<-sapply(gmb,is.numeric)
1209  cor.data <-cor(gmb[,num.cols],use="complete.obs")
1210  corrplot(cor.data)
1211
1212  cor.test(gmb$Cr, gmb$Ni)
1213  ggplot(gmb, aes(x = Ni, y = Cr)) +
1214  geom_point(alpha = 0.3) +
1215  geom_smooth(method = "lm")+ xlab("Ni")+ ylab("Cr")+ ggtitle("regression Cr ...
          vs Ni")
1216
1217
1218  cor.test(gmb$Cd , gmb$As)
1219  ggplot(gmb, aes(x = Cd, y = As)) +
1220  geom_point(alpha = 0.3) +
1221  geom_smooth(method = "lm")+ xlab("Cd")+ ylab("As")+ ggtitle("regression As ...
          vs Cd")
1222
1223  cor.test(gmb$As, gmb$Co)
1224  ggplot(gmb, aes(x = As, y = Co)) +
1225  geom_point(alpha = 0.3) +
```

125

```
1226 geom_smooth(method = "lm")+ xlab("As")+ ylab("Co")+ ggtitle("regression As ...
        vs Co")
1227
1228 cor.test(gmb$As, gmb$Mn)
1229 ggplot(gmb, aes(x = As, y = Mn)) +
1230 geom_point(alpha = 0.3) +
1231 geom_smooth(method = "lm")+ xlab("As")+ ylab("Mn")+ ggtitle("regression As ...
        vs Mn")
```

126